Studies of Renormalization-Group Flows in Quantum Field Theories

A Dissertation presented

by

Gongjun Choi

to

The Graduate School

in Partial Fulfillment of the

Requirements

for the Degree of

Doctor of Philosophy

in

Physics

Stony Brook University

May 2018

Stony Brook University

The Graduate School

Gongjun Choi

We, the dissertation committe for the above candidate for the

Doctor of Philosophy degree, hereby recommend

acceptance of this dissertation

Robert Shrock - Dissertation Advisor
Professor, Department of Physics and Astronomy

Chang Kee Jung - Chairperson of Defense
Professor, Department of Physics and Astronomy

Rouven Essig - Committee Member
Associate Professor, Department of Physics and Astronomy

Hooman Davoudiasl - Committee Member
Physicist, Department of Physics, Brookhaven National Laboratory

This dissertation is accepted by the Graduate School

Charles Taber
Dean of the Graduate School

Abstract of the Dissertation

Studies of Renormalization-Group Flows in Quantum Field Theories

by

Gongjun Choi

Doctor of Philosophy

in

Physics

Stony Brook University

2018

A transformation of the scheme used for regularization and renormalization in a quantum field theory is a map that connects coupling spaces of a theory in different schemes of this type. Especially in quantum chromodynamics, there have been active studies inventing schemes aimed at trying to reduce higher-order corrections in perturbative calculations, which work well for the coupling very close to zero. However, the problem becomes different provided one aims at studying a scheme transformation for values of the coupling away from zero, as is relevant for a vanishing of the beta function away from the origin. It turns out that many existing scheme transformations that work well for the coupling near zero cannot be applied so simply for the coupling away from zero (but still in the perturbative regime, i.e. $g^2/4\pi = \alpha \leq 1$), and may cause violation of unitarity and perturbativity in a given theory. Motivated by this, we study the construction of scheme transformations that are applicable in the vicinity of a zero of the beta function away from the origin [1, 2]. We construct and apply scheme transformations at an infrared (IR) zero of the beta function, $\alpha_{IR,zero}$, in an vectorial, asymptotically free SU(N) gauge theory with N_f fermions in a representation R to study the scheme dependence of $\alpha_{IR,zero}$. We show that the shift of $\alpha_{IR,zero}$ with increasing loop order tends to decrease, providing a quantitative mea-

sure of the size of the scheme-dependence in the calculation of $\alpha_{IR,zero}$ up to four-loop order at not only small but also moderate coupling away from zero.

As the second part of the thesis work, we study the renormalization-group evolution of a $\mathcal{N} = 1$ supersymmetric $SU(N)$ gauge theory by investigating β functions in different schemes [3]. We take two particular schemes and compute Padé approximants to probe the degree of similarity of the respective β functions in these schemes.

Finally, we explore the renormalization-group evolution of the Gross-Neveu model with N-component fermions by examining its β function up to four-loop order [4]. As part of this study, we apply scheme transformations to this β function and also calculate and analyze Padé approximants to the β function. From this analysis, we show that there is no evidence for presence of an infrared zero in the finite-N Gross-Neveu model.

Dedication Page

To Shinhae

Contents

1 Introduction

In this dissertation, we will study some topics in quantum field theory (QFT), including the dependence of a β function calculated to finite loop order, and the corresponding renormalization-group flows of some models, on the scheme used for regularization and renormalization. We will call this simply a scheme in the following. The original research discussed in this thesis was performed in collaboration with Prof. R. Shrock and published in the four papers [1]-[4], the last of which also involved Prof. T. Ryttov (of Southern Denmark University) as a coauthor. Early papers on the renormalization group (RG) include [5]. The specific models we will go through for the study of these topics are

- $SU(N_c)$ gauge theory with N_f massless Dirac fermions
- $\mathcal{N} = 1$ supersymmetric $SU(N_c)$ gauge theory with N_f massless chiral superfields
- Gross-Neveu model with finite N component massless fermions

These theories have the common feature of asymptotic freedom due to the negativity of the one-loop β function for a range of the number of fermion matter fields, N_f, that each theory has. Since we will be investigating the infrared behavior of these asymptotically free theories, our restriction to massless fermions incurs no loss of generality. The reason for this is that if a fermion had a nonzero mass m_0, it would be integrated out of the effective field theory at scales $\mu < m_0$, and hence would not affect the IR limit $\mu \to 0$ considered here. As we will see later, a finite ℓ-loop order β function with $\ell \geq 3$ depends on a choice of scheme used for regularization and renormalization, and thus one may wonder how this fact affects physical observables in perturbative QFT. To be specific, the possible questions that arise due to subtlety lying behind renormalization scheme dependence could be

- How could one map coupling spaces of different schemes in a quantum field theory?
- How much is a finite-loop calculation of a physical observable sensitive to change of scheme?
- How is a renormalization-group flow of quantum field theory affected by change of scheme?

We shall investigate these questions by the method of construction of various scheme transformations and applying those to a physical observable of the theories presented above, with reference to an infrared zero of the associated β functions. To this end, in this introduction section, we review the basic procedure of regularization and renormalization and the way how one defines a scheme in Sec.1.1 and Sec.1.2. Then in Sec.1.3, we briefly review the β function of a non-Abelian gauge theory and define an infrared zero of the β function. In addition, we study several possible infrared phases of an asymptotically free theory, which depend on the value of the infrared zero of β function. Finally in Sec.1.4, we study the basic formalism of scheme transformations mapping coupling spaces of different renormalization schemes.

1.1 Regularization

In computing physical quantities within the framework of QFT, there arise certain divergences, although we know the final answer for a physical quantity must be finite. The expectation is that the divergences may occur in the intermediate steps of the computation of physical observables. In the computational procedure, it is necessary to isolate a meaningful finite part from a divergent expression and the technique for the isolation is called *regularization*. As an explicit example of regularization procedure, we illustrate here the order $\mathcal{O}(g^2)$ fermion loop correction to the gluon propagator in quantum chromodynamics (QCD). Using the fermion propagator

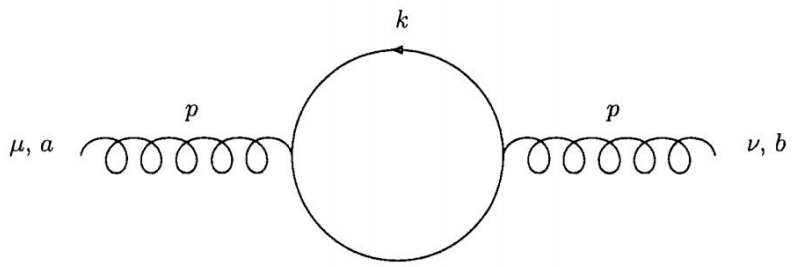

Figure 1: The Feynman diagram for one-loop correction to the gluon propagator. Curly external lines and solid internal lines correspond to gluon and fermion, respectively.

$$i\delta_{ij}\frac{\not{p}+m}{p^2-m^2+i\epsilon} \tag{1}$$

and fermion-fermion-gauge vertex $-ig\gamma^\mu T^a_{ij}$ with i and j color indices, one can evaluate the Feynman diagram in Fig.1 and it reads

$$-i\Pi^{\mu\nu}_{ab}(p^2) = -g^2\mathrm{Tr}(T_aT_b)\int\frac{d^4k}{(2\pi)^4}\frac{\mathrm{Tr}[\gamma^\mu(\not{k}+m)\gamma^\nu(\not{k}+\not{p}+m)]}{(k^2-m^2)([k+p]^2-m^2)} \tag{2}$$

where T_a is generator of the gauge group $SU(3)$ and our metric is $(+,-,-,-)$. The denominator of the integrand can be expressed with the use of the identity

$$\frac{1}{A\cdot B} = \int_0^1\frac{d\alpha}{\left[A(1-\alpha)+B\alpha\right]^2} \tag{3}$$

with $A = k^2-m^2$ and $B = [k+p]^2-m^2$. Then, one sees that $-i\Pi^{\mu\nu}_{ab}(p^2)$ contains term of the form

$$\int_0^1\int\frac{d^4\ell}{(2\pi)^4}\frac{\ell^n d\alpha}{(\ell^2-D)^2} \qquad (\mathrm{n}=0\ ,\ 2) \tag{4}$$

with $\ell \equiv k+\alpha p$ and $D \equiv m^2-\alpha(1-\alpha)p^2$. Now by having spacetime dimension analytically continued to $D = 4-2\epsilon$ dimension [6, 7, 8], we can perform dimensional regularization of the momentum integral in Eq. (4) via

$$\int\frac{d^D\ell}{(2\pi)^D}\frac{\ell^n}{(\ell^2-D)^2} = \frac{\Gamma(-n+\epsilon)\Gamma(n+2-\epsilon)}{(4\pi)^{2-\epsilon}\Gamma(2)\Gamma(2-\epsilon)}D^{n-\epsilon} \tag{5}$$

where $\Gamma(\epsilon)$ is the Euler Gamma function given by

$$\Gamma(\epsilon) = \frac{\Gamma(1+\epsilon)}{\epsilon} = \frac{1}{\epsilon}(1-\epsilon\gamma_E+O(\epsilon^2)) \tag{6}$$

where $\gamma_E = 0.57722...$ is the Euler-Mascheroni constant. In D spacetime dimensions, the Lagrangian density's mass dimension becomes D and thus each field's mass dimension changes accordingly compared to 4 dimensional case. Since the scalar, fermion and gluon field's mass dimensions get converted to $1-\epsilon$, $(3/2)-\epsilon$ and $1-\epsilon$, respectively, one can deduce ϵ as the gauge coupling's mass dimension from the minimal coupling of the scalar and fermion with the gluon field. Now we rewrite the gauge coupling g in terms of the dimensionless renormalized gauge coupling $\tilde{g}$ and a new parameter μ which

carries mass dimension of g. These are related by $g = \tilde{g}\mu^{\epsilon}$. Note that μ is not an actual parameter of the theory, and therefore we require that physical observables are independent of μ.

Now relying on identities of gamma matrices and Eq. (5), one eventually arrives at the following result,

$$-i\Pi^{\mu\nu}_{ab}(p^2) = i\frac{\tilde{g}^2}{12\pi^2}\mathrm{T(R)}\delta_{ab}(p^\mu p^\nu - g^{\mu\nu}p^2)(-\frac{1}{\epsilon} + \text{finite}) \tag{7}$$

where T(R) is Dynkin index of R-representation of the gauge group SU(N) and the finite part in the parenthesis reads

$$\text{finite} = [\gamma_E - \ln(4\pi) + \ln(\frac{-p^2}{\mu^2}) - \frac{5}{3}] - \frac{m^2}{p^2} + \mathcal{O}(\frac{m^6}{p^6}) + \mathcal{O}(\epsilon) \tag{8}$$

Thus the divergent integral in Eq. (2) becomes separated into finite and divergent parts.

1.2 Renormalization and its Scheme

In the procedure of renormalization, one writes a bare Lagrangian as a sum of a renormalized Lagrangian and its corresponding counterterm, i.e.,

$$\mathcal{L}_B = \mathcal{L}_R + \Delta\mathcal{L} \tag{9}$$

where $\Delta\mathcal{L}$ is the counterterm Lagrangian. We use the subscripts B and R to denote the bare and renormalized quantities, respectively. The switch from the left hand side to the right hand side of Eq. (9) is achieved by relating bare quantities to renormalized quantities via renormalization constants, Z_i. For instance, the bare gauge field $A^{a\mu}_B$ is related to the renormalized gauge field $A^{a\mu}_R$ through $A^{a\mu}_B = \sqrt{Z_3}A^{a\mu}_R$ where a is the gauge group generator index and Z_3 is the renormalization constant for the gauge field. In general, the renormalization constants can be written as $Z_i = 1 + \Delta Z_i$, which implies that a bare quantity differs from its renormalized quantity by ΔZ_i. Since $\mathcal{L}_R$ is completely expressed in terms of renormalized quantities, it should be the case that ΔZ_is appear in the counterterm Lagrangian $\Delta\mathcal{L}$. It is this ΔZ_i that incorporates the singularity structure of loop correction diagrams.

Now, having regularized the divergence(s), one still has the freedom to define the finite part of ΔZ_i with divergent part fixed and a choice of the finite part defines a regularization and renormalization *scheme*. Some well-known

examples of such schemes include the minimal subtraction scheme (MS) and the modified minimal subtraction scheme ($\overline{\rm MS}$), which are characterized by setting the finite part of ΔZ_i to be 0 and $\gamma_E - \ln(4\pi)$, respectively [7, 8]. Apart from these examples, one can still choose another value of the finite part and thus define a new renormalization scheme. Note, however, that different renormalization schemes lead on to not only different finite part of ΔZ_i, but the finite values of Feynman diagrams that we are left with after renormalization.

To be more explicit, we can study the effect of renormalization on the fermion one-loop correction to gauge field propagator in Eq. (7). After renormalization, Eq. (7) is converted into

$$-i\Pi^{\mu\nu}_{ab}(p^2) = i\frac{\tilde{g}^2}{12\pi^2}\mathrm{T(R)}\ln(\frac{-p^2}{\mu^2 e^{C_{RS}}}) \tag{10}$$

where C_{RS} varies according to what scheme is chosen for renormalization. For exemplary schemes we mentioned above, the values of C_{RS} are given by $C_{MS} = -\gamma_E + \ln(4\pi) + 5/3$ and $C_{\overline{\rm MS}} = 5/3$. We thus realize that renormalization scheme transformation can be easily carried out by rescaling the parameter μ. In effect, the result we have in Eq. (10) contributes to the renormalization constant of the gauge field, Z_3, as manifested in renormalization of the kinetic term of the gauge field. For further details of regularization and renormalization procedure, we refer the reader to [9]. Although we shall focus on asymptotically free theories in our work, we note that studies of renormalization-group evolution have also been of interest in non-asymptotically free theories, such as [10]-[16].

1.3 Beta Function of Non-Abelian Gauge Theory

In this section we discuss some relevant background of the beta function of non-Abelian gauge theory and possible infrared behavior, relying on the beta function at a finite loop order. We define

$$a \equiv \frac{g^2}{16\pi^2} = \frac{\alpha}{4\pi} \ . \tag{11}$$

where g is the gauge coupling of the non-Abelian gauge theory of interest. Because of loop effects such as the one illustrated in the previous section, the coupling depends on the momentum scale at which it is measured. Formally,

one may take this scale to be μ, although in a particular physical problem, this will be related to the relevant physical momentum scale. The μ dependence of α will often be left implicit in the notation. The beta function is $\beta_g = dg/dt$ or equivalently,

$$\beta_\alpha \equiv \frac{d\alpha}{dt} \ , \tag{12}$$

where $dt = d\ln\mu$. Thus, $\beta_\alpha = [g/(2\pi)]\beta_g$. The function β_α has the series expansion

$$\beta_\alpha = -2\alpha \sum_{\ell=1}^{\infty} b_\ell \, a^\ell = -2\alpha \sum_{\ell=1}^{\infty} \bar{b}_\ell \, \alpha^\ell \ , \tag{13}$$

where b_ℓ is the ℓ-loop coefficient and $\bar{b}_\ell = b_\ell/(4\pi)^\ell$. The n-loop ($n\ell$) β function, denoted $\beta_{\alpha,n\ell}$, is obtained from Eq. (13) by replacing the upper limit on the ℓ-loop summation by n instead of ∞. The coefficients b_1 and b_2 were calculated in [17],

$$b_1 = \frac{1}{3}(11C_A - 4T_f N_f) \ , \tag{14}$$

and [18]

$$b_2 = \frac{1}{3}[34C_A^2 - 4(5C_A + 3C_f)T_f N_f] \ . \tag{15}$$

Here, the group-theoretic quantities are defined as follows. Let T_R^a denote the generators of the Lie algebra of a group G in the representation R, where a is a group index, and let d_R denote the dimension of R. The Casimir invariants $C_2(R)$ is given by $T_R^a T_R^a = C_2(R)I$, where here I is the $d_R \times d_R$ identity matrix, and the trace invariant is given by $\mathrm{Tr}_R(T_R^a T_R^b) = T(R)\delta_{ab}$. For a fermion f transforming according to a representation R, we often use the equivalent compact notation $T_f \equiv T(R)$ and $C_f \equiv C_2(R)$. We also use the notation $C_A \equiv C_2(A) \equiv C_2(G)$. Our normalization of generators is such that $C_A = N_c$ for $G = \mathrm{SU}(N_c)$. Note that from Eq. (14), one sees that $b_1 > 0$ holds provided $N_f < 11C_A/2T_f$ in which the theory is asymptotically free. It is natural to work within a class of schemes where subtractions are performed in the minimal manner as illustrated in the previous section, independent of external masses and momenta. These schemes are called mass-independent and include the MS and $\overline{\mathrm{MS}}$ schemes, and others related to them via scheme transformations. We shall do this in our analysis.

The coefficient b_1 is scheme-independent, and b_2 is also independent of scheme within the class of mass-independent schemes [19]. In contrast,

the coefficients b_ℓ with $\ell \geq 3$ are scheme-dependent [19]. This can be proven by using scheme transformation formalism which will be discussed in Sec.1.4. The widely applied modified minimal subtraction ($\overline{\rm MS}$) scheme [8] uses dimensional regularization of Feynman integrals with minimal subtraction (MS) of the poles and associated constants at dimension $d = 4$ in the resultant Euler Γ functions as discussed in Sec.1.2. Calculations of b_3, b_4 and b_5 in the $\overline{\rm MS}$ scheme were given in [20, 21, 22] for a non-Abelian gauge theory for general gauge group G and fermion representation R. (For the special case $G = {\rm SU}(3)$ and $R = F$, the fundamental representation, b_5 was calculated in [23].)

One of the advantages of the use of the β function is that it can give some indication of what infrared phase a relevant theory would flow to as one moves from high energy to a lower energy regime. Here we discuss some possible infrared phases of the non-Abelian gauge theory with N_f fermions. We start with the notion of infrared zero of a beta function defined to be the coupling α in Eq. (11) satisfying

$$\beta(a) = -2\alpha \sum_{\ell=1}^{\infty} b_\ell a^\ell = 0 \ . \tag{16}$$

By replacing the upper limit ∞ with n, we get the n-loop analong and denote the IR zero of the n-loop beta function $\beta_{\alpha,n\ell}$ as $\alpha_{IR,n\ell} = 4\pi a_{IR,n\ell}$. Now, the 2-loop value of the infrared zero of the beta function is given by

$$\alpha_{IR,2\ell} = -\frac{4\pi b_1}{b_2} \ . \tag{17}$$

In order for a positive $\alpha_{IR,2\ell}$ to exist in an asymptotically free theory ($b_1 > 0$), one need to require $b_2 < 0$. Thus the number of the fermions in the theory must lie in the interval

$$I: \quad N_{f,b2z} < N_f < N_{f,b1z} \ . \tag{18}$$

where $N_{f,b\ell z}$ is the N_f with which b_ℓ vanishes.

As the first possibility of an infrared behavior of a non-Abelian gauge theory, the theory might not have even $\alpha_{IR,2\ell}$ due to $b_2 > 0$ ($N_f < N_{f,b2z}$), not to mention $\alpha_{IR,zero}$. In this case, as one moves toward low energy regime, both the gauge coupling and the magnitude of the beta function value would continue to increase, and eventually these would exceed the regime where

they can be reliably calculated perturbatively. For example, one may not rely on perturbative computational method below the scale Λ_{QCD} where $g(\Lambda_{QCD}) \sim 1$ holds. QCD is one of the theories that belong to this class. We illustrate this situation in Fig. 2.

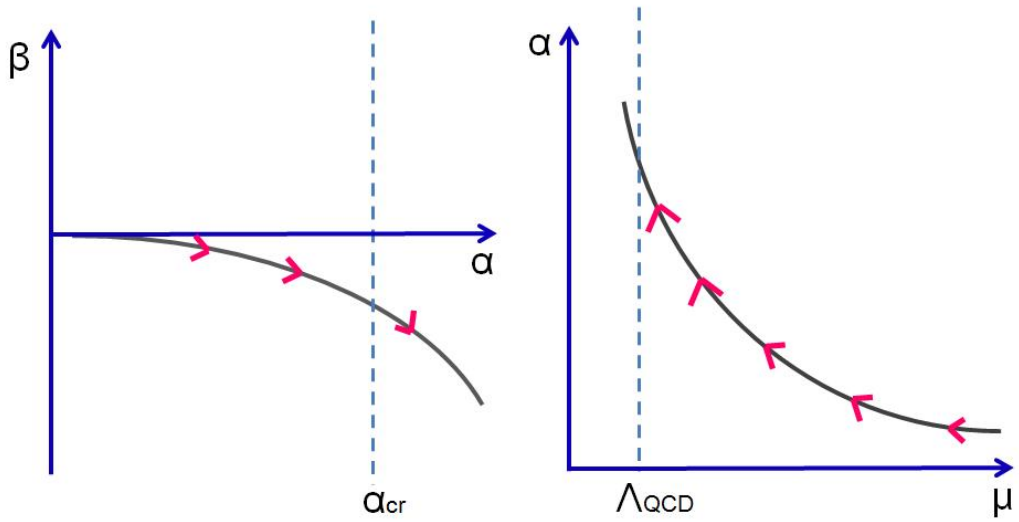

Figure 2: The evolution of β function and gauge coupling of an asymptotically free non-Abelian gauge theory when the theory does not exhibit $\alpha_{IR,zero}$. The arrow is along the direction of renormalization group evolution of the theory of interest.

On the other hand, if there exists a real positive solution to Eq. (16), then relative comparison between $\alpha_{IR,zero}$ and α_{cr} becomes important in the classification of the infrared behavior, where α_{cr} is the coupling beyond which the formation of bilinear fermion condensates takes place in the most attractive channel, with attendant spontaneous chiral symmetry breaking and dynamical generation of effective masses for the fermions involved. In the ladder approximation to the Schwinger-Dyson equation for the fermion propagator, this occurs as α increases through a value α_{cr} given by [24] $\alpha_{cr} = \pi/(3C_f)$. Given the intrinsic uncertainties involved in the strongly coupled physics of fermion condensate formation, one may infer that the actual critical value of α satisfies $\alpha_{cr}C_f \sim O(1)$. If α_{IR} exceeds α_{cr} as the reference scale decreases below a scaled denoted Λ, then α_{cr} is reached before α_{IR} in the renormalization-group evolution of the gauge coupling. Then, forming bi-

linear condensates, fermions gain dynamical masses of order $\mathcal{O}(\Lambda)$. Thus, the fermions are integrated out (N_f decreases) when the energy scale gets below values of the masses and the β function of the theory in lower energy regime than fermion masses becomes modified, so that the gauge coupling increases further, eventually exceeding the perturbatively calculable regime. Interestingly, however, if $\alpha_{IR,zero}$ is just slightly greater than α_{cr}, there is a range of energy scale within which the gauge coupling rarely evolves and the theory becomes *quasi-scale invariant*. This behavior is equivalently referred to as being approximately dilatation-invariant. We illustrate this situation in Fig.3. For this case, we call α_{IR} the approximate infrared zero.

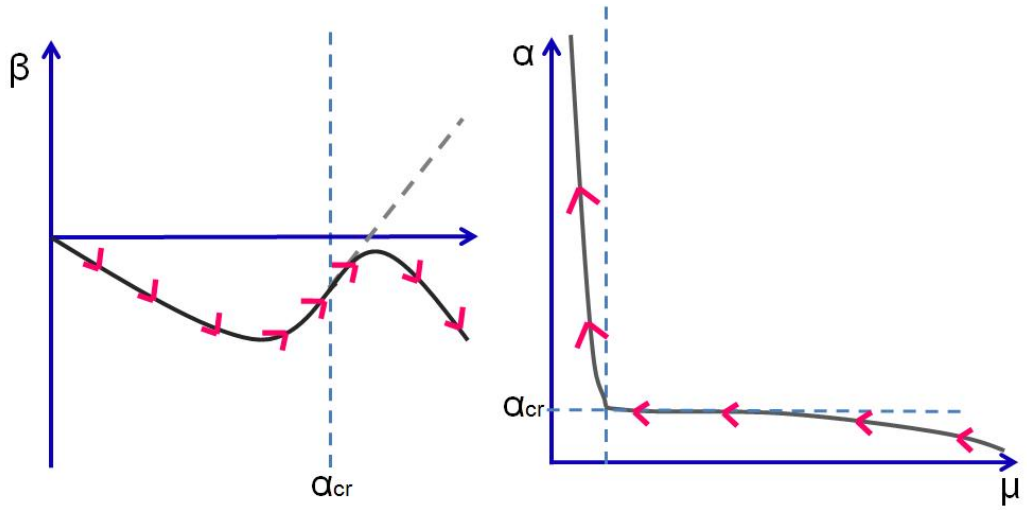

Figure 3: The evolution of β function and gauge coupling of an asymptotically free non-Abelian gauge theory when α_{IR} is just slightly greater than α_{cr}. The arrow is along the direction of renormalization group evolution of the theory of interest.

For a given gauge group G and fermion representation R, we defines a critical value, $N_{f,cr}$, that separates the two types of UV to IR evolution; for $N_f > N_{f,cr}$, this evolution is to a massless non-Abelian Coulomb phase, while for $N_f < N_{f,cr}$, it involves the above-mentioned chiral symmetry breaking. These theories merit study because of their intrinsic field-theoretic interest, and our work focuses mainly on formal aspects of the renormalization-group behavior of these theories. However, it should be noted that they have been of considerable phenomenological interest for a number of years as possible

ultraviolet extensions of the Standard Model involving dynamical electroweak symmetry breaking (EWSB) and a composite Higgs particle. In this application, the fermions transform vectorially under the gauge group G, but have transformation properties under the electroweak group such that the bilinear fermion condensates that form at the scale Λ break electroweak symmetry. These condensates transform in the same manner as a Higgs, namely with weak isospin $I = 1/2$ and unit weak hypercharge. As a result of the breaking of the associated global chiral symmetry, there arise three Nambu-Goldstone bosons, which become the longitudinal modes of the $W^{\pm}$ and Z vector bosons that mediate the charged-current and neutral-current weak interactions. This fermion condensate formation also produces dynamical masses for the fermions and therefore spontaneously breaks the approximate dilatation invariance, giving rise to a light dilaton, which has properties similar to those of the Standard-Model Higgs (e.g., [25]). Such theories have the potential to solve the naturalness problem in the Higgs mass in the original Standard Model because the small mass of the dilaton is protected, as an approximate Nambu-Goldstone boson. The quasi-scale-invariant behavior can be built into a model by choosing a gauge group G, fermion representation R, and value of N_f so that N_f is slightly smaller than $N_{f,cr}$, where $N_{f,cr}$ is such that if $N_f < N_{f,cr}$, then the gauge interaction produces a fermion condensate and confines in the IR, while if $N_f > N_{f,cr}$, then there is no fermion condensate formation or associated spontaneous chiral symmetry breaking and the theory evolves in the infrared to a (deconfined) non-Abelian Coulomb phase. Extensive lattice studies of quasi-scale-invariant theories have been undertaken over the past ten years, both because of their possible role in physics beyond the Standard Model with dynamical EWSB and a composite Higgs, and because of their intrinsic theoretical interest [26, 27]. These have demonstrated the appearance of a light scalar particle in quasi-scale-invariant theories, consistent with being the dilaton. So far, the production and decays of the Higgs particle at the CERN Large Hadron Collider (LHC) are consistent with the predictions of the Standard Model. The question of whether or not it is composite, or is truly pointlike, as predicted by the Standard Model, will continue to be a major goal of experimental study at the LHC. Thus, time will tell whether quasi-scale-invariant theories are realized as part of physics beyond the Standard Model. However, such theories are of definite theoretical interest because of their unusual renormalization-group behavior. As will be discussed below, our thesis research on scheme transformations is quite useful in the analysis of these theories, since it provides a quantitative

measure of the degree of scheme dependence in higher-loop-order perturbative calculations. Indeed, this is analogous to the value of studying scheme dependence in higher-order perturbative QCD calculations relevant for the analysis of experimental data at the Fermilab Tevatron and CERN LHC. The difference is that in our case, we are investigating behavior in the vicinity of an approximate infrared fixed point of the renormalization group, while in the case of QCD, the investigations study the behavior at high momentum transfers in the vicinity of the ultraviolet fixed point at the origin in coupling space. As we will show, scheme transformations that work well near $\alpha = 0$ and hence in the deep UV, may not be applicable at an infrared fixed point located away from the origin.

Lastly, if there exists a real positive solution to Eq. (16) and $\alpha_{IR,zero} < \alpha_{cr}$ holds, then the theory has the exact infrared zero of β function. In contrast to the previous case, now α_{IR} is reached before α_{cr} in the renormalization-group evolution of the gauge coupling. This implies that the β function evolves from zero to zero and the coupling increases and eventually evolves to α_{IR} in renormalization group evolution from ultraviolet (UV) to infrared (IR) regime. Then in the IR limit, the theory has an exact scale invariance and the value of β function approaches zero. In this sense, we call $\alpha_{IR,zero}$ an infrared fixed point (IRFP) and denote it as α_{IRFP}. Here, the UV to IR evolution of the theory leads to a deconfined non-Abelian Coulomb Phase without any spontaneous chiral symmetry breaking [28, 29]. We illustrate this situation in Fig.4.

In this discussion about infrared phase of the theory and IR zero, we have not specified a loop order at which we evaluate the IR zero. Thus one may wonder whether higher loop corrections to IR zero are large enough to change the renormalization group evolution of the theory. This was investigated in [30]-[35]. We discuss the comparison of $\alpha_{IR,2\ell}$, $\alpha_{IR,3\ell}$ and $\alpha_{IR,4\ell}$ in the $\overline{\rm MS}$ scheme. For fermions in the fundamental representation, it was found that, in the $\overline{\rm MS}$ scheme, relative to the (scheme-independent) two-loop value, $\alpha_{IR,2\ell}$.

$$\alpha_{IR,3\ell,\overline{\rm MS}} \ < \ \alpha_{IR,4\ell,\overline{\rm MS}} \ < \ \alpha_{IR,2\ell} \ . \tag{19}$$

The shifts in the value of the IR zero with ascending loop order were found to become smaller as N_f approaches $N_{f,b1z}$. Comparisons were made with the extensive lattice studies of this physics for various gauge groups and fermion representations [26]. Because the coefficients b_ℓ for $\ell \geq 3$ are scheme-dependent, these higher-loop calculations naturally led to studies of scheme-

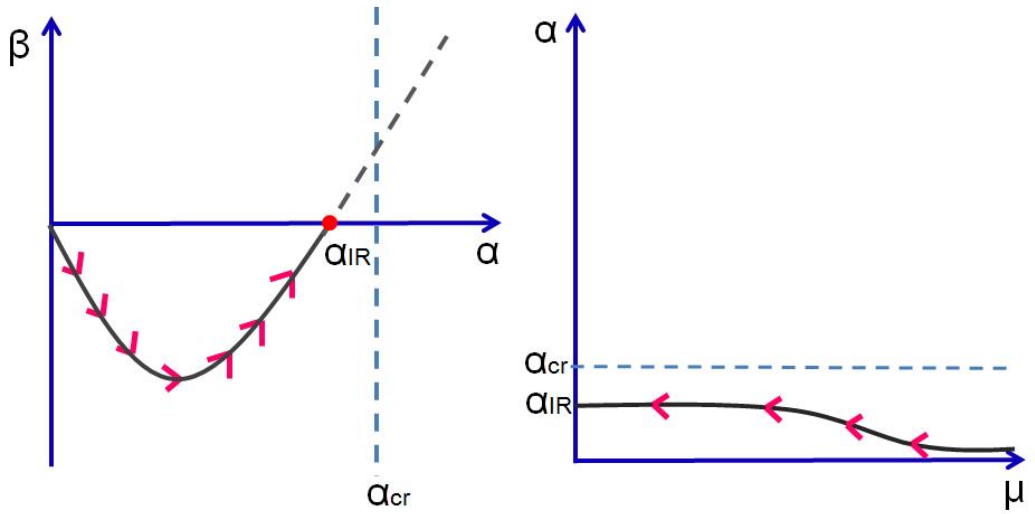

Figure 4: The evolution of β function and gauge coupling of an asymptotically free non-Abelian gauge theory when there exists an exact infrared fixed point with $\alpha_{IR} < \alpha_{cr}$. The arrow is along the direction of renormalization group evolution of the theory of interest. In the left panel, the red circular point on α axis represents IR zero of the theory of interest and it is smaller than α_{cr} in this case.

dependence in [36]-[41]. A different approach to study an IR fixed point of an asymptotically free theory [28] that has been pursued in [42]-[47] is to calculate scheme-independent series expansions for physical quantities. In addition to this thesis research, the author is also carrying out research in cosmology in collaboration with Prof. M. Loverde and Dr. Chi-Ting Chiang [48].

1.4 Scheme Transformations

Having reviewed relevant background in previous sections, we now begin to describe the original research carried out by the author in collaboration with Prof. Shrock, which comprises the author's Ph.D. thesis work and was published in the four papers [1]-[4], the last of which also coauthored with Prof. T. Ryttov.

A scheme transformation can be expressed as a mapping between α and

α' or equivalently, between a and a', namely

$$a = a' f(a') = F(a') \ . \tag{20}$$

In the limit where a and a' vanish, the theory becomes free, so a scheme transformation has no effect. This implies the condition

$$f(0) = 1 \ . \tag{21}$$

The functions $f(a')$ that we consider have Taylor series expansions about $a = a' = 0$ of the form

$$f(a') = 1 + \sum_{s=1}^{s_{max}} k_s (a')^s \tag{22}$$

where the k_s are constants, and s_{max} may be finite or infinite. Thus, these functions $f(a')$ automatically satisfy the condition (21). Equivalently,

$$F(a') = a' + \sum_{s=1}^{s_{max}} k_s (a')^{s+1} \ . \tag{23}$$

A number of the scheme transformations studied in [1, 36, 37, 38, 39] depend on a parameter (denoted r in these works) and hence are actually one-parameter families of scheme transformations. Here and below, we shall often refer to a one-parameter family of scheme transformations as a single scheme transformation, with the dependence on the parameter r taken to be implicit. In accordance with the series expansion (23), $F(a')$ has the property

$$F'(0) \equiv \frac{dF(a')}{da'}\Big|_{a'=0} = 1 \ . \tag{24}$$

(No confusion should result from the prime used here for differentiation and the prime on a', which does not indicate any differentiation but just distinguishes a' from a.) For the relevant region of small a (and hence also small a') where the perturbative beta function is applicable, we mention the following general result. Let us denote the lowest-order nonzero coefficient k_s in Eq. (22) as $k_{s_{min}}$. Then for small a (and hence a'),

$$\begin{aligned} k_{s_{min}} > 0 &\implies a > a' \ , \\ k_{s_{min}} < 0 &\implies a < a' \ . \end{aligned} \tag{25}$$

Given the form (22), it follows that the Jacobian

$$J = \frac{da}{da'} = \frac{d\alpha}{d\alpha'} \tag{26}$$

has the series expansion

$$J = 1 + \sum_{s=1}^{s_{max}} (s+1) k_s (a')^s \tag{27}$$

and thus satisfies

$$J = 1 \quad \text{at} \quad a = a' = 0 \ . \tag{28}$$

The beta function in the transformed scheme is

$$\beta_{\alpha'} \equiv \frac{d\alpha'}{dt} = \frac{d\alpha'}{d\alpha} \frac{d\alpha}{dt} = J^{-1} \beta_\alpha \ . \tag{29}$$

with the series expansion

$$\beta_{\alpha'} = -2\alpha' \sum_{\ell=1}^{\infty} b'_\ell (a')^\ell = -2\alpha' \sum_{\ell=1}^{\infty} \bar{b}'_\ell (\alpha')^\ell \ , \tag{30}$$

where $\bar{b}'_\ell = b'_\ell/(4\pi)^\ell$. Since Eqs. (29) and (30) define the same function, one can solve for the b'_ℓ in terms of the b_ℓ and k_s. This yields the results $b'_1 = b_1$ and $b'_2 = b_2$. In [36, 37], explicit expressions were calculated for higher-loop b'_ℓ with $\ell \geq 3$ in terms of the b_ℓ and k_s. In general, it was shown that the coefficient b'_ℓ with $\ell \geq 3$ in the transformed scheme is a linear combination of b_n with $1 \leq n \leq \ell$ with coefficients that are algebraic functions of the various k_s. We present expressions of b'_ℓ for $\ell = 3, 4$ and 5 below, from [36]:

$$b'_3 = b_3 + k_1 b_2 + (k_1^2 - k_2) b_1 \ , \tag{31}$$

$$b'_4 = b_4 + 2k_1 b_3 + k_1^2 b_2 + (-2k_1^3 + 4k_1 k_2 - 2k_3) b_1 \ . \tag{32}$$

$$\begin{aligned} b'_5 &= b_5 + 3k_1 b_4 + (2k_1^2 + k_2) b_3 + (-k_1^3 + 3k_1 k_2 - k_3) b_2 \\ &+ (4k_1^4 - 11 k_1^2 k_2 + 6k_1 k_3 + 4k_2^2 - 3k_4) b_1 \ . \end{aligned} \tag{33}$$

Given that the b_ℓ for $\ell \geq 3$ are scheme-dependent, one may ask whether it is possible to transform to a scheme in which the b'_ℓ are all zero for $\ell \geq 3$, i.e., a

scheme in which the two-loop β function is exact. Near the UV fixed point at $\alpha = 0$, this is possible, as emphasized by 't Hooft [49]. The resultant scheme, in which the beta function truncates at two-loop order is commonly called the 't Hooft scheme. Ref. [37] presented an explicit scheme transformation which, starting from an arbitrary scheme, transforms to the 't Hooft scheme. This necessarily has $s_{max} = \infty$. However, Refs. [37, 38] also noted that although this scheme transformation is acceptable in the vicinity of a zero of the beta function at $\alpha = 0$ (UV zero for an asymptotically free theory or IR zero for an infrared-free theory), it cannot, in general, be applied to a generic zero of the beta function (IR zero of an asymptotically free theory or UV zero of an infrared-free theory) away from $\alpha = 0$. Ref. [39] constructed and studied a one-parameter class of scheme transformations, denoted S_{R,m,k_1} having $s_{max} = m \geq 2$, with the property that an S_{R,m,k_1} scheme transformation eliminates the ℓ-loop terms in the beta function of a gauge theory from loop order $\ell = 3$ to order $\ell = m + 1$, inclusive. In Ref. [39], scheme transformations in this S_{R,m,k_1} family were applied to the higher-loop calculation of the infrared zero of the beta function of an asymptotically free gauge theory with multiple fermions and it was shown that they were acceptable over a reasonably large range of couplings.

In order to be physically acceptable, a scheme transformation must satisfy several conditions C_i, as was discussed in [37]. These are as follows:

1. C_1: the scheme transformation must map a real positive α to a real positive α'.

2. C_2: the scheme transformation should not map a moderate value of α, for which perturbation theory may be reliable, to a value of α' that is so large that perturbation theory is unreliable, or vice versa.

3. C_3: the Jacobian J should not vanish (or diverge) or else the transformation would be singular. Since $J = 1$ for $a = a' = 0$, a corollary of condition C_3 is that J must be positive.

4. C_4: since the existence of an IR zero of β is a scheme-independent property of theory, a scheme transformation must satisfy the condition that β_α has an IR zero if and only if $\beta_{\alpha'}$ has an IR zero.

Since one can define a transformation from α to α' and the inverse from α' to α, these conditions apply going in both directions. These four conditions

can always be satisfied by scheme transformations used to study the UV fixed point in an asymptotically free theory. However, as was pointed out in [36] and shown with a number of examples in [36]-[39], they are not automatically satisfied, and indeed, are quite restrictive conditions when one applies the scheme transformation at a zero of the beta function away from the origin, $\alpha = 0$, i.e., at an IR zero of the beta function for an asymptotically free theory or a UV zero of the beta function for an infrared-free theory. For example, recall the scheme transformation denoted $S_{\rm th_r}$ [36, 37], defined by

$$a = \frac{1}{r}\,\tanh(ra')\ , \tag{34}$$

depending on a parameter r. Since this transformation is an even function of r, one may take $r \geq 0$ without loss of generality. The $S_{\rm th_r}$ transformation is well-behaved near the UVFP at $a = a' = 0$ in an asymptotically free theory, but is not acceptable at a generic IR zero of the beta function. The reason is evident from its inverse,

$$a' = \frac{1}{2r}\,\ln\left[\frac{1+ra}{1-ra}\right] \tag{35}$$

As ra approaches 1 from below, $a' \to \infty$, and for $ra > 1$, a' is complex. Hence, this transformation violates conditions C_1, C_2, and C_4. For example, for $r = 4\pi$, this scheme transformation is

$$\alpha = \tanh\alpha' \tag{36}$$

and the inverse is

$$\alpha' = \frac{1}{2}\ln\left[\frac{1+\alpha}{1-\alpha}\right] \tag{37}$$

with the pathologies occurring as α approaches 1 from below. For $r = 8\pi$, the pathologies occur as α approaches the value 0.5 from below. As this example and the others analyzed in [36]-[39] show, the construction and application of a physically acceptable scheme transformation at a zero of the beta function away from the origin is considerably more difficult than at a zero of the beta function at the origin, as in scheme transformations used in QCD [50, 52, 54].

In the following, to avoid overly complicated notation, we will use the generic notation α' for the result of the application of each scheme transformation to an initial α, with it being understood that this refers to the specific transformation under consideration. Where it is necessary for clarification, we will use a subscript to identify the specific scheme S being discussed.

2 Construction and Application of Renormalization Scheme Transformation

In this section, we shall carry out explicit construction of renormalization scheme transformations that satisfy the four necessary conditions presented in Sec.1.4. Furthermore, taking the $\overline{\rm MS}$ scheme as our initial scheme, we shall apply some of the scheme transformations we construct in this section to compute $\alpha_{IR,zero,n\ell}$ $(2 \le \ell \le 4)$ in another schemes. As a result of this application, we will be able to measure the scheme dependence of an infrared zero of the β function in a quantitative manner. Our original research in this area has been published in collaboration with Prof. R. Shrock in the two papers [1, 2]. Related papers include [36]-[39].

As noted, Refs.[36, 37] observed that it is significantly more difficult to construct scheme transformations that can be applied away from the origin in coupling-constant space than it is to construct such transformations that are applicable in the vicinity of the origin (such as those used QCD calculations in the perturbative region, i.e., for small α_s). An example of this was given by the scheme transformation (34) above. This is well-behaved near zero coupling, $\alpha = \alpha' = 0$, where it approaches the identity transformation, but is unacceptable at a generic zero of the beta function. This is clear from the inverse transformation (35), which has a singularity as ra approaches 1 from below, i.e., as α approaches $4\pi/r$ from below, and yields a complex α' for $ra > 1$, i.e., for $\alpha > 4\pi/r$. For the illustrative value $r = 8\pi$, this unphysical behavior occurs at $\alpha = 0.5$. In other words, even though one might succeed in designing a scheme transformation that works very well for coupling near zero by satisfying the necessary four conditions presented in Sec.1.4, this does not guarantee the scheme transformation's validity for coupling away from the origin, which makes construction of the latter much more challenging and restrictive.

In this context, our construction and application of scheme transformations in this section are aimed at such scheme transformations that are applicable not only near the origin of coupling space, but also at a zero of β function away from the origin. We succeeded in devising this sort of scheme transformation in the papers [1, 2]. Let us consider a well-behaved (family of) scheme transformation(s) S_r where in this paragraph, r symbolizes a set of one or more parameters, such that S_0 is the identity. Since we are going to apply the scheme transformations to calculation of infrared zeros of β

function, it is worthwhile to make some remarks on the comparison between $\alpha_{IR,n\ell,S_{\{r\}}}$ and $\alpha_{IR,n\ell,\overline{\rm MS}}$. It follows that if one applies the transformation S_r to the $\overline{\rm MS}$ scheme, then, for a given loop order n,

$$\lim_{r\to 0} \alpha'_{IR,n\ell,S_r} = \alpha_{IR,n\ell,\overline{\rm MS}} \ . \tag{38}$$

Furthermore, since the IR zero in β_α approaches zero as N_f approaches $N_{f,b1z}$ from below, one has the formal result that, with N_f extended from a nonnegative integer variable to a nonnegative real variable,

$$\lim_{N_f \nearrow N_{f,b1z}} \alpha_{IR,n\ell,S_r} = \lim_{N_f \nearrow N_{f,b1z}} \alpha_{IR,n\ell,\overline{\rm MS}} = 0 \ . \tag{39}$$

Moreover, if the set of parameters $\{r\}$ specifying a general scheme transformation is such that this transformation is sufficiently close to the identity, then it preserves the relative order of the values of the IR zeros of the n-loop beta function. We recall that for fermions in the fundamental representation, in the $\overline{\rm MS}$ scheme, the three-loop and four-loop values of the IR zero, $\alpha_{IR,3\ell,\overline{\rm MS}}$ and $\alpha_{IR,4\ell,\overline{\rm MS}}$, are in the order, relative to the (scheme-independent) two-loop value, $\alpha_{IR,2\ell}$, given by Eq. (19).

In Sec.2.1, we construct and study scheme transformation denoted S_{L_r} which makes use of a logarithmic $f(a')$. In Sec.2.2, we construct and study a scheme transformation denoted S_{Q_r} based on a rational type of function $f(a')$. Finally, in Sec.2.3, we introduce an integral formalism for constructing scheme transformations. This method has some convenient features, as we will describe.

2.1 The S_{L_r} Scheme Transformation

Here we introduce and study a scheme transformation, denoted S_{L_r}, where L stands for logarithm and r for the parameter on which a transformation in this family depends [1]. This is thus actually a one-parameter family of scheme transformations. We show that the S_{L_r} scheme transformation satisfies the necessary conditions to be acceptable at a zero of the beta function away from the origin, for a reasonable range of $|r|$, and we then apply it to the calculation, at higher-loop order, of an IR zero of the beta function for an asymptotically free non-Abelian gauge theory. This calculation provides a measure of the scheme dependence of the value of this IR zero.

The S_{L_r} scheme transformation is defined as

$$S_{L_r}: \quad a = \frac{\ln(1+ra')}{r} \ , \tag{40}$$

where r is a (real) parameter. Writing Eq. (40) in the form of Eq. (20), the transformation function is

$$S_{L_r}: \quad f(a') = \frac{\ln(1+ra')}{ra'} \ . \tag{41}$$

This transformation function satisfies

$$\lim_{a' \to 0} f(a') = 1 \ , \tag{42}$$

in accordance with the requirement that $f(0) = 1$. Note also that

$$\lim_{r \to 0} f(a') = 1 \ , \tag{43}$$

where the limit may be taken through either positive or negative values of r. The scheme transformation (40) has the inverse

$$a' = \frac{e^{ra} - 1}{r} \ . \tag{44}$$

The Jacobian $J = da/da'$ is

$$J = \frac{1}{1+ra'} = e^{-ra} \ . \tag{45}$$

This Jacobian always satisfies condition C_3. The transformation function $f(a')$ has the Taylor series expansion

$$f(a') = 1 + \sum_{s=1}^{\infty} \frac{(-ra')^s}{s+1} \ , \tag{46}$$

so, in the notation of Eq. (22), the expansion coefficients are

$$k_s = \frac{(-r)^s}{s+1} \ . \tag{47}$$

Thus, for small $|r|a'$,

$$a = a' \Big[1 - \frac{ra'}{2} + O\Big((ra')^2\Big) \ \Big] \ . \tag{48}$$

It follows that with the application of the S_{L_r} scheme transformation,

$$S_{L_r} \quad : \qquad \begin{aligned} a' &> a \quad \text{if } r > 0 \\ a' &< a \quad \text{if } r < 0. \end{aligned} \tag{49}$$

The requirement that the right-hand side of Eq. (40) must be real implies that the argument of the log must be positive, which, in turn, yields the formal lower bound on this parameter

$$r > -\frac{1}{a'} \ . \tag{50}$$

This is also required by the condition C_3, that the Jacobian must be (finite and) positive. If $r > 0$, this inequality is obviously satisfied, since a and a' are positive. Let us then consider negative r. Substituting Eq. (44), the inequality (50) becomes $r > r/(1-e^{ra})$. Since we have restricted to negative r, this can be rewritten as $-|r| > -|r|/(1-e^{-|r|a})$, i.e., $1 < 1/(1-e^{-|r|a})$, which is always satisfied. Thus, r may be positive or negative, and the actual range of r is determined by the conditions C_1 and C_2, that given a value of $\alpha = 4\pi a$ for which perturbative calculations are reasonably reliable, the same should be true of $\alpha' = 4\pi a'$. This will be discussed further below.

Substituting the result (47) for k_s into the general expressions for the b'_ℓ from [37], we obtain

$$b'_3 = b_3 - \frac{r}{2}\, b_2 - \frac{r^2}{12}\, b_1 \ , \tag{51}$$

$$b'_4 = b_4 - r b_3 + \frac{r^2}{4}\, b_2 + \frac{r^3}{12}\, b_1 \ , \tag{52}$$

$$b'_5 = b_5 - \frac{3r}{4}\, b_4 + \frac{5r^2}{6}\, b_3 - \frac{r^3}{8}\, b_2 - \frac{13r^4}{180} b_1 \ , \tag{53}$$

$$b'_6 = b_6 - 2r b_5 + \frac{5r^2}{3}\, b_4 - \frac{2r^3}{3}\, b_3 + \frac{7r^4}{120}\, b_2 + \frac{11r^5}{180}\, b_1 \ , \tag{54}$$

and so forth for the b'_ℓ with $\ell \geq 7$.

We next apply this S_{L_r} scheme transformation to the β function in the $\overline{\rm MS}$ scheme. For $N_f \in I$, so the two-loop β function has an IR zero, we then calculate the resultant IR zero in $\beta_{\alpha'}$ at the three- and four-loop order. We have carried out these calculations with a range of values of N and r. For $N_f \in I$ and various values of r we list the results for $G = {\rm SU}(3)$ in Table 1

for the zero of the three-loop beta function and in Table 2 for the zero of the four-loop beta function. We denote the IR zero of $\beta_{\alpha'}$ at the n-loop level as $\alpha'_{IR,n\ell} \equiv \alpha'_{IR,n\ell,S_{L_r}}$, and, to save space in the tables we further shorten this to $\alpha'_{IR,n\ell,r}$. Here and below, for this SU(3) theory, the lower end of the interval I, namely $N = N_{f,b2z}$, is at $N = 8.05$ [51], so, for physical, integral values of N_f, it is $N_f = 9$. The lowest value we show in Table 1 and the later tables is $N_f = 10$, because for $N_f = 9$, $\alpha_{IR,2\ell}$ is too large for the perturbative methods that we use to be reliable. Our results for $N = 2,\ 4$, and other values are similar, so the $N = 3$, i.e., SU(3) results displayed in Tables 1 and 2 will be sufficient for our discussion here. The range of r for which we list results in these tables is $-3 \le r \le 3$. This range evidently satisfies the conditions C_1-C_4. However, if one were to increase the magnitude of $|r|$ to excessively large values, with either sign of r, this scheme transformation would violate conditions C_1 and C_2. For the SU(3) theory, taking the value $N_f = 12$ for illustration, as one increases r beyond the upper end of the range that we show, for the values $r = 4,\ 5,\ 6,\ 7$, one gets the four-loop result $\alpha_{IR,4\ell,S_{L_r}}$ equal to $0.529,\ 0.550,\ 0.578,\ 0.618$. However, for $r = 8$, the transformation yields a complex, unphysical result for $\alpha_{IR,4\ell,S_{L_r}}$. Similarly, for this $N_f = 12$ case, as one decreases r below the lowest negative value, $r = -3$, the solution for $\alpha_{IR,4\ell,S_{L_r}}$ decreases smoothly to 0.390 at $r = -10$, but becomes complex for $r = -11$. The resultant restriction on the range of the parameter r is generic. That is, as was discussed before in [36]-[39], in applying scheme transformations, one must necessarily restrict the form of the transformation so as to satisfy the conditions C_1-C_4.

We also observe the following additional general properties in our calculations of $\alpha'_{IR,n\ell,S_{L_r}}$. First, it follows from

$$\lim_{r\to 0} \alpha'_{IR,n\ell,S_r} = \alpha_{IR,n\ell,\overline{\rm MS}} \ . \tag{55}$$

together with the fact that Eq. (40) is a continuous transformation, that for small $|r|$, the relative order of the values of the n-loop IR zeros of $\beta_{\alpha'}$ in the transformed scheme are the same as those in the original $\overline{\rm MS}$ scheme, as given in (19). This is evident from the illustrative $N = 3$ results given in Tables 1 and 2. In accord with (39), the shifts of the value of the IR zero as a function of loop order are larger for smaller N_f and get smaller as N_f approaches $N_{f,b1z}$.

Second, for a given N, $N_f \in I$, loop order $n = 3$ or $n = 4$, and r values

Table 1: Values of the IR zero, $\alpha'_{IR,3\ell,S_{L_r}}$, of the three-loop beta function $\beta_{\alpha',3\ell}$ obtained by applying the S_{L_r} scheme transformation to the three-loop beta function in the $\overline{\rm MS}$ scheme, for an SU(3) gauge theory with N_f fermions in the fundamental representation. For compact notation, we set $\alpha'_{IR,3\ell,S_{L_r}} \equiv \alpha'_{IR,3\ell,r}$ in the table. For each N_f, we list these values as a function of r for r from $r = -3$ to $r = 3$ in steps of 1. For $r = 0$, $\alpha'_{IR,3\ell,S_{L_r}} = \alpha_{IR,3\ell,\overline{\rm MS}}$. For reference, we also list the (scheme-independent) IR zero of the beta function, $\alpha_{IR,2\ell}$.

N_f	$\alpha_{IR,2\ell}$	$\alpha'_{IR,3\ell,r=-3}$	$\alpha'_{IR,3\ell,r=-2}$	$\alpha'_{IR,3\ell,r=-1}$	$\alpha_{IR,3\ell,\overline{MS}}$	$\alpha'_{IR,3\ell,r=1}$	$\alpha'_{IR,3\ell,r=2}$	$\alpha'_{IR,3\ell,r=3}$
10	2.21	0.749	0.754	0.759	0.764	0.769	0.774	0.778
11	1.23	0.566	0.570	0.574	0.578	0.583	0.587	0.591
12	0.754	0.426	0.429	0.432	0.435	0.438	0.441	0.444
13	0.468	0.311	0.313	0.315	0.317	0.319	0.321	0.323
14	0.278	0.211	0.212	0.213	0.2145	0.216	0.217	0.218
15	0.143	0.122	0.122	0.123	0.123	0.124	0.124	0.125
16	0.0416	0.0396	0.0396	0.0397	0.0397	0.0398	0.0398	0.0399

for which the S_{L_r} transformation satisfies the conditions C_1-C_4,

$$\alpha'_{IR,n\ell,S_{L_r}} \quad \text{is an increasing function of } r. \tag{56}$$

This second property, in conjunction with the general property (55), implies that, for a given N, $N_f \in I$, and r,

$$\begin{aligned} &\alpha'_{IR,n\ell,S_{L_r}} > \alpha_{IR,n\ell,\overline{MS}} \quad \text{if } r > 0 \text{ and} \\ &\alpha'_{IR,n\ell,S_{L_r}} < \alpha_{IR,n\ell,\overline{MS}} \quad \text{if } r < 0 \ . \end{aligned} \tag{57}$$

This holds for arbitrary loop order n and, in particular, for the loop orders $n = 3$ and $n = 4$ for which we have done calculations using the known $\overline{\rm MS}$ beta function coefficients. The result (57) is evident in the illustrative $N = 3$ results given in Tables 1 and 2. In accord with (39), the shifts of the value of the IR zero as a function of $|r|$ become quite small as N_f approaches $N_{f,b1z}$ from below. In this region, these shifts in the position of the IR zero of the ℓ-loop beta function in the transformed scheme can be sufficiently small that the entries may coincide to the given number of significant figures displayed in the tables.

Table 2: Values of the IR zero, $\alpha'_{IR,4\ell,S_{L_r}}$, of the four-loop beta function $\beta_{\alpha',4\ell}$ obtained by applying the S_{L_r} scheme transformation to the four-loop beta function in the $\overline{\rm MS}$ scheme, for an SU(3) gauge theory with N_f fermions in the fundamental representation. For compact notation, we set $\alpha'_{IR,4\ell,S_{L_r}} \equiv \alpha'_{IR,4\ell,r}$ in the table. For each N_f, we list these values as a function of r for r from $r = -3$ to $r = 3$ in steps of 1. For $r = 0$, $\alpha'_{IR,4\ell,S_{L_r}} = \alpha_{IR,4\ell,\overline{\rm MS}}$. For reference, we also list the (scheme-independent) IR zero of the beta function, $\alpha_{IR,2\ell}$ and $\alpha_{IR,3\ell,\overline{\rm MS}}$.

N_f	$\alpha_{IR,2\ell}$	$\alpha_{IR,3\ell,\overline{\rm MS}}$	$\alpha'_{IR,4\ell,r=-3}$	$\alpha'_{IR,4\ell,r=-2}$	$\alpha'_{IR,4\ell,r=-1}$	$\alpha_{IR,4\ell,\overline{MS}}$	$\alpha'_{IR,4\ell,r=1}$	$\alpha'_{IR,4\ell,r=2}$	$\alpha'_{IR,4\ell,r=3}$
10	2.21	0.764	0.734	0.760	0.785	0.815	0.851	0.895	0.956
11	1.23	0.578	0.576	0.591	0.607	0.626	0.648	0.673	0.705
12	0.754	0.435	0.441	0.450	0.460	0.470	0.482	0.496	0.511
13	0.468	0.317	0.322	0.327	0.332	0.337	0.343	0.349	0.356
14	0.278	0.2145	0.217	0.219	0.221	0.224	0.226	0.228	0.231
15	0.143	0.123	0.124	0.124	0.125	0.126	0.126	0.127	0.128
16	0.0416	0.0397	0.0396	0.0397	0.0398	0.0398	0.0399	0.0400	0.0400

2.2 The Rational Scheme Transformation $S_{[p,q]}$

Here we discuss the construction and study of scheme transformations for which the function $f(a')$ a rational function of a', i.e.,

$$a = a' f(a')_{[p,q]} \tag{58}$$

where

$$S_{[p,q]}: \quad f(a')_{[p,q]} = \frac{N(a')}{D(a')} \ , \tag{59}$$

where the numerator and denominator functions $N(a')$ and $D(a')$ are polynomials of respective finite degrees p and q in a':

$$N(a') = \sum_{i=0}^{p} u_i \, (a')^i \quad \text{with } u_0 = 1 \tag{60}$$

and

$$D(a') = \sum_{j=0}^{q} v_j \, (a')^j \quad \text{with } v_0 = 1 \ . \tag{61}$$

This discussion follows Ref. [1]. The restrictions that $u_0 = v_0 = 1$ are imposed so that $f(a')$ satisfies the necessary condition that $f(0) = 1$. Thus, a general $S_{[p,q]}$ scheme transformation depends on the $p + q$ parameters u_i,

$i = 1, ..., p$ and v_j, $j = 1, ..., q$. As indicated, we label this class of scheme transformations as $S_{[p,q]}$, with the dependence on the coefficients u_i and v_j kept implicit. If $q = 0$, then this gives a Taylor series expansion (22) with $s_{max} = p$, while if $q \geq 1$, then $s_{max} = \infty$.

We note that, as one may recall from the theory of Padé approximants, for a given series expansion (22) calculated to a given finite order s_h, it is possible to construct a set of rational functions $f(a')$ of the form (59) whose Taylor series expansion coefficients match the given set k_s, $s = 1, ..., s_h$. Viewed the other way, if one starts with a set of rational functions of the form (59), one knows that certain subsets of these can be chosen to yield the same Taylor series expansion to a given order s_h.

The scheme transformation function $S_{[p,q]}$ introduces p zeros and q poles, so a necessary requirement is that one must choose the coefficients u_i with $i = 1, ..., p$ and v_j with $j = 1, ..., q$ such that the zeros and poles occur away from the relevant physical region in a. Obviously, scheme transformations with polynomial transformation functions $f(a')$ are special cases of $S_{[p,q]}$ with $q = 0$. Thus, the scheme transformation S_1 studied in [36, 37] and [39] is a special case of $S_{[p,q]}$ with $p = 1$ and $q = 0$; the S_2 and S_3 transformations in [36, 37, 38] are special cases of $S_{[p,q]}$ with $p = 2$ and $q = 0$, and the $S_{R,m}$ and S_{R,m,k_1} transformations studied in [38, 39] are special cases of $S_{[p,q]}$ with $p = m$ and $q = 0$. We proceed in the next section to study the simplest member of the class of $S_{[p,q]}$ scheme transformations with $q \neq 0$, namely one with $p = 0$ and $q = 1$.

2.2.1 The S_{Q_r} Scheme Transformation

In this section we introduce and apply a scheme transformation that we call S_{Q_r}, defined as $S_{[p,q]}$ with $p = 0$ and $q = 1$,

$$S_{Q_r} \equiv S_{[0,1]} \text{ with } v_1 = -r \ . \tag{62}$$

Thus, explicitly,

$$S_{Q_r}: \quad a = \frac{a'}{1 - ra'} \ , \tag{63}$$

where r is a (real) parameter, whose allowed range will be determined below. As before, we show this satisfies the necessary conditions to be acceptable at a zero of the beta function away from the origin for a reasonable range of $|r|$, and we then apply it to assess the scheme dependence of the IR zero in the

beta function of an asymptotically free non-Abelian gauge theory at higher loop order. The transformation function corresponding to (63) is

$$S_{Q_r}: \quad f(a') = \frac{1}{1 - ra'} \ . \tag{64}$$

Clearly, $f(a') = 1$ for $a' = 0$ and separately for $r = 0$. The inverse of Eq. (63) is

$$a' = \frac{a}{1 + ra} \ . \tag{65}$$

The Jacobian $J = da/da'$ is

$$J = \frac{1}{(1 - ra')^2} = (1 + ra)^2 \ . \tag{66}$$

The transformation function has the Taylor series expansion

$$f(a') = 1 + \sum_{s=1}^{\infty} (ra')^s \ , \tag{67}$$

so, in the notation of Eq. (22), the expansion coefficients are

$$k_s = r^s \ . \tag{68}$$

Thus, for small $|r|a'$,

$$a = a' \Big[\, 1 + ra' + O\Big((ra')^2\Big) \, \Big] \ . \tag{69}$$

It follows that after application of the S_{Q_r} scheme transformation,

$$\begin{aligned} S_{Q_r} \quad : \qquad & a' < a \quad \text{if } r > 0 \\ & a' > a \quad \text{if } r < 0 \ . \end{aligned} \tag{70}$$

The condition C_1 requires that the denominator of the right-hand side of Eqs. (65) be finite and positive, which implies that the (real) parameter r is bounded below according to

$$r > -\frac{1}{a} \ . \tag{71}$$

Clearly, in order for conditions C_1 and C_2 to be satisfied, r cannot be too close to saturating this lower bound. These conditions applied to the original

transformation (63) yield the formal inequality $r < 1/a'$. However, substituting (65), this becomes $r < a^{-1} + r$, which is always valid, since $a > 0$. Thus, the actual upper bound on r is determined by the conditions C_1 and C_2, that, given a value of α for which perturbative calculations are reasonably reliable, the same should be true of α'.

Inserting the result (68) for k_s into the general expressions for the b'_ℓ from [37], we obtain

$$b'_3 = b_3 + r b_2 \ , \tag{72}$$

$$b'_4 = b_4 + 2r b_3 + r^2 b_2 \ , \tag{73}$$

$$b'_5 = b_5 + 3r b_4 + 3r^2 b^3 + r^4 b_2 \ , \tag{74}$$

$$b'_6 = b_6 + 4r b_5 + 6r^2 b_4 + 4r^3 b_3 + r^4 b_2 \ , \tag{75}$$

and so forth for the b'_ℓ with $\ell \ge 7$. A general property of these beta function coefficients resulting from the application of the S_{Q_r} scheme transformation to an arbitrary initial scheme is that

$$S_{Q_r}: \quad b'_\ell \quad \text{is independent of} \quad b_1 \quad \text{for} \ \ell \ge 3 \ . \tag{76}$$

The reason for this can be seen as follows. The coefficient b'_ℓ with $\ell \ge 3$ resulting from the application of a scheme transformation is a linear combination of the b_n with $1 \le n \le \ell$. The structure of the coefficients multiplying these b_n, $1 \le n \le \ell$ was discussed in [36, 37]. In particular, the respective coefficients of b_1 in the expressions for b'_ℓ with $\ell \ge 3$ have the property that they vanish if $k_s = (k_1)^s$. This property is satisfied by the present S_{Q_r} scheme transformation, as is evident from Eq. (68). For example, in the expression (31) for b'_3, the coefficient of b_1 is $k_1^2 - k_2$, and in Eq. (32) for b'_4, the coefficient of b_1 is $-2k_1^3 + 4k_1 k_2 - 2k_3$, which vanish if $k_s = (k_1)^s$. Similar results hold for the b'_ℓ with higher values of ℓ that were calculated in [36]-[38].

We next apply this S_{Q_r} scheme transformation to the β function in the $\overline{\rm MS}$ scheme. We present results in Table 3 for the three-loop calculation and Table 4 for the four-loop calculation. The range of r that we use is $-3 \le r \le 3$. For the lowest two values of N_f, namely $N_f = 10$ and $N_f = 11$, and the lowest values of r, namely $r = -3$, although the $S_{Q,r}$ scheme transformations yields acceptable values of the three-loop zero, $\alpha'_{IR,3\ell,S_{Q_r}}$, it yields complex values of the four-loop zero, $\alpha'_{IR,4\ell,S_{Q_r}}$. To avoid these, one may restrict the lower range of r to, e.g., $r = -2$. The S_{Q_r} transformation obeys the conditions C_1 and C_2 for values of r somewhat beyond the upper end of the range that we

Table 3: Values of the IR zero, $\alpha'_{IR,3\ell,S_{Q_r}}$, of the three-loop beta function $\beta_{\alpha',3\ell}$ obtained by applying the S_{Q_r} scheme transformation to the three-loop beta function in the $\overline{\rm MS}$ scheme, for an SU(3) gauge theory with N_f fermions in the fundamental representation. For compact notation, we set $\alpha'_{IR,3\ell,S_{Q_r}} \equiv \alpha'_{IR,3\ell,r}$ in the table. For each N_f, we list these values as a function of r for r from $r = -3$ to $r = 3$ in steps of 1. For $r = 0$, $\alpha'_{IR,3\ell,S_{Q_r}} = \alpha_{IR,3\ell,\overline{\rm MS}}$. For reference, we also list the (scheme-independent) IR zero of the beta function, $\alpha_{IR,2\ell}$.

N_f	$\alpha_{IR,2\ell}$	$\alpha'_{IR,3\ell,r=-3}$	$\alpha'_{IR,3\ell,r=-2}$	$\alpha'_{IR,3\ell,r=-1}$	$\alpha_{IR,3\ell,\overline{MS}}$	$\alpha'_{IR,3\ell,r=1}$	$\alpha'_{IR,3\ell,r=2}$	$\alpha'_{IR,3\ell,r=3}$
10	2.21	0.795	0.785	0.774	0.764	0.755	0.746	0.737
11	1.23	0.605	0.596	0.587	0.5785	0.571	0.563	0.556
12	0.754	0.455	0.448	0.441	0.435	0.429	0.423	0.418
13	0.468	0.330	0.325	0.321	0.317	0.313	0.309	0.305
14	0.278	0.222	0.219	0.217	0.215	0.212	0.210	0.208
15	0.143	0.126	0.125	0.124	0.123	0.122	0.122	0.121
16	0.0416	0.0401	0.0400	0.0398	0.0397	0.0396	0.0395	0.0394

show, but eventually, if one were to use excessively large values of r, it would again fail to satisfy these.

We remark on some general features of the S_{Q_r} scheme transformation. As with the S_{L_r} transformation, it follows from (55) together with the fact that Eq. (63) is a continuous transformation, that for small $|r|$, the relative order of the values of the n-loop IR zeros of $\beta_{\alpha'}$ in the transformed scheme are the same as those in the original $\overline{\rm MS}$ scheme, as given in (19). This is evident in Table 3 and from Table 4. Second, for a given N, $N_f \in I$, and r, we find

$$\begin{aligned} &\alpha'_{IR,n\ell,S_{Q_r}} < \alpha_{IR,n\ell,\overline{MS}} \quad \text{if } r > 0 \text{ and} \\ &\alpha'_{IR,n\ell,S_{Q_r}} > \alpha_{IR,n\ell,\overline{MS}} \quad \text{if } r < 0 \quad \text{for } n = 3,\ 4\ . \end{aligned} \tag{77}$$

Third, for a given N, $N_f \in I$, and loop order $n = 3$ or $n = 4$,

$$\alpha'_{IR,n\ell,S_{Q_r}} \quad \text{is a decreasing function of } r. \tag{78}$$

2.2.2 $S_{[1,1]}$ Scheme Transformation

In this section we remark on some other $S_{[p,q]}$ scheme transformations with $q \neq 0$. We begin with $S_{[1,1]}$, This is defined by the $p = q = 1$ special case of

Table 4: Values of the IR zero, $\alpha'_{IR,4\ell,S_{Q_r}}$, of the four-loop beta function $\beta_{\alpha',4\ell}$ obtained by applying the S_{Q_r} scheme transformation to the four-loop beta function in the $\overline{\rm MS}$ scheme, for an SU(3) gauge theory with N_f fermions in the fundamental representation. For compact notation, we set $\alpha'_{IR,4\ell,S_{Q_r}} \equiv \alpha'_{IR,4\ell,r}$ in the table. For each N_f, we list these values as a function of r for r from $r = -3$ to $r = 3$ in steps of 1. For $r = 0$, $\alpha'_{IR,4\ell,S_{Q_r}} = \alpha_{IR,4\ell,\overline{\rm MS}}$. For reference, we also list the (scheme-independent) IR zero of the beta function, $\alpha_{IR,2\ell}$ and $\alpha_{IR,3\ell,\overline{\rm MS}}$. The notation $-$ means that the transformation yields an unphysical (here, complex) value for $\alpha'_{IR,4\ell,S_{Q_r}}$.

N_f	$\alpha_{IR,2\ell}$	$\alpha_{IR,3\ell,\overline{\rm MS}}$	$\alpha'_{IR,4\ell,r=-3}$	$\alpha'_{IR,4\ell,r=-2}$	$\alpha'_{IR,4\ell,r=-1}$	$\alpha_{IR,4\ell,\overline{MS}}$	$\alpha'_{IR,4\ell,r=1}$	$\alpha'_{IR,4\ell,r=2}$	$\alpha'_{IR,4\ell,r=3}$
10	2.21	0.764	–	1.062	0.896	0.815	0.760	0.719	0.685
11	1.23	0.578	–	0.750	0.674	0.626	0.591	0.563	0.540
12	0.754	0.435	0.581	0.530	0.496	0.470	0.450	0.433	0.418
13	0.468	0.317	0.380	0.363	0.349	0.337	0.327	0.318	0.309
14	0.278	0.2145	0.239	0.233	0.228	0.224	0.219	0.215	0.211
15	0.143	0.123	0.130	0.128	0.127	0.126	0.124	0.123	0.122
16	0.0416	0.0397	0.0402	0.0401	0.0400	0.0398	0.0397	0.0396	0.0395

(58), namely

$$S_{[1,1]}: \quad f(a') = \frac{1+u_1 a'}{1+v_1 a'} \ , \tag{79}$$

where u_1 and v_1 are (real) parameters. The inverse of Eq. (79) formally involves two solutions to a quadratic equation, but only one is physical because it is the only one for which $a' \to a$ as $(u_1, v_1) \to (0, 0)$. This inverse transformation is

$$a' = \frac{-1 + v_1 a + \sqrt{(1-v_1 a)^2 + 4u_1 a}}{2u_1} \ . \tag{80}$$

The Jacobian is

$$J = \frac{1 + 2u_1 a' + u_1 v_1 (a')^2}{(1+v_1 a')^2} \ . \tag{81}$$

The transformation function has a Taylor series expansion of the form (22) with

$$k_s = (u_1 - v_1)(-v_1)^{s-1} \ . \tag{82}$$

2.2.3 $S_{[1,2]}$ Scheme Transformation

The $S_{[1,2]}$ scheme transformation is the special case of (58) with $p = 1$ and $q = 2$, namely

$$S_{[1,2]}: \quad f(a') = \frac{1 + u_1 a'}{1 + v_1 a' + v_2 (a')^2} \ , \tag{83}$$

depending on the three (real) parameters u_1, v_1, and v_2. As with $S_{[1,1]}$, the inverse of (83) formally involves two solutions to a quadratic equation, but only one is physical because it is the only one for which $a' \to a$ as $(u_1, v_1, v_2) \to (0, 0, 0)$. This inverse transformation is

$$a' = \frac{-1 + v_1 a + \sqrt{(1 - v_1 a)^2 + 4a(u_1 - v_2 a)}}{2(u_1 - v_2 a)} \ . \tag{84}$$

The Jacobian is

$$J = \frac{1 + 2u_1 a' + (u_1 v_1 - v_2)(a')^2}{(1 + v_1 a' + v_2 (a')^2)^2} \tag{85}$$

The transformation function has a Taylor series expansion of the form (22), but with coefficients k_s that are more complicated than those for $S_{[0,1]}$ or $S_{[1,1]}$. The first few of these coefficients k_s are

$$k_1 = (u_1 - v_1) \ , \tag{86}$$

$$k_2 = -(u_1 - v_1) v_1 - v_2 \ , \tag{87}$$

$$k_3 = (u_1 - v_1) v_1^2 + (2v_1 - u_1) v_2 \ , \tag{88}$$

$$k_4 = -(u_1 - v_1) v_1^3 + (v_2 - 3v_1^2 + 2u_1 v_1) v_2 \ , \tag{89}$$

and so forth for higher s.

For sufficiently small $|u_1|$ and $|v_1|$, the $S_{[1,1]}$ scheme transformation obeys the conditions to be applicable at a (perturbatively calculated) IR zero of the beta function of an asymptotically free gauge theory. Similarly, for sufficiently small $|u_1|$, $|v_1|$, and $|v_2|$, the $S_{[1,2]}$ scheme also obeys these conditions. Because these scheme transformations involve two and three parameters, respectively, the analysis of the allowed ranges of these parameters is more complicated than the corresponding analyses given in [36, 38, 39] and for the one-parameter scheme transformations S_{L_r} and S_{Q_r} here.

One could also consider $S_{[p,q]}$ scheme transformations with higher (finite) values of p and/or q, but the inverses generically involve equations of cubic and higher degree, rendering the analytic calculations more cumbersome. We will thus not pursue these here.

2.3 Scheme Transformations from an Integral Formalism

Here we introduce and apply a general integral formalism for the construction of one-parameter families of scheme transformations. This work was published in Ref. [2]. In this formalism, the starting point is a choice of a Jacobian $J(y)$ that will be used as the integrand of an integral representation of the function $F(a')$ defined in Eq. (20):

$$a = F(a') = \int_0^{a'} J(y)\, dy \ . \tag{90}$$

We choose $J(y)$ to be an analytic function of y satisfying the condition

$$J(0) = 1 \ . \tag{91}$$

This guarantees that $J(a')$ and $f(a')$ have the respective Taylor series expansions (27) and (22) and hence that $f(a')$ satisfies the condition $f(0) = 1$. As discussed above, the condition C_3 for an acceptable scheme transformation is that the Jacobian must not vanish, since otherwise the transformation is singular. The property $J(0) = 1$ together with analyticity of J imply that J must be positive for the ranges of couplings a and a' that are relevant for perturbative calculations for which these scheme transformations are applicable. Thus, we require that $J(y) > 0$ throughout the range of the integration variable y in Eq. (90).

We can include dependence of the scheme transformation on a (real) auxiliary parameter, denoted r. Differentiating Eq. (90) and using a basic theorem from calculus yields the relation $dF(a')/da' = da/da' = J(a')$, in agreement with Eq. (26). Using an appropriate choice for the Jacobian $J(z)$, we can also satisfy conditions C_1-C_4.

In addition to these general conditions for the acceptability of a scheme transformation, another important aspect of the analysis is the ease of inverting the transformation to solve for a' from a. As was evident in Refs. [37]-[39], for algebraic scheme transformations with finite values of s_{max} in Eq. (22), the inversion required the solution of an algebraic equation and a choice of which root to take for this solution. In contrast, for cases of algebraic or transcendental scheme transformations with $s_{max} = \infty$, the inverse transformations were often simpler, in the sense that one did not have to make such a choice of which root of an algebraic equation to take.

To show the usefulness of this integral formalism for the construction of acceptable scheme transformations, we give some examples. We first illustrate how the method works with some scheme transformations that have already been studied in [1, 36, 37], which are acceptable for the analysis of a zero in a beta function located away from the origin in coupling constant space, in particular, an IR zero of the beta function of an asymptotically free non-Abelian gauge theory. Let us consider, for example, the scheme transformation

$$a \equiv F(a') = \frac{1}{r} \sinh(ra') \tag{92}$$

that was presented in [37] and applied there to study the dependence of the location of an IR zero in the beta function of an asymptotically free SU(N) gauge theory on the scheme. This is an example of a class of one-parameter families of scheme transformations that are invariant under reversal in sign of the auxiliary parameter r. Hence, for such transformations, we can, without loss of generality, take this parameter r to be nonnegative, and, as in [37], we shall do so. This scheme transformation has the inverse

$$a' = \frac{1}{r} \ln \left[ra + \sqrt{1 + (ra)^2} \, \right] \tag{93}$$

and the Jacobian

$$J = \frac{da}{da'} = \cosh(ra') = \sqrt{1 + (ra)^2} \ . \tag{94}$$

As was shown in [37], this transformation satisfies all of the conditions C_1-C_4. To show how one could use our present integral formalism to construct this scheme transformation, we start with J and replace the variable a' by the integration variable y to get $J(y) = \cosh(ry)$. Substituting this function into Eq. (90), we obtain

$$a = F(a') = \int_0^{a'} \cosh(ry) \, dy = \frac{1}{r} \sinh(ra') \ , \tag{95}$$

thereby rederiving the transformation (92).

Another example is provided by one of the scheme transformations that we studied in [1], namely

$$a = \frac{1}{r} \ln(1 + ra') \tag{96}$$

with inverse

$$a' = \frac{e^{ra} - 1}{r} \ . \tag{97}$$

The Jacobian is

$$J = \frac{1}{1 + ra'} = e^{-ra} \ . \tag{98}$$

Again replacing the variable a' by y to get $J(y) = 1/(1 + ry)$ and then substituting this into Eq. (90), we reproduce the original transformation:

$$a = F(a') = \int_0^{a'} \frac{dy}{1 + ry} = \frac{1}{r} \ln(1 + ra') \ . \tag{99}$$

Here, as we discussed in [1], the parameter r is restricted to lie in the range $r > -1/a'$ to avoid a singularity in the transformation and is further restricted by the condition that the scheme transformation satisfies conditions C_1-C_4.

2.3.1 Transformation with an Algebraic $J(y)$

We next proceed to present new scheme transformations that we have constructed using our integral formalism [2]. Recall that the starting point for the procedure is a choice of the Jacobian function $J(y)$ that serves as the integrand in Eq. (90) and that satisfies the requisite conditions that it is analytic and that $J(0) = 1$. For our first new transformation, we choose a $J(y)$ of algebraic form, namely

$$J(y) = (1 + ry)^p \ , \tag{100}$$

where the power p is a positive real number. Then, calculating the integral in Eq. (90), we obtain the scheme transformation

$$a = F(a') = \frac{(1 + ra')^{p+1} - 1}{r(p + 1)} \ . \tag{101}$$

The resultant series expansion for $f(a') = F(a')/a'$ has the form of Eq. (22) with

$$k_s = \frac{r^s}{(s + 1)} \binom{p}{s} = \frac{r^s}{(s + 1)!} \prod_{\ell=0}^{s-1} (p - \ell) \ , \tag{102}$$

where $\binom{a}{b} = a!/[b!(a - b)!]$ is the binomial coefficient. This is a finite series if p is an integer, and an infinite series otherwise. We list the coefficients k_s

explicitly for the first few values of s for this scheme transformation and for others discussed in this paper in Table 5. The series (102) has $s_{min} = 1$ and

$$k_{s_{min}} = k_1 = \frac{p\,r}{2} \ . \tag{103}$$

The inverse transformation is

$$a' = \frac{1}{r}\Big[\Big\{(p+1)ra + 1\Big\}^{\frac{1}{p+1}} - 1\Big] \ . \tag{104}$$

Using this inverse transformation, one can express the Jacobian equivalently as a function of a':

$$J = (1 + ra')^p = \Big[(p+1)ra + 1\Big]^{\frac{p}{p+1}} \ . \tag{105}$$

There are two immediate restrictions on the parameter r arising from the requirement that $J > 0$ and that there not be any singularity in the scheme transformation (101), namely

$$r > -\frac{1}{a'} \quad \text{and} \quad r > -\frac{1}{(p+1)a} \ . \tag{106}$$

These restrictions are easily met, for example, by requiring that r be non-negative. Moreover, the interval in the couplings α where one could use perturbative calculations reliably only extends up to values $\alpha \sim O(1)$, and since $a = \alpha/(4\pi)$, this interval only extends up to $a \sim O(0.1)$, so for moderate p, the lower bounds (106) evaluate to $r \geq -O(10)$. This lower bound can easily be satisfied even with moderate negative values of r. With the restrictions (106) satisfied, the scheme transformation (101) satisfies the conditions C_1-C_4. If $r > 0$, then since $k_{s_{min}} > 0$ (where $s_{min} = 1$ here), it follows from our general result (25) above that $a > a'$ for small $a,\ a'$. If r is negative (in the range allowed by above restrictions) then $k_1 < 0$, so $a < a'$ for small $a,\ a'$.

2.3.2 Transformation with a Transcendental $J(y)$

For an application of our integral formalism using a Jacobian that is a transcendental function, we choose

$$J(y) = 1 + \tanh(ry) \ . \tag{107}$$

Then, doing the integral in Eq. (90), we obtain

$$a = F(a') = a' + \frac{1}{r} \ln \Big[\cosh(ra') \Big] \ . \tag{108}$$

The resultant series expansion for $f(a') = F(a')/a'$ has the form of Eq. (22) with $k_s = 0$ for s even and

$$k_1 = \frac{r}{2}, \quad k_3 = -\frac{r^3}{12}, \quad k_5 = \frac{r^5}{45}, \quad k_7 = -\frac{17r^7}{2520} \ , \tag{109}$$

etc. for higher values of s. For comparative purposes, we list these k_s for s up to 4 in Table 5. The Jacobian of this transformation, expressed as a function of a', is given by Eq. (107) with $y = a'$. The inverse of the scheme transformation has a simple form for certain values of r. For example, for $r = 1$, the inverse is

$$a' = \frac{1}{2} \ln(2e^a - 1) \ . \tag{110}$$

Using Eq. (110), one can also express J as a function of a for this $r = 1$ case, obtaining $J = 2 - e^{-a}$.

The allowed range of the parameter r is determined by the requirement that the scheme transformation must satisfy the conditions C_1-C_4. If $r > 0$, then, since $k_{s_{min}} > 0$ (where $s_{min} = 1$ here), it follows that $a > a'$ for small $a,\ a'$, while if $r < 0$, then $k_1 < 0$, so $a < a'$ for small $a,\ a'$.

2.3.3 Scheme Transformations for which $J(y) = (d/dy) \ln h(y)$

One requirement for the general integral formalism that we have presented above to be useful is one should be able to do the integral (90). It is therefore helpful to consider a class of Jacobian functions for which one is guaranteed to be able to calculate the the integral (90). Clearly, if $J(y)$ is the derivative of another function, then one can always do this integral. In this section we present one such class of Jacobian functions [2]. These are functions that can be expressed as logarithmic derivatives (LDs) of smooth functions denoted $h(y)$:

$$J(y) = \frac{d}{dy} \ln h(y) = \frac{h'(y)}{h(y)} \ . \tag{111}$$

where $h'(y) \equiv dh(y)/dy$. To obtain acceptable scheme transformation functions, we require that $h(y)$ is positive for physical (nonnegative) values of the argument y and that

$$h(0) = h'(0) \ . \tag{112}$$

The equality (112) guarantees that the present construction satisfies the condition (91) that $J(0) = 1$ and, as will be shown below, that it also satisfies the condition (21) that $f(0) = 1$. With $J(y)$ as specified in Eq. (111), we can perform the integral (90) immediately, obtaining the transformation function

$$a = F(a') = \int_0^{a'} \frac{h'(y)}{h(y)}\, dy = \ln\Big[\frac{h(a')}{h(0)}\Big] \ . \tag{113}$$

This shows why we required that $h(y)$ be positive for physical values of y, since otherwise $h(0)$ and/or $h(a')$ might vanish, rendering the logarithm singular. Since only the ratio $h(a')/h(0)$ enters in $F(a')$, it follows that $F(a')$ is invariant under a rescaling of $h(y)$. Consequently, we can, without loss of generality, normalize $h(y)$ so that $h(0) = 1$, and we shall do this. Combining this with Eq. (112), we have

$$h(0) = h'(0) = 1 \ , \tag{114}$$

and combining Eq. (114) with Eq. (113), we obtain

$$F(a') = \ln[h(a')] \ . \tag{115}$$

To prove that this construction satisfies the condition $f(0) = 1$, we use the definition (20) together with the analyticity of $h(a')$ at $a' = 0$. We write out the Taylor series expansion for $h(a')$ at the origin and use the property (112) that we have imposed:

$$h(a') = 1 + a' + \frac{1}{2!}\, h''(0)\, (a')^2 + ... \tag{116}$$

where here and below, the dots ... denote higher powers of a'. Therefore,

$$\begin{aligned} f(0) &= \lim_{a'\to 0} \frac{F(a')}{a'} \\ &= \lim_{a'\to 0} \frac{1}{a'} \ln\Big[1 + a' + \frac{1}{2}\, h''(0)\, (a')^2 + ...\Big] \\ &= 1 \ . \end{aligned} \tag{117}$$

Secondly, as noted above, this construction satisfies the condition $J(0) = 1$. Since $a = F(a')$ by Eq. (20), Eq. (115) is equivalent to $e^a = h(a')$, so the inverse transformation is given formally as

$$a' = h^{-1}(e^a) \ , \tag{118}$$

where h^{-1} denotes the inverse of the function h. We have found several cases where this inverse can be calculated explicitly present some of these explicit examples below.

Our first example of a function h to be used in Eq. (111) and (113) is

$$h(y) = 1 + \frac{1}{r}\ln(1+ry) \ . \tag{119}$$

Hence, $h'(y) = 1/(1+ry)$. By construction, this satisfies the condition that both $h(y)$ and $h'(y)$ are positive functions for physical (i.e., nonnegative) y and the condition that $h(0) = h'(0)$. Here, $h(0) = h'(0) = 1$. From (113), we have

$$a = F(a') = \ln\Big[1 + \frac{1}{r}\ln(1+ra')\Big] \ . \tag{120}$$

We remark that for the families of scheme transformations studied so far in [36, 37, 39] that are dependent on an auxiliary parameter r, such as $a = (1/r)\sinh(ra')$ and the transformations studied in [1] such as $a = (1/r)\ln(1+ra')$ and $a = a'/(1-ra')$, setting $r = 0$ yields the identity transformation $a = F(a') = a'$. However, this is not the case for the transformation of Eq. (120). Instead, setting $r = 0$ in (120) yields the scheme transformation

$$r = 0 \quad \Longrightarrow \quad a = F(a') = \ln(1+a') \ . \tag{121}$$

This property also holds for the transformations (127) and (131) discussed below. As is necessary, Eq. (121) obeys the requirement (21) that $f(0) = 1$, i.e., that the transformation becomes an identity $a = a'$ in the free-field limit $a \to 0$.

The resultant series expansion for $f(a') = F(a')/a'$ has the form of Eq. (22) with the k_s coefficients displayed in Table 5. In the special case $r = 0$, the coefficients k_s are given by the Taylor series expansion of $(1/a')\ln(1+a')$ around $a' = 0$, namely

$$r = 0 \quad \Longrightarrow \ k_s = \frac{(-1)^s}{s+1} \ . \tag{122}$$

The inverse transformation is

$$a' = \frac{1}{r}\Big[\exp[r(e^a - 1)] - 1\Big] \ . \tag{123}$$

For the Jacobian, expressed in terms of a' and a, we calculate

$$\begin{aligned} J &= \frac{1}{(1+ra')\Big[1+\frac{1}{r}\ln(1+ra')\Big]} \\ &= \exp[-a-r(e^a-1)] \ . \end{aligned} \tag{124}$$

The parameter r is restricted to the range

$$r > -\frac{1}{a'} \tag{125}$$

in order to avoid singularities in $h(y)$ and $F(a')$ and is further restricted by the requirement that this scheme transformation must satisfy the conditions C_1-C_4. These conditions can be satisfied for small positive r. With r positive (indeed with $r > -1$), $k_{s_{min}} < 0$ (where $s_{min} = 1$ here), so our general result (25) implies that $a < a'$ for small $a,\ a'$.

Next, a second example is provided by the function

$$h(y) = 1 + \frac{1}{r}\sinh(ry) \ . \tag{126}$$

Then $h'(y) = \cosh(ry)$. Without loss of generality, the parameter r can be taken to be nonnegative, and we shall do this. Evidently, this function $h(y)$ satisfies the condition (114). From the general result (113), we obtain

$$a = F(a') = \ln\Big[1 + \frac{1}{r}\sinh(ra')\Big] \ . \tag{127}$$

The resultant series expansion for $f(a') = F(a')/a'$ has the form of Eq. (22), and we list the first few coefficients k_s in Table 5. The invariance of the transformation $F(a')$ in Eq. (127) under the reversal in sign of the auxiliary parameter r is reflected in the property that the k_s involve only even powers of r. Here $s_{min} = 1$ and $k_{s_{min}} < 0$, so by our general result (25), it follows that $a < a'$ for small $a,\ a'$.

The inverse transformation is

$$a' = \frac{1}{r}\ln\Big[r(e^a-1) + \sqrt{1+[r(e^a-1)]^2}\ \Big] \ . \tag{128}$$

for the Jacobian we calculate

$$J = \frac{\cosh(ra')}{1+\frac{1}{r}\sinh(ra')} \ . \tag{129}$$

This transformation satisfies all of the conditions C_1-C_4.

Lastly we discuss a third function h for use in Eq. (111) and (113), namely

$$h(y) = 1 + \frac{1}{r}\tanh(ry) \ . \tag{130}$$

Thus, $h'(y) = 1/\cosh^2(ry)$. This satisfies the condition (114). As with the previous $h(y)$ function in Eq. (126), we can, without loss of generality, take the parameter r to be nonnegative, and we shall do this. From the general result (113), we obtain

$$a = F(a') = \ln\Big[1 + \frac{1}{r}\tanh(ra')\Big] \ . \tag{131}$$

The resultant series expansion for $f(a') = F(a')/a'$ has the form of Eq. (22) with the first few k_s coefficients listed in Table 5.

The inverse transformation is

$$a' = \frac{1}{2r}\ \ln\left[\frac{1 + r(e^a - 1)}{1 - r(e^a - 1)}\right] \ . \tag{132}$$

The Jacobian, expressed as a function of a' and of a, is

$$\begin{aligned} J(a') &= \frac{1}{\cosh^2(ra')\left[1 + \frac{1}{r}\tanh(ra')\right]} \\ &= e^{-a}\Big[1 + r(e^a - 1)\Big]\Big[1 - r(e^a - 1)\Big] \ . \end{aligned} \tag{133}$$

Although the transformation in Eq. (131) and the Jacobian in Eq. (133) are nonsingular for any r, the inverse transformation (132) does contain a singularity which restricts the range of r. This singularity occurs at $r = \pm 1/(e^a - 1)$. Recalling that, without loss of generality, r has been taken to be nonnegative, we restrict r to be substantially less than $1/(e^a - 1)$ to avoid the singularity in the inverse transformation.

2.3.4 Scheme Transformations for which $J(y) = (d/dy)e^{\phi(y)}$

Here we present another class of $J(y)$ functions that can be used in conjunction with our integral formalism to construct scheme transformations [2]. As was true of the functions in Section 2.3.3, these function have the form of

total derivatives, which guarantees that one can do the integral (90). We begin with an analytic function $\phi(y)$ that satisfies the conditions

$$\phi(0) = 0, \quad \phi'(0) = 1 \ . \tag{134}$$

We then set $J(y)$ equal to the derivative of the exponential of this function:

$$J(y) = \frac{d}{dy}\, e^{\phi(y)} = \phi'(y) e^{\phi(y)} \ . \tag{135}$$

Substituting this into the integral (90), we obtain

$$a = F(a') = e^{\phi(a')} - e^{\phi(0)} = e^{\phi(a')} - 1 \ . \tag{136}$$

This yields $J(a') = dF(a')/da' = \phi'(a') e^{\phi(a')}$ so that, taking into account the property (134), it follows that $J(0) = 1$. Furthermore, this construction guarantees that the condition $f(0) = 1$ in Eq. (21) is satisfied. To prove this, we use the defining relation $a = a' f(a') = F(a')$ in Eq. (20) to obtain

$$f(a') = \frac{e^{\phi(a')} - 1}{a'} \ . \tag{137}$$

Expanding the numerator in a Taylor series around $a' = 0$, we get

$$\begin{aligned} f(a') &= \frac{1}{a'}\Big[e^{\phi(0)} - 1 + \phi'(0) a' + O((a')^2)\Big] \\ &= 1 + O(a') \ , \end{aligned} \tag{138}$$

from which it follows that $f(0) = 1$. The inverse is, formally,

$$a' = \phi^{-1}[\ln(a+1)] \ , \tag{139}$$

where here ϕ^{-1} denotes the function that is the inverse of ϕ. We have found several cases where this inverse can be calculated explicitly present some of these explicit examples below.

As a first example of this type of construction, we take

$$\phi(y) = \frac{1}{r}(e^{ry} - 1) \ . \tag{140}$$

This function satisfies the condition (134). Substituting the resultant $J(y) = e^{ry} \exp[(1/r)(e^{ry} - 1)]$ into Eq. (90), we obtain the scheme transformation

$$a = F(a') = \exp\left[\frac{1}{r}(e^{ra'} - 1)\right] - 1 \ . \tag{141}$$

The resultant series expansion for $f(a') = F(a')/a'$ has the form of Eq. (22) with the first few k_s coefficients listed in Table 5. Note that in the limit as $r \to 0$, the scheme transformation (141) becomes

$$r = 0 \quad \Longrightarrow \quad a = F(a') = e^{a'} - 1 \ . \tag{142}$$

Hence, in this limit the coefficients are given by

$$r = 0 \quad \Longrightarrow \quad k_s = \frac{1}{s!} \ . \tag{143}$$

These results also hold for the transformation (147) to be discussed below.

The inverse transformation is

$$a' = \frac{1}{r} \ln\left[1 + r \ln(a+1)\right] \ . \tag{144}$$

Using this, we may express the Jacobian in terms of a:

$$\begin{aligned} J &= e^{ra'} \exp\left[\frac{1}{r}(e^{ra'} - 1)\right] \\ &= (a+1)[1 + r \ln(a+1)] \ . \end{aligned} \tag{145}$$

This transformation satisfies conditions C_1-C_4.

In the second place, we use

$$\phi(y) = \frac{1}{r} \sinh(ry) \ . \tag{146}$$

As before, without loss of generality, we take the auxiliary parameter r to be nonnegative. This function satisfies the condition (134). Substituting the resultant $J(y) = (d/dy)\, e^{(1/r)\sinh(ry)}$ into Eq. (90), we obtain the scheme transformation

$$a = F(a') = e^{(1/r)\sinh(ra')} - 1 \ . \tag{147}$$

The resultant series expansion for $f(a') = F(a')/a'$ has the form of Eq. (22) with the k_s coefficients listed in Table 5. Because $k_{s_{min}} > 0$ (where $s_{min} = 1$ here), our general result (25) implies that $a > a'$ for small $a,\ a'$.

The inverse transformation is

$$a' = \frac{1}{r} \ln \left[r \ln(a+1) + \sqrt{1 + [r \ln(a+1)]^2} \, \right] . \tag{148}$$

The Jacobian is

$$J = \cosh(ra') \, e^{(1/r) \sinh(ra')} . \tag{149}$$

This transformation satisfies conditions C_1-C_4.

Table 5: Values of the coefficients k_s in Eq. (22) for scheme transformations discussed in the text. The transformation $F(a')$ is defined by Eq. (20): $a = a' f(a') = F(a')$.

$F(a')$	k_1	k_2	k_3	k_4
$(1/r)\sinh(ra')$	0	$r^2/6$	0	$r^4/120$
$(1/r)\tanh(ra')$	0	$-r^2/3$	0	$2r^4/15$
$(1/r)\ln(1+ra')$	$-r/2$	$r^2/3$	$-r^3/4$	$r^4/5$
$a'/(1-ra')$	r	r^2	r^3	r^4
$\frac{(1+ra')^{p+1}-1}{r(p+1)}$	$\frac{r}{2}\,p$	$\frac{r^2}{3}\binom{p}{2}$	$\frac{r^3}{4}\binom{p}{3}$	$\frac{r^4}{5}\binom{p}{4}$
$\ln[1+(1/r)(a+ra')]$	$-(r+1)/2$	$(2r^2+3r+2)/6$	$-(6r^3+11r^2+12r+6)/24$	$(12r^4+25r^3+35r^2+30r+12)/60$
$a'+(1/r)\ln[1+\cosh(ra')]$	$(1/2)r$	0	$-(1/12)r^3$	0
$\ln[1+(1/r)\sinh(ra')]$	$-1/2$	$(r^2+2)/6$	$-(2r^2+3)/12$	$(r^4+20r^2+24)/120$
$\ln[1+(1/r)\tanh(ra')]$	$-1/2$	$(1-r^2)/3$	$(4r^2-3)/12$	$(r^2-1)(2r^2-3)/15$
$\exp[(1/r)(e^{ra'}-1)]-1$	$(r+1)/2$	$(r^2+3r+1)/6$	$(r^3+7r^2+6r+1)/24$	$(r^4+15r^3+25r^2+10r+1)/120$
$\exp[(1/r)\sinh(ra')]-1$	$1/2$	$(r^2+1)/6$	$(4r^2+1)/24$	$(r^4+10r^2+1)/120$

3 Renormalization-Group Evolution of $\mathcal{N} = 1$ Supersymmetric Gauge Theories

It is of considerable interest to study scheme-dependence in supersymmetric gauge theories. In this section we shall discuss our use of Padé methods to study the beta function of vectorial, asymptotically free, $\mathcal{N} = 1$ supersymmetric SU(N_c) gauge theories. This work was published with Prof. R. Shrock in Ref. [3]. We investigate both the purely gluonic supersymmetric Yang-Mills (SYM) gauge theory and theories with matter content consisting of N_f copies of massless chiral superfields Φ_i and $\tilde{\Phi}_i$, $i = 1, ..., N_f$, which transform according to the respective representations R and $\bar{R}$ of SU(N_c). We consider the cases where R is the fundamental representation and where R is the symmetric and antisymmetric rank-2 tensor representation of SU(N_c).

In our analysis, we will make use of the closed-form calculation of β_α by Novikov, Shifman, Vainshtein, and Zakharov (NSVZ) in [55] (see also [56]), denoted $\beta_{\alpha,NSVZ}$, which is written in a closed form within the scheme used for its calculation (called the NSVZ scheme). This beta function exhibits a pole at a certain value of the coupling [55, 56, 57] (see Eq. (162) below). Furthermore, we will make use of a number of exact results that have been obtained using effective holomorphic action methods concerning the infrared properties of this theory [58, 59]. The beta function of an $\mathcal{N} = 1$ supersymmetric gauge theory with general chiral superfield matter content has been calculated up to three-loop order [60, 62], and, for the pure gluonic SYM theory, up to four-loop order [63] in the dimensional reduction scheme with minimal subtraction [64], denoted $\overline{\rm DR}$. Using these results, we calculate Padé approximants to the beta function of the pure gluonic SYM theory up to four-loop order and to the beta functions of the theories with chiral superfields in the fundamental and rank-2 tensor representations up to three-loop order. The theories with sufficiently large matter superfield content have a perturbative IR zero in the beta function. Previously, Refs. [33] by Profs. T. Ryttov and R. Shrock, and Refs. [31]-[32] by Shrock, presented calculations of properties of the beta function, including an IR zero, from the two and three-loop beta function. In the present work we extend these studies in several ways. Using our calculation of Padé approximants for the SYM theory and for theories with various matter superfield content, we address and answer several questions:

1. How the value of the IR zero in the Padé approximants compares with

the IR zero in the $\overline{\rm DR}$ and NSVZ beta functions, for cases where such an IR zero is present.

2. Whether these Padé approximants to the $\overline{\rm DR}$ beta function exhibit a robust indication of a pole, as in the NSVZ beta function.

3. If the answer to question (ii) is affirmative, whether this pole occurs at a value of α near to the value in the NSVZ beta function and, moreover, closer to the origin than an IR zero (if the latter is present) and hence dominates the UV to IR evolution.

Our calculations and analysis provide a quantitative measure, for these various supersymmetric theories, of how well finite-order perturbative results calculated in the $\overline{\rm DR}$ scheme reproduce the properties of the NSVZ beta function. Some related work is in Refs. [65]-[70]. A different approach is to calculate scheme-independent series expansions for physical quantities [42, 47].

This section is organized as follows. In Sec.3.1 we discuss the beta function and exact results on the properties of the theory. In Sect.3.2 we calculate and analyze Padé approximants for the pure gluonic supersymmetric Yang-Mills theory. Sec.3.3 is devoted to the corresponding calculation and analysis of Padé approximants for the theory with chiral superfields in the fundamental and conjugate fundamental representation. In Sec.3.4. we investigate the theory with chiral superfields in the rank-2 tensor and conjugate tensor representations.

3.1 Beta Function and Exact Results

3.1.1 Beta Function

In this section we review some basic results on the beta function and also some exact results that we will use for our analysis. The beta function has a series expansion of the form given above in (13). The first two coefficients in the expansion (13), which are scheme-independent [60], are [61]

$$b_1 = 3C_A - 2T_f N_f \tag{150}$$

and

$$b_2 = 6C_A^2 - 4(C_A + 2C_f)T_f N_f \ . \tag{151}$$

In the commonly used $\overline{\rm DR}$ scheme, the three-loop coefficient is [62]

$$\begin{aligned} b_3 &= 21C_A^3 + 4(-5C_A^2 - 13C_AC_f + 4C_f^2)T_fN_f \\ &+ 4(C_A + 6C_f)(T_fN_f)^2 \ . \end{aligned} \tag{152}$$

For pure $\mathcal{N} = 1$ supersymmetric Yang-Mills theory (with no matter chiral superfields, i.e., $N_f = 0$), the four-loop coefficient, b_4, has also been calculated [63] and will be used in our analysis of this SYM theory below.

If $N_f = 0$, then $b_1 > 0$; as N_f increases from zero, b_1 decreases monotonically and passes through zero, reversing sign, at the value $N_f = N_{f,b1z}$, where [51]

$$N_{f,b1z} = \frac{3C_A}{2T_f} \tag{153}$$

(and the subscript $b1z$ stands for "b_1 zero"). If N_c and R are such that $N_{f,b1z}$ is an integer and if $N_f = N_{f,b1z}$, so that $b_1 = 0$, then b_2 has the negative value $-12C_AC_f$. Hence, the requirement of asymptotic freedom, which means $\beta < 0$ near the origin, is true (given the minus sign that we have extracted in Eq. (13)) if and only if $b_1 > 0$. Therefore, we restrict to

$$N_f < N_{f,b1z} \ . \tag{154}$$

Similarly, for $N_f = 0$, $b_2 > 0$, and as N_f increases from zero, b_2 decreases monotonically and passes through zero, reversing sign, at the value $N_f = N_{f,b2z}$, where

$$N_{f,b2z} = \frac{3C_A^2}{2T_f(C_A + 2C_f)} \ . \tag{155}$$

For an arbitrary fermion representation R, $N_{f,b2z} < N_{f,b1z}$, so there is always an interval I in N_f where $b_1 > 0$ and $b_2 < 0$. This interval is $N_{f,b2z} < N_f < N_{f,b1z}$, i.e.,

$$I: \quad \frac{3C_A^2}{2T_f(C_A + 2C_f)} < N_f < \frac{3C_A}{2T_f} \ . \tag{156}$$

For $N_f \in I$, the two-loop (2ℓ) beta function has an IR zero at

$$\begin{aligned} \alpha_{IR,2\ell} &= -\frac{\bar{b}_1}{\bar{b}_2} = -\frac{4\pi b_1}{b_2} \\ &= \frac{2\pi(3C_A - 2T_fN_f)}{2(C_A + 2C_f)T_fN_f - 3C_A^2} \ . \end{aligned} \tag{157}$$

Clearly, if N_f is too close to $N_{f,b2z}$, then b_2 is sufficiently small that $\alpha_{IR,2\ell}$ is too large for this perturbative two-loop result to be reliable. As noted, the two-loop beta function encodes the maximal scheme-independent perturbative information about the theory.

Given that $N_f \in I$ and that $\alpha_{IR,2\ell}$ is sufficiently small for the perturbative analysis of the beta function to be reasonable, a natural next step in the analysis of the UV to IR evolution of the theory is to examine the three-loop beta function. The three-loop beta function has two zeros away from the origin, given by the equation $b_1 + b_2 a + b_3 a^2 = 0$ or equivalently, $\bar{b}_1 + \bar{b}_2 \alpha + \bar{b}_3 \alpha^2 = 0$. The solutions are

$$\alpha = \frac{1}{2\bar{b}_3}\Big[-\bar{b}_2 \pm \sqrt{\bar{b}_2^2 - 4\bar{b}_1\bar{b}_3}\ \Big] \ . \tag{158}$$

The smaller one of these two solutions is the one that will be relevant for our analysis, and we label it as $\alpha_{IR,3\ell}$.

3.1.2 NSVZ Beta Function

A closed-form expression for the beta function was derived by Novikov, Shifman, Vainshtein, and Zakharov in [55] and discussed further in [56]; this is

$$\beta_{\alpha,NSVZ} = \frac{d\alpha}{dt} = -\frac{\alpha^2}{2\pi}\Big[\frac{b_1 - 2T_f N_f \gamma_m}{1 - 2C_A a}\Big] \ , \tag{159}$$

where γ_m is the anomalous dimension of the fermion bilinear product $\psi_i^T C \tilde{\psi}_i$, or equivalently, $\bar{\psi}_i \psi_i$, of component fermion fields in the quadratic superfield operator product $\Phi_i \tilde{\Phi}_i$ (no sum on the flavor index i). As noted above, this beta function can be written in closed form in the NSVZ scheme used in [55]. This anomalous dimension has the series expansion

$$\gamma_m = \sum_{\ell=1}^{\infty} c_\ell \, a^\ell = \sum_{\ell=1}^{\infty} \bar{c}_\ell \, \alpha^\ell \ , \tag{160}$$

where $\bar{c}_\ell = c_\ell/(4\pi)^\ell$ is the ℓ-loop series coefficient. Only the one-loop coefficient c_1 is scheme-independent, and is

$$c_1 = 4C_f \ . \tag{161}$$

Given our restriction to asymptotically free supersymmetric gauge theories, $\beta_{\alpha,NSVZ}$ has a UV zero at $\alpha = 0$. For the pure gluonic SYM theory,

$\beta_{\alpha,NSVZ}$ has no IR zero; for theories with nonzero matter superfield content, it may or may not have an IR zero, depending on this content. This will be discussed further below. As is evident from Eq. (159), $\beta_{\alpha,NSVZ}$ has a pole at

$$a_{pole,NSVZ} = \frac{\alpha_{NSVZ}}{4\pi} = \frac{1}{2C_A} \ . \tag{162}$$

An important property of this pole is that its position is independent of R and N_f.

3.1.3 General Result on IR Phase Properties

A number of exact results have been established for this asymptotically free supersymmetric gauge theory [55, 56, 58] (see also [59, 69]). We recall one property that is particularly relevant to our present work: if N_f is in the interval $N_{f,cr} < N_f < N_{f,b1z}$, where

$$N_{f,cr} = \frac{3C_A}{4T_f} = \frac{N_{b1z}}{2} \ , \tag{163}$$

i.e., explicitly, the interval

$$I_{N_f,NACP}: \quad \frac{3C_A}{4T_f} < N_f < \frac{3C_A}{2T_f} \ , \tag{164}$$

then the theory flows from weak coupling in the UV to a superconformal IR fixed point. The resultant theory is in a (deconfined) non-Abelian Coulomb phase (NACP) without any spontaneous chiral symmetry breaking. In Eqs. (163) and (164), it is understood that, physically, N_f must be an integer [51], so the actual values of N_f in the NACP are understood to be the integers that satisfy the inequality (164).

3.2 $\mathcal{N} = 1$ Supersymmetric Yang-Mills Theory

In this section we study the case $N_f = 0$, i.e., supersymmetric Yang-Mills theory. We use Padé approximants to the n-loop beta function with $2 \le n \le 4$ calculated in the $\overline{\rm DR}$ scheme to investigate how the properties of this beta function compare with those of the NSVZ beta function. This comparison elucidates the question of how sensitive these properties are to the scheme used for the calculation.

In this SYM theory the calculated coefficients b_ℓ depend on a and C_A via the product

$$x \equiv C_A a \ . \tag{165}$$

or equivalently, $\xi \equiv C_A \alpha$. Consequently, it is natural to re-express the beta function in terms of this product as the expansion variable. We thus define

$$\beta_x \equiv \frac{dx}{dt} = C_A \frac{da}{dt} = \frac{C_A}{4\pi}\,\beta_\alpha \ . \tag{166}$$

Since $b_\ell \propto C_A^\ell$, we define

$$\hat{b}_\ell \equiv \frac{b_\ell}{C_A^\ell} \ . \tag{167}$$

From Eqs. (150)-(152), one has the two scheme-independent coefficients

$$\hat{b}_1 = 3 \ , \quad \hat{b}_2 = 6 \tag{168}$$

and, in the $\overline{\rm DR}$ scheme,

$$\hat{b}_3 = 21 \ . \tag{169}$$

For this SYM theory, the four-loop coefficient has also been calculated in the $\overline{\rm DR}$ scheme [63], and it is

$$\hat{b}_4 = 102 \ . \tag{170}$$

The beta function can be written as

$$\beta_x = -2x^2 \sum_{\ell=1}^{\infty} \hat{b}_\ell \, x^{\ell-1} \ . \tag{171}$$

The n-loop beta function $\beta_{x,n\ell}$ is defined by Eq. (171) with the upper limit on the sum given by $\ell = n$. Explicitly, using the $\overline{\rm DR}$ scheme for b_3 and b_4,

$$SYM: \quad \beta_{x,4\ell,\overline{\rm DR}} = -6x^2(1 + 2x + 7x^2 + 34x^3) \ . \tag{172}$$

It will be convenient to define a reduced (rd) beta function, $\beta_{x,rd}$:

$$\beta_{x,rd} \equiv -\frac{\beta_x}{2x^2\,\hat{b}_1} = 1 + \frac{1}{\hat{b}_1} \sum_{\ell=2}^{\infty} \hat{b}_\ell \, x^{\ell-1} \ . \tag{173}$$

This separates off the factor that gives rise to a UV zero at $x = 0$ so that we can concentrate on the region of interest, namely the IR behavior. The point here is that both $\beta_{x,NSVZ}$ and $\beta_{x,\overline{\rm DR}}$ are guaranteed to have the same

UV behavior in the vicinity of the origin because of the asymptotic freedom of the theory and the fact that the first two orders in the loop expansion are scheme-independent. The question is how well they agree in the IR. As with the full beta function, we also define the n-loop truncation of $\beta_{x,rd}$, denoted $\beta_{x,rd,n\ell}$, as Eq. (173) with the upper limit on the sum given by $\ell = n$; this is thus a polynomial of degree $n-1$ in x. In the $\overline{\rm DR}$ scheme, the four-loop reduced beta function is

$$SYM: \quad \beta_{x,rd,4\ell,\overline{\rm DR}} = 1 + 2x + 7x^2 + 34x^3 \ . \tag{174}$$

We first analyze the zeros of $\beta_{x,rd,n\ell}$ for $2 \le n \le 4$. Since each term is positive, it is clear that at the two-loop level and also, in the $\overline{\rm DR}$ scheme, at the $n = 3,\ 4$ loop level, the respective n-loop reduced beta function has no physical zero. Specifically, the reduced two-loop beta function $\beta_{x,rd,2\ell}$ has only an unphysical zero away from the origin, at $x = -1/2$. With b_3 calculated in the $\overline{\rm DR}$ scheme, the reduced three-loop beta function $\beta_{x,rd,3\ell}$ has an unphysical pair of complex-conjugate zeros, at

$$x = \frac{1}{7}\left(-1 \pm \sqrt{6}\, i\right) = -0.14286 \pm 0.34993i \tag{175}$$

(Here and below, floating-point numbers are listed to the indicated accuracy.) The reduced four-loop beta function $\beta_{x,rd,4\ell,\overline{\rm DR}}$ has three unphysical roots, at

$$x = -0.3152, \quad x = 0.05466 \pm 0.3005i \ . \tag{176}$$

We now compare the properties of $\beta_{x,\overline{\rm DR}}$ and $\beta_{x,NSVZ}$ for the SYM theory. The series expansions of these two beta functions about $x = 0$ are necessarily equal up to two-loop order inclusive, since the beta function is scheme-independent up to and including this order. Beyond two-loop order they differ, as is to be expected, since they are calculated in different schemes. An important question is whether, although they differ in detail, these two beta functions at least exhibit qualitatively similar physical properties. To answer this question, we first express the NSVZ beta function for the SYM theory in terms of β_x, obtaining

$$\beta_{x,NSVZ,SYM} = -\frac{6x^2}{1-2x} \ , \tag{177}$$

so that the reduced NSVZ beta function for the SYM theory is

$$\beta_{x,rd,NSVZ,SYM} = \frac{1}{1-2x} \ . \tag{178}$$

This $\beta_{x,rd,NSVZ,SYM} = 1/(1-2x)$ is in the form of a [0,1] Padé approximant, a property that will be used below. Clearly, $\beta_{x,rd,NSVZ,SYM}$ has no IR zero and, as is evident from Eq. (162) (or equivalently, Eq. (178)), it has a pole at $x = 1/2$:

$$x_{pole,NSVZ} = \frac{1}{2} \ . \tag{179}$$

Interestingly, the $\beta_{x,rd,n\ell,\overline{\rm DR}}$ functions at the $n = 2,\ 3,\ 4$ loop levels all share the same property as $\beta_{x,NSVZ}$ in having no (physical) IR zero. This property will be discussed further below.

We next carry out our Padé calculations and analysis. In general, the n-loop reduced beta function $\beta_{x,rd,n\ell}$ is a polynomial of degree $n-1$ in x. At loop order $n \geq 3$, the coefficients in this function depend on the scheme used for the calculation, and hence, where this is not obvious from context, we shall indicate the scheme with an additional subscript. Since all of the $[p,q]$ Padé approximants that we calculate will apply to the beta function in the $\overline{\rm DR}$ scheme, it is not necessary to indicate this. We can thus calculate $[p,q]$ Padé approximants of the form

$$[p,q]_{\beta_{x,rd,n\ell}} = \frac{1 + \sum_{j=1}^{p} n_j x^j}{1 + \sum_{k=1}^{q} d_k \, x^k} \tag{180}$$

with

$$p + q = n - 1 \ , \tag{181}$$

where the n_j and d_j are x-independent coefficients of the respective polynomials in the numerator and denominator of $[p,q]_{\beta_{x,rd,n\ell}}$. (Our notation for Padé approximants follows the notation in, e.g., [71].) Thus, as with $\beta_{x,rd,n\ell}$ itself, each Padé approximant is normalized so that $[p,q]_{\beta_{x,rd,n\ell}} = 1$ at $x = 0$. For a given $\beta_{x,rd,n\ell}$, there are thus n Padé approximants, namely the set

$$\{\ [n-k,k-1]_{\beta_{x,rd,n\ell}}\ \} \quad \text{with } 1 \leq k \leq n \ . \tag{182}$$

We shall generically denote one of the p zeros of a $[p,q]]_{\beta_{x,rd,n\ell}}$ Padé approximant as $[p,q]_{zero}$ and one of the q poles of this approximant as $[p,q]_{pole}$; in each case, the value of n is given by Eq. (181) as $n = p + q + 1$ and will sometimes be omitted for brevity.

Since

$$[n-1,0]_{\beta_{x,rd,n\ell}} = \beta_{x,rd,n\ell} \ , \tag{183}$$

i.e., the $[n-1,0]_{\beta_{x,rd,n\ell}}$ Padé approximant is identical to the n-loop reduced beta function itself, whose zeros we have already analyzed, we mainly restrict our consideration below to Padé approximants $[p,q]_{\beta_{x,rd,n\ell}}$ with $q \neq 0$. Since b_1 and b_2 are scheme-independent, it follows that for $n = 1,\ 2$, the corresponding Padé approximants are scheme-independent. Note that for an arbitrary polynomial $1 + \sum_j f_j x^j$, the zero of the $[1,0]$ Padé approximant, $1 + f_1 x$, denoted as $[1,0]_{zero}$, occurs at minus the value of the pole in the $[0,1]$ approximant $1/(1 - f_1 x)$, denoted as $[0,1]_{pole}$, i.e.,

$$[1,0]_{zero} = -\frac{1}{f_1} = -[0,1]_{pole} \ . \tag{184}$$

We can also explore the correspondence between the pole at $x = 1/2$ in $\beta_{x,rd,NSVZ}$ and the structure of $\beta_{x,rd,n\ell,\overline{\rm DR}}$. Although $\beta_{x,rd,n\ell,\overline{\rm DR}}$ is a polynomial and hence obviously has no poles, we can investigate whether $[p,q]$ Padé approximants to $\beta_{x,rd,n\ell,\overline{\rm DR}}$ with $q \neq 0$ share properties in common with $\beta_{x,rd,NSVZ}$.

We shall address and answer the following specific questions concerning the $[p,q]$ Padé approximants:

1. Considering the $[p,q]$ Padé approximants to $\beta_{x,rd,n\ell,\overline{\rm DR}}$, do the $[p,q]$ approximants with $p \neq 0$ exhibit a physical IR zero?

2. Considering the $[p,q]$ Padé approximants to $\beta_{x,rd,n\ell,\overline{\rm DR}}$, do the $[p,q]$ approximants with $q \neq 0$ exhibit a physical pole?

3. If a given $[p,q]$ Padé approximant with $q \neq 0$ does exhibit a physical pole, does this pole dominate the UV to IR evolution? This is the case if and only if this pole occurs closer to the origin $x = 0$ than a physical IR zero.

4. If the answers to the previous two questions are affirmative, then is the value of the pole in the given $[p,q]$ Padé approximant with $q \neq 0$ close to the value $x_{IR,NSVZ} = 1/2$?

5. If the answers to questions 1 and 2 are affirmative, then, independent of whether the poles in the $[p,q]$ approximants with $q \neq 0$ are close to $x_{IR,NSVZ} = 1/2$, do different approximants at least exhibit a stable physical pole? That is, do these $[p,q]$ Padé approximants with $q \neq 0$ exhibit a stable physical pole?

The answers to these questions elucidate how general and robust are the properties of the SYM beta function calculated in different schemes, in particular, the absence of an IR zero and the presence of a pole in the NSVZ SYM beta function. We have already partially answered the first question, since we have shown that there is no IR zero in the two-loop beta function and also none in the three-loop or four-loop beta function in the $\overline{\rm DR}$ scheme, in agreement with the absence of an IR zero in the NSVZ beta function for this SYM theory. We complete this first answer by examining $[p, q]$ Padé approximants with both p and q nonzero and also address the questions pertaining to a pole.

From the two-loop reduced beta function $\beta_{x,rd,2\ell}$, we can calculate one Padé approximant with $q \neq 0$, namely

$$[0,1]_{\beta_{x,rd,2\ell}} = \frac{1}{1-2x} \ . \tag{185}$$

This is the same as the reduced NSVZ beta function, $\beta_{x,rd,NSVZ,SYM}$ in Eq. (178), and hence their poles are at the same location:

$$[0,1]_{pole,\beta_{x,rd,n\ell}} = \frac{1}{2} = x_{pole,NSVZ} \ . \tag{186}$$

Although $\beta_{x,rd,NSVZ,SYM} = 1/(1-2x)$ was obtained by a sum to infinite-loop order and hence is scheme-dependent, the pole in the [0,1] Padé approximant was derived from the two-loop beta function $\beta_{x,rd,2\ell}$ and hence is scheme-independent.

We proceed next to the comparison at the three-loop order. From the reduced three-loop reduced beta function, $\beta_{x,rd,3\ell,\overline{\rm DR}}$, we can calculate two Padé approximants with $q \neq 0$, namely

$$[1,1]_{\beta_{x,rd,3\ell}} = \frac{1-(3/2)x}{1-(7/2)x} \tag{187}$$

and

$$[0,2]_{\beta_{x,rd,3\ell}} = \frac{1}{(1+x)(1-3x)} \ . \tag{188}$$

As is evident from (187), the $[1,1]_{\beta_{x,rd,3\ell}}$ Padé has a pole at $x = 2/7 = 0.2857$ and a zero at $x = 2/3$. These are listed in Table 6. As the theory flows from the UV to the IR, x increases from 0 and reaches the IR pole at 2/7 before it reaches the zero, so the latter is not relevant to this UV to IR evolution from

Table 6: Values of zeros and poles, in the variable x, of various Padé approximants to $\beta_{x,rd,2\ell}$ and $\beta_{x,rd,n\ell,\overline{\rm DR}}$ with $n = 3,\ 4$ for $\mathcal{N} = 1$ supersymmetric Yang-Mills theory, SYM. Results are given to the indicated floating-point accuracy. The abbreviation NA means "not applicable".

n	$[p,q]$	zero(s)	pole(s)
2	[1,0]	$-1/2$	NA
2	[0,1]	NA	$1/2$
3	[2,0]	$0.143 \pm 0.350i$	NA
3	[1,1]	$2/3$	$2/7 = 0.286$
3	[0,2]	NA	$-1,\ 1/3$
4	[3,0]	$-0.315,\ 0.0547 \pm 0.3005i$	NA
4	[2,1]	$-1.330,\ 0.277$	$7/34 = 0.206$
4	[1,2]	$3/14 = 0.214$	$0.181,\ 0.871$
4	[0,3]	NA	$0.265,\ -0.240 \pm 0.461i$

weak coupling. The $[0,2]_{\beta_{x,rd,3\ell}}$ Padé exhibits an unphysical pole at $x = -1$ and a physical pole at $x = 1/3$. Since this Padé has no zero, the pole at $x = 1/3$ again dominates the UV to IR evolution.

From the four-loop reduced beta function $\beta_{x,rd,4\ell,\overline{\rm DR}}$, we can calculate three $[p,q]$ Padé approximants with $q \neq 0$, namely

$$[2,1]_{\beta_{x,rd,4\ell}} = \frac{1 - (20/7)x - (19/7)x^2}{1 - (34/7)x} \ , \tag{189}$$

$$[1,2]_{\beta_{x,rd,4\ell}} = \frac{1 - (14/3)x}{1 - (20/3)x + (19/3)x^2} \ , \tag{190}$$

and

$$[0,3]_{\beta_{x,rd,4\ell}} = \frac{1}{1 - 2x - 3x^2 - 14x^3} \ . \tag{191}$$

The $[2,1]_{\beta_{x,rd,4\ell}}$ Padé has zeros at $x = (1/19)(-10 \pm \sqrt{233}\ )$, i.e, $x = 0.2771$ and $x = -1.3297$, and a pole at $x = 7/34 = 0.2059$. The $[1,2]_{\beta_{x,rd,4\ell}}$ Padé has a zero at $x = 3/14 = 0.2143$ and two poles, at $x = (1/19)(10 \pm \sqrt{43}\ )$, i.e., $x = 0.8714$ and $x = 0.1812$. Finally, the $[0,3]_{\beta_{x,rd,4\ell}}$ Padé has three poles, at $x = 0.26481$ and $x = -0.23955 \pm 0.4608i$. As with our other Padé results for the SYM theory, these are listed in Table 6.

These results provide answers to the five questions that we posed above. Concerning the first question, the [1,0] approximant to $\beta_{x,rd,2\ell}$ and the [2,0], and [3,0] approximants to $\beta_{x,rd,n\ell,\overline{\rm DR}}$ for $n = 3,\ 4$ have no IR zero, in agreement with the NSVZ beta function. Although the [1,1] approximant to $\beta_{x,rd,3\ell\overline{\rm DR}}$ and the [2,1] and [1,2] approximants to $\beta_{x,rd,4\ell,\overline{\rm DR}}$ do have (physical) IR zeros, in each case, the IR zero occurs farther from the origin than the pole in the respective approximant and hence does not directly influence the UV to IR evolution. Thus, the results from all of these Padé approximants to $\beta_{x,rd,n\ell,\overline{\rm DR}}$ for $2 \le n \le 4$ are in agreement with the NSVZ beta function for this SYM theory as regards the absence of an IR zero affecting the UV to IR evolution.

The answer to the second question is yes; that is, all of the Padé approximants to the various n-loop reduced beta functions in the $\overline{\rm DR}$ scheme, $\beta_{x,rd,n\ell,\overline{\rm DR}}$, up to $n = 4$ loop order, agree with $\beta_{x,rd,NSVZ}$ as regards the property that they exhibit a physical IR pole. The answer to the third question is also yes; in each case where a $[p, q]$ Padé approximant to $\beta_{x,rd,n\ell,\overline{\rm DR}}$ exhibits a physical pole, this pole occurs closer to the origin than any physical zero(s) (if such a zero is present at all) and hence dominates the UV to IR evolution.

We come next to question 4, concerning the numerical agreement of the (physical) pole in the $[p, q]$ Padé approximants with $q \neq 0$ with the position of the pole at $x = 1/2$ in the NSVZ beta function. To answer this question, for each $[p, q]$ approximant to $\beta_{x,rd,n\ell,\overline{\rm DR}}$ with $q \neq 0$, one takes the pole among the q poles at a physical (positive real) value of x (if there is such a pole) closest to the origin. This is the IR pole for this approximant. As noted, this agreement is automatic in the two-loop case, so the question really applies at the three-loop and four-loop level. As is evident in Table 6, the two Padé approximants with $q \neq 0$ formed from the three-loop beta function, namely [1,1] and [0,2], have poles at the respective values $x = 0.286$ and $x = 0.333$. At the four-loop level, the values of the poles closest to the origin in the [2,1], [1,2], and [0,3] Padé approximants are $x = 0.206,\ 0.181,\ 0.265$, respectively. However, none of these is particularly close to the value $x = 0.5$ of the pole in the NSVZ beta function. Nevertheless, we can at least say that the values of the (physical) pole in the various $[p, q]$ approximants to $\beta_{x,rd,n\ell,\overline{DR}}$ with $n = 3,\ 4$ do not differ from the value $x = 1/2$ in $\beta_{x,rd,NSVZ}$ by more than a factor of about 2.8.

Finally, we address the fifth question. The importance of this question stems from the fact that when one switches schemes, one does not expect a pole (or zero) to occur at the same position as in another scheme, but

at least different $[p,q]$ Padé approximants should yield a reasonably stable value of this pole, especially as one calculates to progressively higher-loop order. There are thus two categories of comparisons that one can make here, namely comparing the stability of the position of a pole appearing in $[p,q]$ Padé approximants for different loop orders n, and comparing this stability for a given n-loop order in $[p,q]$ Padé approximants with different p and q (satisfying $p+q=n-1$), at a high-enough order so that there are several $[p,q]$ approximants with poles. Regarding the comparison among different loop orders, as is evident from Table 6, the values of the poles range from the value from the two-loop result, which is automatically equal to $x=0.5$, to a low of $x=0.181$ for the physical pole in the $[1,2]_{\beta_{x,rd,4\ell}}$ Padé, a factor of 2.8 smaller. Regarding the range of values of physical pole positions from the Padé approximants at a given loop order, the range is given, at the three-loop order, by the ratio

$$\frac{[0,2]_{pole}}{[1,1]_{pole}} = \frac{7}{6} = 1.167 \ , \tag{192}$$

and, at the four-loop order, by two independent ratios, which may be taken to be

$$\frac{[0,3]_{pole}}{[1,2]_{pole}} = 1.462 \ , \tag{193}$$

and

$$\frac{[1,2]_{pole}}{[2,1]_{pole}} = 0.88005 \ . \tag{194}$$

One also has

$$\frac{[0,3]_{pole}}{[2,1]_{pole}} = \frac{[0,3]_{pole}}{[1,2]_{pole}} \, \frac{[1,2]_{pole}}{[2,1]_{pole}} = 1.286 \ . \tag{195}$$

Summarizing the findings from our Padé analysis for the SYM theory, the results show excellent agreement between the beta function, calculated up to four-loop order in the $\overline{\rm DR}$ scheme, and the NSVZ beta function, concerning the absence of an IR zero that affects the UV to IR evolution. Furthermore, the answers to questions 2 and 3 show that the Padé approximants to this beta function in the $\overline{\rm DR}$ scheme are consistent with the existence of an IR pole that dominates the UV to IR evolution, again in agreement with the NSVZ beta function. The answer to the fourth question can be interpreted as a consequence of the scheme-dependence of a pole in a beta function. The answer to the fifth question suggests that, assuming that the beta function in the $\overline{\rm DR}$ scheme does, indeed, encode evidence for a physical pole that

dominates the UV to IR evolution in this SYM theory, one must calculate this beta function to higher than four-loop order in order for the $[p, q]$ Padé approximants with $q \neq 0$ to yield a stable value for the location of this zero.

3.3 Supersymmetric SU(N_c) Quantum Chromodynamics

In this section we discuss our investigation in [3] of an asymptotically free vectorial gauge theory with $\mathcal{N} = 1$ supersymmetry, gauge group SU(N_c), and N_f copies (flavors) of massless chiral superfields Φ_i and $\tilde{\Phi}_i$, $i = 1, ..., N_f$, transforming according to the fundamental and conjugate fundamental representations of SU(N_c).

This theory is often called supersymmetric quantum chromodynamics (SQCD), and we shall also use this nomenclature, keeping in mind that the gauge group is generalized from the actual SU(3) color group of real-world QCD to SU(N_c). We restrict our consideration to values $N_f \neq 0$ here, since if $N_f = 0$, the present theory reduces to a pure supersymmetric Yang-Mills gauge theory, which we have also discussed above. As we did with the SYM theory, we shall use Padé approximants to investigate the question of the extent to which the beta function for this theory, as calculated in the $\overline{\rm DR}$ scheme, exhibits properties in agreement with the properties of the NSVZ beta function, (159).

3.3.1 Some General Properties

We recall some basic well-known properties of this theory, many of which follow as special cases of the general discussion in Sect. 3.1 for the fundamental representation. For this case, the upper bound on N_f imposed by the condition of asymptotic freedom, Eq. (154), reads

$$N_f < 3N_c \ . \tag{196}$$

The exact result (163) on the value of N_f at the lower boundary of the IR non-Abelian Coulomb phase reads [51]

$$N_{f,cr} = \frac{3N_c}{2} \ , \tag{197}$$

If N_c is odd, this is only a formal result, since $N_{f,cr}$ must be integral. Thus, the (chirally symmetric, deconfined) IR non-Abelian Coulomb phase is specified, from Eq. (198), by N_f in the interval

$$\frac{3N_c}{2} < N_f < 3N_c \ . \tag{198}$$

For our present case with R being the fundamental representation, Eq. (155) specializes to

$$N_{f,b2z} = \frac{3N_c}{2 - N_c^{-2}} \ . \tag{199}$$

Hence, the range of values of N_f in Eq. (156) where the two-loop beta function has an IR zero is [51]

$$\frac{3N_c}{2 - N_c^{-2}} < N_f < 3N_c \ . \tag{200}$$

Numerical values of $N_{f,cr}$, $N_{f,b2z}$, $N_{f,b3z}$, and $N_{f,b1z} = N_{f,max}$ were listed for $2 \le N_c \le 5$ in Table II of Ref. [33]. As was noted in [33], the value of $N_{f,b2z}$ in Eq. (199) is greater (for all finite N_c) than the exactly known lower boundary of the non-Abelian Coulomb phase in Eq. (197). Results for the values of the IR zero in the two-loop and three-loop beta function, $\alpha_{IR,2\ell}$ and $\alpha_{IR,3\ell}$, were given in [33].

3.3.2 Calculations of Padé Approximants

We now proceed to calculate and analyze the Padé approximants to the n-loop beta function for this SQCD theory. As before with the SYM theory, since our analysis concerns the behavior away from the UV fixed point at $\alpha = 0$, it is convenient to deal with the reduced beta function defined by (173). Because the beta function β_α is known up to three-loop order, the reduced beta function has the form

$$\beta_{\alpha,rd,3\ell} = 1 + (b_2/b_1)a + (b_3/b_1)a^2 \ . \tag{201}$$

Since $G = \mathrm{SU}(N_c)$, it follows that $C_A = N_c$ and the variable x in Eq. (165) has the explicit form

$$x \equiv a\, N_c \equiv \frac{\xi}{4\pi} \ . \tag{202}$$

In general, the beta function and hence the Padé approximants to it depend on the two parameters N_c and N_f. It is natural to apply the Padé analysis to address the question of how the properties of the beta function calculated in the $\overline{\rm DR}$ scheme compare with those of the NSVZ beta function in the simplest context, namely the limit where the (appropriately scaled) beta function depends on only one variable. This is the 't Hooft-Veneziano or LNN (Large N_c and N_f) limit

$$\begin{aligned} LNN: \qquad & N_c \to \infty, \quad N_f \to \infty, \\ & \text{with } r \equiv \frac{N_f}{N_c} \text{ fixed and finite} \end{aligned} \tag{203}$$

with $x(\mu) = a(\mu)\, N_c$ a finite function of the Euclidean scale μ.

Our constraint of asymptotic freedom implies $r < 3$. We divide our analysis into two parts corresponding to two subdivisions of this interval, namely the NACP interval

$$I_{r,NACP}: \quad \frac{3}{2} < r < 3 \ , \tag{204}$$

where the UV to IR evolution leads to a non-Abelian Coulomb phase without any spontaneous chiral symmetry breaking, and the remaining interval $0 < r < 3/2$. In addition to simplifying the analysis of the beta function from dependence on variables to two to one variable, the LNN limit has the appeal that the interval (204) in which the two-loop beta function has an IR zero coincides with the interval leading to a non-Abelian Coulomb phase. This is in contrast to the situation for general N_c and N_f, in which b_2 vanishes in the interior of the NACP.

In the LNN limit, one focuses on the scaled beta function, which is finite in this limit. For this we use the same notation, β_x, as in Eq. (166), with it being understood that the LNN limit is taken, so that

$$\beta_x = \lim_{LNN} \frac{dx}{dt} \ , \tag{205}$$

equivalent to $\beta_\xi = \frac{d\xi}{dt}$. The function β_x has the expansion (171) with

$$\hat{b}_\ell \equiv \lim_{LNN} \frac{b_\ell}{N_c^\ell} \ . \tag{206}$$

As before, we denote the n-loop truncation of Eq. (205) as $\beta_{x,n\ell}$, and, where appropriate, we indicate the scheme used for loop order $n \geq 3$ by a subscript, as $\beta_{x,n\ell,\overline{\rm DR}}$. From Eqs. (150) and (151), it follows that the scheme-independent scaled coefficients are

$$\hat{b}_1 = 3 - r \tag{207}$$

and

$$\hat{b}_2 = 2(3 - 2r) \ . \tag{208}$$

From the expression (152) for b_3 calculated in the $\overline{\rm DR}$ scheme, one has

$$\hat{b}_3 = 21 - 21r + 4r^2 \ . \tag{209}$$

Thus,

$$\beta_{x,3\ell,\overline{\rm DR}} = -2x^2\Big[(3-r) + 2(3-2r)x + (21 - 21r + 4r^2)x^2 \ \Big] \ , \tag{210}$$

and hence

$$\begin{aligned} \beta_{x,rd,3\ell,\overline{\rm DR}} &= 1 + \frac{\hat{b}_2}{\hat{b}_1}\, x + \frac{\hat{b}_3}{\hat{b}_1}\, x^2 \\ &= 1 + 2\Big(\frac{3-2r}{3-r}\Big)\, x + \Big(\frac{21 - 21r + 4r^2}{3-r}\Big)\, x^2 \ . \end{aligned} \tag{211}$$

It will be convenient to define

$$D_s = -\hat{b}_3 = -21 + 21r - 4r^2 \ . \tag{212}$$

This polynomial D_s has the property that

$$D_s > 0 \quad \text{for} \quad \frac{1}{8}(21 - \sqrt{105}\ ) < r < \frac{1}{8}(21 + \sqrt{105}\ ) \ , \tag{213}$$

i.e., for $1.3441 < r < 3.9059$, which includes all of the interval $I_{r,NACP}$. (If r lies outside of the interval in Eq. (213), then $D_s < 0$.)

We recall from [31, 32, 34] that if the two-loop beta function has an IR zero, then, since this is a scheme-independent property, one may require a physically acceptable scheme to maintain the existence of this IR zero at loop level $n \geq 3$ and the condition that it should maintain it at the three-loop level implies that $b_3 < 0$ (see the proof in Section II.E of [31]). This condition is thus satisfied by the $\overline{\rm DR}$ scheme, since $\hat{b}_3 < 0$ for the interval $I_{r,NACP}$, where $\beta_{x,2\ell}$ has an IR zero.

3.3.3 Analysis for Interval $r \in I_{r,NACP}$

IR Zero of $\beta_{x,rd,2\ell}$ At the two-loop level, $\beta_{x,rd,2\ell}$ has a (scheme-independent) IR zero at

$$x_{IR,2\ell} = \frac{\xi_{IR,2\ell}}{4\pi} = \frac{(3-r)}{2(2r-3)} \ , \tag{214}$$

which is physical for $3/2 < r < 3$, i.e., for $r \in I_{r,NACP}$. The value of $x_{IR,2\ell}$ increases monotonically from 0 to arbitrarily large values as r decreases from 3 to 3/2 in the interval I_{NACP}. Clearly, for the values of r in the lower part of this interval, where $x_{IR,2\ell}$ becomes large, the perturbative calculation that yielded the expression for $x_{IR,2\ell}$ cannot be reliably applied.

IR Zero of $\beta_{x,rd,3\ell,\overline{\rm DR}}$ At the three-loop level, $\beta_{x,rd,3\ell,\overline{\rm DR}}$ has an IR zero at [32, 33]

$$x_{IR,3\ell} = \frac{-(2r-3) + \sqrt{C_s}}{D_s} \ , \tag{215}$$

where

$$C_s = -54 + 72r - 29r^2 + 4r^3 \ . \tag{216}$$

The polynomial C_s has only one real zero, at $r = 1.3380$, and is positive (negative) for r greater (less) than this value. Thus, C_s is positive for all $r \in I_{r,NACP}$. Since $\hat{b}_3 < 0$ for $r \in I_{r,NACP}$, it follows that

$$x_{IR,3\ell} \leq x_{IR,2\ell} \ , \tag{217}$$

as a special case of an inequality that was proved in [31] (see Eq. (2.29) of [31]). The inequality (217) is a strict inequality except at the upper end of $I_{r,NACP}$ at $r = 3$, where both $x_{IR,3\ell}$ and $x_{IR,2\ell}$ vanish.

Analysis of IR Zero Using Padé Approximants For $r \in I_{r,NACP}$, where the beta function has an IR zero, we address and answer the following set of questions concerning the comparison of the three-loop beta function calculated in the $\overline{\rm DR}$ scheme, the Padé approximants to it, and the NSVZ beta function:

1. Considering (i) the n-loop beta function and (ii) the $[p, q]$ Padé approximants to this beta function with $p \neq 0$, do these exhibit a physical IR zero?

2. If (i) the n-loop beta function and (ii) the $[p,q]$ Padé approximant to this beta function with $p \neq 0$ do exhibit a physical IR zero, does this IR zero dominate the UV to IR evolution? This is the case if and only if this IR zero occurs closer to the origin $x = 0$ than a physical IR pole (if the latter is present in a $[p,q]$ Padé with $q \neq 0$).

3. In each of the cases (i) and (ii), if the answers to the previous two questions are affirmative, then is the value of the IR zero close to the value $x_{IR,cfs,NSVZ}$ in $\beta_{x,rd,NSVZ}$, given in Eq. (232)?

4. In each of the cases (i) and (ii), if the answers to questions 1 and 2 are affirmative, then, independent of the closeness of the IR zero to $x_{IR,cfs,NSVZ}$, are the values at least close to each other?

5. For the $[p,q]$ Padé approximants with $q \neq 0$, if there is a physical pole, is its location near to the value $x = 1/2$ in the NSVZ beta function?

We recall that the $[p,0] = [n-1]$ Padé approximant is identical to the reduced n-loop beta function $\beta_{x,rd,n\ell}$, as noted above in Eq. (183). As a special case of this, the two-loop reduced beta function $\beta_{x,rd,2\ell}$ yields only one Padé approximant with a zero, namely [1,0], which coincides with $\beta_{x,rd,2\ell}$, itself, so no further analysis is necessary. The three-loop reduced beta function $\beta_{x,rd,3\ell,\overline{\rm DR}}$ yields two Padé approximants with $p \neq 0$, namely [2,0] and [1,1]. The [2,0] approximant coincides with $\beta_{x,rd,3\ell,\overline{\rm DR}}$, which has already been analyzed. We calculate the [1,1] approximant to be

$$[1,1]_{\beta_{x,rd,3\ell}} = \frac{1 - \left[\frac{E_s}{2(3-r)(2r-3)}\right] x}{1 - \left[\frac{D_s}{2(2r-3)}\right] x} \ , \tag{218}$$

where

$$E_s = -27 + 36r - 17r^2 + 4r^3 \ . \tag{219}$$

The polynomial E_s has only one real zero, at $r = 1.3118$ and is positive (negative) for r greater (less) than this value. Therefore, E_s is positive for all $r \in I_{r,NACP}$. As r decreases from 3 to 3/2, E_s decreases from 36 to 9/4. Thus, the $[1,1]_{\beta_{x,rd,3\ell,\overline{\rm DR}}}$ Padé approximant has a zero at

$$x_{[1,1],zero} = \frac{2(3-r)(2r-3)}{E_s} \ . \tag{220}$$

This is positive semidefinite for all $r \in I_{r,NACP}$; it vanishes at both ends of this interval and reaches a maximum at $r = 1.8321$ (a zero of the function $81 - 198r + 189r^2 - 72r^3 + 8r^4$), where it has the value $x_{[1,1],zero} = 0.23898$. In order for $x_{[1,1],zero}$ to be relevant for the UV to IR evolution of the theory (from weak coupling in the UV), it is necessary that if this Padé approximant has a pole at a physical value of x, then this pole must occur farther from the origin than the zero. Below, when we analyze poles of the various Padé approximants, we will show that this condition is satisfied (although the distance between the zero and the pole vanishes as $r \searrow 3/2$). We thus denote

$$x_{[1,1],zero} = x_{IR,3\ell,[1,1]} \ . \tag{221}$$

We prove two inequalities. First,

$$x_{IR,3\ell,[1,1]} \le x_{IR,2\ell} \quad \text{for } r \in I_{r,NACP} \ . \tag{222}$$

This is proved by computing the difference

$$x_{IR,2\ell} - x_{IR,3\ell,[1,1]} = \frac{(3-r)^2 \, D_s}{2(2r-3) \, E_s} \ . \tag{223}$$

This difference is positive semidefinite for $r \in I_{r,NACP}$, vanishing only as $r \nearrow 3$ at the upper end of this interval.

Second, we obtain the stronger inequality

$$x_{IR,3\ell,[1,1]} \le x_{IR,3\ell} \quad \text{for } r \in I_{r,NACP} \ . \tag{224}$$

(This is a stronger inequality since $x_{IR,3\ell} \le x_{IR,2\ell}$, by (217).) We have proved the inequality (224) by calculating the difference, $x_{IR,3\ell} - x_{IR,3\ell,[1,1]}$ and showing that it is positive semidefinite for $r \in I_{r,NACP}$, vanishing only at $r = 3$. Combining these inequalities, we have

$$x_{IR,3\ell,[1,1]} \le x_{IR,3\ell} \le x_{IR,2\ell} \quad \text{for } r \in I_{r,NACP} \ , \tag{225}$$

with equality only at $r = 3$, where all three terms in the inequality vanish.

IR Zero from NSVZ Beta Function Applying the LNN limit to the NSVZ beta function (159) and calculating the resultant β_x in Eq. (205), we obtain

$$\beta_{x,NSVZ,LNN} = -2x^2 \left[\frac{3 - r(1+\gamma_m)}{1-2x} \right] \ . \tag{226}$$

Here,

$$\gamma_m = \sum_{\ell=1}^{\infty} \hat{c}_\ell x^\ell \ , \tag{227}$$

where the maximal scheme-independent coefficient in γ_m is the one-loop coefficient

$$\hat{c}_1 = 2 \ . \tag{228}$$

In terms of the closed-form (cf) and series (s) functions defined in [34], this beta function can be expressed as

$$\beta_{x,NSVZ} = -2x^2 \hat{b}_1 \, f_{x,cf,NSVZ} \, f_{x,s,NSVZ} \ , \tag{229}$$

where

$$f_{x,cf,NSVZ} = \frac{1}{1-2x} \tag{230}$$

and

$$f_{x,s,NSVZ} = 1 - \frac{r\gamma_m}{\hat{b}_1} = 1 - \frac{r\gamma_m}{3-r} \ , \tag{231}$$

where here the subscript s connotes the dependence on the series (227) for γ_m.

There are different approaches to calculating the IR zero of $\beta_{x,NSVZ}$. If one expands it in a series in x around $x = 0$ and calculates the resultant zero, one necessarily reproduces the one-loop and two-loop results obtained starting from the original series expansion, since these are scheme-independent. This analysis was carried out in [31, 32, 33]. An alternate approach proposed and analyzed in [34] is to incorporate the information obtained from the summation to infinite-loop order that yields the structure in Eqs. (229)-(231). Since the factor $f_{x,cf,NSVZ}$ has no zero, one thus calculates the IR zero as the zero in $f_{x,s,NSVZ}$. Substituting the expansion of γ_m to its maximal scheme-independent order $\gamma_m = 2x$, one thus solves the equation $1 - 2rx/(3-r) = 0$, obtaining

$$x_{IR,NSVZ} = \frac{\xi_{IR,NSVZ}}{4\pi} = \frac{3-r}{2r} \ , \tag{232}$$

As r decreases from 3 to 3/2 in the interval $I_{r,NACP}$, this IR zero, $x_{IR,NSVZ}$, increases from 0 to 1/2. The IR zero $x_{IR,NSVZ}$ has much better behavior than $x_{IR,2\ell}$ in that it increases to a finite value as r decreases to the lower end of the interval $I_{r,NACP}$, while $x_{IR,2\ell}$ diverges at this lower boundary of $I_{r,NACP}$. (As noted above, this divergence is only formal, since the perturbative calculation

that yielded the expression for $x_{IR,2\ell}$ ceases to apply when the value of x becomes too large.)

In order for the IR zero $x_{IR,NSVZ}$ to be relevant to the UV to IR evolution of the theory, it is necessary and sufficient that this IR zero of the beta function should occur closer to the origin than the pole in $\beta_{x,NSVZ}$, which occurs at $x = 1/2$, as given in Eq. (179). The requisite condition

$$x_{IR,NSVZ} \leq x_{pole,NSVZ} \quad \text{for } \frac{3}{2} < r < 3 \tag{233}$$

is satisfied, since, as we have observed above, $x_{IR,NSVZ} < 1/2$ in this interval, $3/2 < r \leq 3$. As r approaches the lower boundary of $I_{r,NACP}$ at $r = 3/2$, $x_{IR,NSVZ}$ approaches $x_{pole,NSVZ}$ from below. The inequality (233) is a strict inequality except at the single point $r = 3$, where both $x_{IR,NSVZ}$ and $x_{pole,NSVZ}$ vanish.

As r decreases below $3/2$ in the interval $0 < r < 3/2$, $x_{IR,NSVZ}$ increases monotonically above $1/2$. Thus, for $0 < r < 3/2$, this IR zero at $x_{IR,NSVZ}$ occurs farther from the origin $x = 0$ than the IR pole in $\beta_{x,NSVZ}$ at $x = 1/2$ and hence is not directly relevant to the UV to IR evolution of the theory from weak coupling.

We next prove some additional inequalities. First,

$$x_{IR,NSVZ} \leq x_{IR,2\ell} \quad \text{for } r \in I_{r,NACP} \ . \tag{234}$$

This is proved by calculating the difference, which is

$$x_{IR,2\ell} - x_{IR,NSVZ} = \frac{(3-r)^2}{2r(2r-3)} \ . \tag{235}$$

This is evidently positive-semidefinite, vanishing only at the upper end of the interval $I_{r,NACP}$ at $r = 3$, where both $x_{IR,2\ell}$ and $x_{IR,NSVZ}$ vanish. Next, we obtain the stronger inequality,

$$x_{IR,NSVZ} \leq x_{IR,3\ell} \quad \text{for } r \in I_{r,NACP} \ , \tag{236}$$

with equality only at $r = 3$, where both $x_{IR,NSVZ}$ and $x_{IR,3\ell}$ both vanish. This is again proved by calculating the difference:

$$x_{IR,3\ell} - x_{IR,NSVZ} = \frac{63 - 78r + 29r^2 - 4r^3 + 2r\sqrt{C_s}}{2rD_s} \ . \tag{237}$$

The denominator of this expression is positive for $r \in I_{r,NACP}$. In the numerator, although the polynomial $63-78r+29r^2-4r^3$ is negative for $r \in I_{r,NACP}$, it is smaller in magnitude than the second term, $2r\sqrt{C_s}$, so the numerator is positive semidefinite in this interval, vanishing only at the upper end, at $r = 3$.

Comparing $x_{IR,NSVZ}$ with $x_{IR,3\ell,[1,1]}$, we find that

$$x_{IR,3\ell,[1,1]} - x_{IR,NSVZ} = \frac{(3-r)^2(r-1)(4r-9)}{2rE_s} \ . \tag{238}$$

Therefore, the relative size of $x_{IR,NSVZ}$ and $x_{IR,3\ell,[1,1]}$ is reversed between upper and lower subsections of the interval $I_{r,NACP}$:

$$x_{IR,NSVZ} \le x_{IR,3\ell,[1,1]} \quad \text{if } 2.25 \le r \le 3 \tag{239}$$

(with equality only at $x = 2.25$ and $r = 3$), while

$$x_{IR,NSVZ} > x_{IR,3\ell,[1,1]} \quad \text{if } 1.5 < r < 2.25 \ . \tag{240}$$

We summarize these results in Table 7. The entries in Table 7 for $x_{IR,n\ell}$ with $n = 2,\ 3$ are equivalent to the entries for $\xi_{IR,n\ell} = 4\pi x_{IR,n\ell}$ with $n = 2,\ 3$ given in Table VII of [31]; the entries for $x_{IR,3\ell,[1,1]}$ are new here. As is evident, the numerical results in Table 7 obey the general inequalities (222) and (224) that we have proved above, as well as the inequality (217) proved in [31].

Poles of Padé Approximants Here we investigate the poles of the Padé approximants to $\beta_{x,rd,2\ell}$ and $\beta_{x,rd,3\ell,\overline{\rm DR}}$ in order to answer the questions posed above. At the two-loop level, from $\beta_{x,rd,2\ell}$ we can obtain one $[p,q]$ Padé approximant with $q \neq 0$, namely

$$[0,1]_{\beta_{x,rd,2\ell}} = \frac{1}{1 + \left[\frac{2(2r-3)}{3-r}\right]x} \ . \tag{241}$$

This has a pole at

$$x_{[0,1]_{pole}} = -\left[\frac{3-r}{2(2r-3)}\right] \ . \tag{242}$$

Since we are considering $r \in I_{NACP}$, i.e., $3/2 \le r \le 3$, this occurs at negative x and hence is unphysical. As a special case of the general result (184), we have $x_{[0,1]_{pole}} = -x_{IR,2\ell}$. So the fact that $x_{IR,2\ell}$ is physical guarantees that this pole is irrelevant.

Table 7: Values of the IR zero of the beta function in the LNN limit of the SQCD theory, as a function of $r \in I_{r,NACP}$. The entries in the columns are: (i) $x_{IR,2\ell}$, IR zero of the 2-loop beta function $\beta_{x,2\ell}$, (ii) $x_{IR,3\ell}$, IR zero of the 3-loop beta function $\beta_{x,3\ell,\overline{\rm DR}}$, (iii) the IR zero calculated from the Padé approximant [1,1] to $\beta_{x,3\ell,\overline{\rm DR}}$, and (iv) $x_{IR,cfs}$ obtained from $\beta_{x,NSVZ}$. Since $x_{IR,2\ell}$ formally diverges as $r \searrow 1.5$, the perturbative calculation is not applicable (NA) there.

r	$x_{IR,2\ell}$	$x_{IR,3\ell}$	$x_{IR,3\ell,[1,1]}$	$x_{IR,cfs,NSVZ}$
1.5	NA	1.000	0.000	0.500
1.6	3.500	0.690	0.162	0.438
1.7	1.625	0.529	0.220	0.382
1.8	1.000	0.424	0.238	0.333
1.9	0.6875	0.349	0.236	0.289
2.0	0.500	0.290	0.222	0.250
2.1	0.375	0.242	0.202	0.214
2.2	0.286	0.201	0.179	0.182
2.3	0.219	0.166	0.154	0.152
2.4	0.167	0.135	0.129	0.125
2.5	0.125	0.107	0.104	0.100
2.6	0.0909	0.0811	0.0801	0.0769
2.7	0.0625	0.0579	0.0576	0.05555
2.8	0.0385	0.0368	0.0367	0.0367
2.9	0.0179	0.0175	0.0175	0.0172
3.0	0	0	0	0

We next proceed to the three-loop level. From $\beta_{x,rd,3\ell,\overline{\rm DR}}$ we can obtain two $[p,q]$ Padé approximants with $q \neq 0$. The first is the [1,1] approximant, given in Eq. (218). This has a pole at

$$x_{[1,1]_{pole}} = \frac{2(2r-3)}{D_s} \ . \tag{243}$$

We list values of $x_{[1,1]_{pole}}$ as a function of r in Table 8. As r decreases from 3 to 3/2 in the interval $I_{r,NACP}$, the position of this pole decreases monotonically from 1 to 0. For a given $r \in I_{r,NACP}$, this pole occurs farther from the origin than the zero, i.e. $x_{[1,1]_{pole}} \geq x_{[1,1]_{zero}}$. We show this by calculating the difference,

$$x_{[1,1]_{pole}} - x_{[1,1]_{zero}} = \frac{8(2r-3)^3}{D_s \, E_s} \ . \tag{244}$$

The right-hand side of (244) is positive for $3/2 < r \leq 3$ in I and vanishes as r decreases to 3/2 at the lower end of this interval I. Thus, the $[1,1]_{\beta_{x,rd,3\ell}}$ approximant exhibits a physical zero closer to the origin than the pole, and hence the pole is not relevant to the UV to IR evolution described by this Padé approximant. This irrelevance of the pole is similar to what we found for the $[0,1]_{\beta_{x,rd,2\ell}}$ Padé approximant; indeed in that case, the pole occurred at an unphysical, negative value of x. The confluence of the pole and the zero of the $[1,1]_{\beta_{x,rd,3\ell}}$ approximant as $r \searrow 3/2$ in I reflects the fact that as $r \searrow 3/2$, $[1,1]_{x,rd,3\ell} \to 1$, independent of x.

For the analysis of an IR zero, as was carried out in [33, 32, 34], the [0,2] Padé is not of interest, since it cannot reproduce an IR zero that is present in the analysis of $\beta_{x,rd,3\ell,\overline{\rm DR}}$. However, it is of interest for the questions that we address in this subsection. We calculate

$$[0,2]_{\beta_{x,rd,3\ell}} = \frac{1}{1 + \left[\frac{2(2r-3)}{3-r}\right] x + \left[\frac{E_s}{(3-r)^2}\right] x^2} \ . \tag{245}$$

Since the coefficients of both the x and x^2 terms in the denominator of $[0,2]_{\beta_{x,rd,3\ell}}$ are positive, this approximant clearly has no pole for physical (non-negative) x. Explicitly, the poles in $[0,2]_{\beta_{x,rd,3\ell}}$ occur at

$$x_{[0,2],pole} = \frac{(3-r)\Big[-(2r-3) \pm \sqrt{F_s} \ \Big]}{E_s} \ , \tag{246}$$

Table 8: Values of the IR pole(s) of the $[p, q]$ Padé approximants, with $q = 1$ and $q = 2$, to $\beta_{x,2\ell}$ and $\beta_{x,3\ell,\overline{\rm DR}}$, as functions of r, in the LNN limit of the SQCD theory. The entries in the columns are (i) $x_{[0,1]_{pole}}$, pole of [0,1] approximant to $\beta_{x,rd,2\ell}$; (ii) $x_{[1,1]_{pole}}$, pole of [1,1] approximant to $\beta_{x,rd,3\ell,\overline{\rm DR}}$; (iii) $\{x_{[0,2]_{pole}}\}$, poles of [0,2] approximant to $\beta_{x,rd,3\ell,\overline{\rm DR}}$.

r	$x_{[0,1]_{pole}}$	$x_{[1,1]_{pole}}$	$\{x_{[0,2]_{pole}}\}$
0.0	0.500	0.286	$-1, \quad 0.333$
0.1	0.518	0.296	$-1.034, \quad 0.345$
0.2	0.538	0.307	$-1.070, \quad 0.358$
0.3	0.5625	0.319	$-1.109, \quad 0.373$
0.4	0.591	0.332	$-1.150, \quad 0.390$
0.5	0.625	0.348	$-1.195, \quad 0.410$
0.6	0.667	0.366	$-1.245, \quad 0.434$
0.7	0.719	0.387	$-1.304, \quad 0.463$
0.8	0.786	0.414	$-1.376, \quad 0.500$
0.9	0.875	0.449	$-1.473, \quad 0.549$
1.0	1.000	0.500	$-1.618, \quad 0.618$
1.1	1.1875	0.584	$-1.876, \quad 0.727$
1.2	1.500	0.769	$-2.519, \quad 0.940$
1.3	2.125	1.739	$-11.368, \quad 1.790$
1.4	4.000	-0.7143	$0.303 \pm 1.527i$
1.5	∞	0	$\pm i$
1.6	-3.500	0.1695	$-0.0808 \pm 0.748i$
1.7	-1.625	0.255	$-0.110 \pm 0.588i$
1.8	-1.000	0.3125	$-0.119 \pm 0.473i$
1.9	-0.6875	0.359	$-0.118 \pm 0.385i$
2.0	-0.500	0.400	$-0.111 \pm 0.314i$
2.1	-0.375	0.440	$-0.101 \pm 0.256i$
2.2	-0.286	0.479	$-0.0895 \pm 0.208i$
2.3	-0.219	0.521	$-0.0770 \pm 0.167i$
2.4	-0.167	0.566	$-0.0644 \pm 0.132i$
2.5	-0.125	0.615	$-0.0519 \pm 0.101i$
2.6	-0.0909	0.671	$-0.0400 \pm 0.0753i$
2.7	-0.0625	0.734	$-0.0288 \pm 0.0526i$
2.8	-0.0385	0.807	$-0.0184 \pm 0.0328i$
2.9	-0.0179	0.895	$-0.00875 \pm 0.0154i$
3.0	0	1	0

where

$$F_s = 36 - 48r + 21r^2 - 4r^3 \ . \tag{247}$$

The polynomial F_s has only one real zero, at $r = 1.3223$, and is positive (negative) for r less (greater) than this value. Hence, F_s is negative for all $r \in I_{r,NACP}$. We list values of $x_{[0,2],pole}$ as a function of r in Table 8.

These results answer the five questions that we posed above. The answer to the first question is yes, the quantities $\beta_{x,rd,2\ell} = [1,0]_{\beta_{x,rd,2\ell}}$, $\beta_{x,rd,3\ell} = [2,0]_{\beta_{x,rd,3\ell,\overline{\rm DR}}}$, and $[1,1]_{\beta_{x,rd,3\ell,\overline{\rm DR}}}$ all exhibit (physical) IR zeros. This property is in agreement with existence of an IR in the NSVZ beta function for $r \in I_{r,NACP}$. Second, in each case, the respective IR zero controls the UV to IR evolution, and this again agrees with the NSVZ beta function. Actually, the only case to check is the $[1,1]_{\beta_{x,rd,3\ell,\overline{\rm DR}}}$ Padé approximant, for which we have proved that the pole is always farther from the origin than the IR zero. This is also evident from an inspection of the entries for zeros and poles in Tables 7. and 8.

Concerning the third and fourth questions, for r in the upper part of the interval $I_{r,NACP}$, where the IR zero in the n-loop beta function occurs at a rather small value, one expects that the values of this IR zero calculated from this beta function itself, from the Padé approximants to the (reduced) beta function, and from the NSVZ beta function should agree, and this expectation is borne out by the results, as listed in Table 7. For example, for the illustrative value $r = 2.5$, $x_{IR,2\ell} = 0.125$, $x_{IR,3\ell} = 0.107$, $x_{IR,3\ell,[1,1]} = 0.104$, and $x_{IR,NSVZ} = 0.100$. Aside from the lowest-order, two-loop value, the last three values of the IR zero are quite close to each other. As r decreases in the interval $I_{r,NACP}$, the differences tend to grow somewhat. Thus, for $r = 2.0$, $x_{IR,2\ell} = 0.500$, $x_{IR,3\ell} = 0.290$, $x_{IR,3\ell,[1,1]} = 0.222$, and $x_{IR,NSVZ} = 0.250$. Again, aside from the lowest-order, two-loop value, the last three values are within about 10 % of each other.

Finally, concerning the fifth question, pertaining to the pole in the $[p,q]$ Padé approximants with $q \neq 0$, one should remark at the outset that since this pole occurs farther from the origin than the IR zero, it does not directly affect the evolution from weak coupling in the UV to the IR, so its precise value is not directly relevant for this evolution. The values of the pole position from the $[0,1]$, $[1,1]$ and $[0,2]$ Padé approximants are listed in Table 8. As discussed in connection with Eq. (184), given the fact that the series expansion of the NSVZ beta function must agree with the $\overline{\rm DR}$ to two-loop order and given the identity (184), it follows that since the two-loop beta function

(equivalently, the [1,0] Padé) has a physical IR zero, the pole in the [0,1] Padé approximant to $\beta_{x,r,2\ell}$ must occur at a negative and hence unphysical value of x. At the three-loop level, the two relevant two Pad'e approximants, [1,1] and [0,2] have poles at different values of x, and only one, namely [1,1], has a pole at a physical value of x. Furthermore, the position of this pole varies as a function of r, decreasing from 1 at $r = 3$ to 0 at $r = 3/2$, in contrast to the pole in $\beta_{x,NSVZ}$, which has a fixed value at $x_{pole,NSVZ} = 1/2$. More generally, even the unphysical poles in the [0,1] and [0,2] Padé approximants vary considerably as functions of r. Thus, these Padé approximants do not exhibit evidence of a stable pole. Of course, these results do not preclude the possibility that if the beta function in the $\overline{\rm DR}$ scheme could be calculated to higher order, one might begin to see evidence of a stable pole in the $[p, q]$ Padé approximants with $q \neq 0$.

3.3.4 Analysis for $0 < r < 3/2$

In this interval of r, $\hat{b}_1$ and $\hat{b}_2$ have the same sign, so the two-loop beta function does not have any IR zero, and this is the maximum scheme-independent information that one has concerning the IR zero. Hence, using this two-loop beta function, one infers that as the scale μ decreases from the deep UV to the IR, the gauge coupling continuously increases, eventually exceeding the region where one can use perturbative methods to calculate it reliably. Formally, the three-loop beta function calculated in the $\overline{\rm DR}$ scheme continues to exhibit an IR zero, $x_{IR,3\ell,\overline{\rm DR}}$, given in Eq. (215), for a small interval of r below 3/2. However, one cannot take this to be a physically compelling result, in view of the fact that the maximal scheme-independent information available (from the two-loop beta function) does not exhibit any IR zero. Furthermore, as r decreases from 3/2 to the zero of D_s at $r = (21 - \sqrt{105}\,)/8 = 1.3441$ (see Eq. (213)), $x_{IR,3\ell,\overline{\rm DR}}$ grows without bound, so that one can ignore it, since the value of the IR zero is beyond the regime where one would consider perturbation theory to be reliable. Indeed, as is evident from the expression for $[1,1]_{zero}$ in Eq. (221), the [1,1] Padé approximant to $\beta_{x,r,3\ell,\overline{\rm DR}}$ ceases to have a physical IR zero as r decreases through 3/2. The absence of a (physical) IR zero from a perturbatively reliable calculation using the beta function in the $\overline{\rm DR}$ scheme for $0 < r < 3/2$ is in agreement with the prediction from the NSVZ beta function; as discussed above, for r in the interval $0 < r < 3/2$, the formal zero at $x_{IR,NSVZ}$ lies farther from the origin than the pole at $x = 1/2$ and hence is not directly relevant to the UV to IR evolution of the theory.

We proceed to address and answer the following questions for this interval $0 \leq r < 3/2$:

1. Do the $[p, q]$ Padé approximants with $q \neq 0$ exhibit a physical pole?

2. If the answer to the first question is affirmative, then does this pole occur closer to the origin than any IR zero (if such a zero is present) and hence dominate the UV to IR evolution of the theory?

3. If the answers to the first two questions are affirmative, then is this IR pole close to the value $x_{pole,NSVZ} = 1/2$ of the pole in the NSVZ beta function?

4. If the answers to the first two questions are affirmative, then, independent of whether the poles in different $[p, q]$ Padé approximants with $q \neq 0$ are close to $x_{IR,NSVZ} = 1/2$, do these different approximants at least exhibit a stable (physical) pole?

In the present case, the relevant Padé approximants are [0,1], [1,1], and [0,2]. As is clear from the explicit expressions for these approximants and their poles given above, the poles do not occur at a fixed value of x and are not, in general, equal to $x_{IR,NSVZ}$. As is evident from (242), the pole in the [0,1] Padé approximant to $\beta_{x,r,2\ell}$ occurs at $x = 1/2$ only if $r = 0$ and increases monotonically without bound as r increases from 0 to 3/2. The pole in the [1,1] Padé approximant to $\beta_{x,r,3\ell,\overline{\rm DR}}$ increases monotonically as a function of r from 0.286 at $r = 0$ and diverges as r approaches the value $(21 - \sqrt{105}\,)/8 = 1.3441$ from below. In the small interval $1.3441 < r < 3/2$, this pole occurs at negative x and hence is unphysical. Only at the value $r = 1$ is the position of this pole in the [1,1] Padé equal to 1/2. The [0,2] Padé approximant to $\beta_{x,r,3\ell,\overline{\rm DR}}$ has two poles, one of which is always unphysical. The other pole of the [0,2] Padé occurs at an r-dependent value that increases from 1/3 at $r = 0$ and diverges as r approaches the zero in E_s at $r = 1.3118$ from below. It is negative for r in the small interval $1.3118 < r < 1.3223$, where $r = 1.3223$ is the point where F_s has a zero; finally, in the small interval $1.3223 < r < 3/2$, it is complex. This pole in the [0,2] Padé is approximately equal to 1/2 for $r = 0.8$.

These results provide answers to the questions stated above. The answer to the first question is that over much of the interval $0 \leq r < 3/2$, the [0,1], [1,1], and [0,2] Padé approximants do exhibit physical poles, but these all vary

as functions of r and are not stable at any particular fixed value. Second, since there is no robust, scheme-independent IR zero in the beta function, these poles do dominate the UV to IR evolution. Third, the values of the poles in the various Padé approximants exhibit some scatter and are not, in general, equal to (the r-independent) value $x_{IR,NSVZ} = 1/2$. Concerning the fourth question, although the pole in the [0,1] Padé is not very close to the pole in the [1,1] Padé or the physical pole in the [0,2] Padé, the latter two poles are in fair agreement with each other. For example (see Table 8) over much of the interval $0 \le r < 3/2$, the ratio of the physical pole in the [0,2] Padé divided by the pole in the [1,1] Padé is about 1.2, which is reasonably close to unity. One may interpret this as indicating that, at least for the three-loop beta function calculated in the $\overline{\rm DR}$ scheme for this theory, there is rough agreement, at about the 20 % level, between the pole in the [1,1] Padé approximant and the physical pole in the [0,2] Padé approximant.

3.4 Chiral Superfields in Symmetric and Antisymmetric Rank-2 Tensor Representations

3.4.1 Beta Function and IR Zeros

Here we consider a (vectorial, asymptotically free) $\mathcal{N} = 1$ supersymmetric SU(N_c) gauge theory with N_f copies of massless chiral superfields Φ_i and $\tilde{\Phi}_i$, $i = 1, ..., N_f$, transforming according to the symmetric and antisymmetric rank-2 tensor representations and their conjugates. We denote these symmetric and antisymmetric rank-2 tensor representations as S_2 and A_2, respectively. While the S_2 theory is defined for all $N_c \ge 2$, the A_2 theory is defined for $N_c \ge 3$, since the A_2 representation is a singlet if $N_c = 2$. We restrict our consideration to values $N_f \ne 0$ here, since if $N_f = 0$, the present theory reduces to a pure supersymmetric Yang-Mills gauge theory, which we have already analyzed above. The one-loop and two-loop coefficients in the beta function are (e.g., [33])

$$b_1 = 3N_c - (N_c \pm 2)N_f \ , \tag{248}$$

and

$$b_2 = 2\Big[3N_c^2(1 - N_f) \mp 8(N_c - N_c^{-1})N_f\Big] \ . \tag{249}$$

where the upper and lower signs apply for the S_2 and A_2 theories, respectively. Evaluating Eq. (152), we obtain, for b_3 in the $\overline{\rm DR}$ scheme,

$$b_3 \ = \ 7N_c^3(N_f - 1)(N_f - 3) \pm 2N_c^2 N_f(-33 + 17N_f)$$

$$
\begin{aligned}
&+ \quad 8N_cN_f(1+5N_f) \mp 24N_f(N_f-1) \\
&- \quad 16N_c^{-1}N_f(2+3N_f) \pm 64N_c^{-2}N_f \ . \qquad (250)
\end{aligned}
$$

It will often be convenient to refer to these two cases together as T_2 (standing for tensor, rank-2) with the above sign convention, and we shall do so. The one-loop coefficient decreases with increasing N_f and passes through zero with sign reversal for $N_f = N_{f,b1z,T_2}$, where

$$
N_{f,b1z,T_2} = \frac{3N_c}{N_c \pm 2} \ . \qquad (251)
$$

In the S_2 theory, $N_{f,b1z,S_2}$ increases monotonically from 3/2 for $N_c = 2$, approaching the limiting value 3 from below as $N_c \to \infty$, while in the A_2 theory, $N_{f,b1z,A_2}$ decreases monotonically from 9 for $N_c = 3$, approaching the limiting value 3 from above as $N_c \to \infty$. The two-loop coefficient also decreases with increasing N_f and passes through zero with sign reversal for $N_f = N_{f,b2z,T_2}$, where

$$
N_{f,b2z,T_2} = \frac{3N_c^2}{3N_c^2 \pm 8(N_c - N_c^{-1})} \ . \qquad (252)
$$

From the exact results recalled above, it follows that the lower boundary of the IR non-Abelian Coulomb phase is

$$
N_{f,cr,T_2} = \frac{N_{f,b1z,T_2}}{2} = \frac{3N_c}{2(N_c \pm 2)} \ . \qquad (253)
$$

In the S_2 theory, $N_{f,cr}$ increases monotonically from 3/4 for $N_c = 2$, approaching 3/2 from below as $N_c \to \infty$, while in the A_2 theory, $N_{f,cr}$ decreases monotonically from 9/2 for $N_c = 3$, approaching 3/2 from above as $N_c \to \infty$. Hence, the IR non-Abelian Coulomb phase exists for (integral) N_f values in the interval

$$
I_{NACP,(S_2,A_2}: \quad \frac{3N_c}{2(N_c \pm 2)} < N_f < \frac{3N_c}{N_c \pm 2} \ . \qquad (254)
$$

In the S_2 theory, as noted in [33], $N_{f,b2z,S_2} < N_{f,cr,S_2}$, so $b_2 < 0$ if N_f is in the non-Abelian Coulomb interval (254). In the A_2 theory, $N_{f,b2z,A_2} < N_{f,cr,A_2}$ if $N_f = 1$ or $N_f = 2$, while $N_{f,b2z,A_2} > N_{f,cr,A_2}$ if $N_f = 3$.

Assuming that N_f is in the respective ranges where $b_2 < 0$ in the S_2 and A_2 theories, the theory has an IR zero in the beta function at the two-loop

level, occuring at $a_{IR,2\ell,T_2} = -b_{1,T_2}/b_{2,T_2}$, i.e.,

$$a_{IR,2\ell,T_2} = \frac{3N_c - (N_c \pm 2)N_f}{2[3N_c^2(N_f-1) \pm 8(N_c - N_c^{-1})N_f]} \ . \tag{255}$$

As noted above, this two-loop result is scheme-independent. To calculate the IR zero of the NSVZ beta function using the corresponding maximal scheme-independent information in γ_m, we use Eq. (161) for the one-loop term in γ_m and thus solve the equation $b_{1,T_2} - 2N_f T_f c_1 a = 0$, obtaining the result

$$a_{IR,NSVZ,T_2} = \frac{N_c[N_c(3-N_f) \mp 2N_f]}{4N_f(N_c \pm 2)^2(N_c \mp 1)} \ . \tag{256}$$

To analyze the extent to which the perturbative beta functions of the S_2 and A_2 theories, calculated in the $\overline{\rm DR}$ scheme, exhibit similarities with the NSVZ beta function, we proceed to consider these functions at the three-loop level. To carry out this analysis, we focus on the case $N_c \to \infty$ and again work with the scaled beta function $\beta_x = dx/dt$. In this limit, the beta functions β_{x,S_2} and β_{x,A_2} and for the S_2 and A_2 theories become the same, and we shall denote the resulting beta function as β_{x,T_2}. Similarly, the intervals given in Eq. (254) also become the same, reducing to

$$I_{NACP,T_2}: \quad \frac{3}{2} < N_f < 3 \quad \text{for } N_c \to \infty \tag{257}$$

Hence, the interval I_{NACP,T_2} contains only one physical, integral value of N_f in this limit, namely $N_f = 2$.

With the definition (326), we have, for the (scheme-independent) one-loop and two-loop rescaled coefficients $\hat{b}_\ell$, the results

$$\hat{b}_{1,T_2} = 3 - N_f \ , \tag{258}$$

and

$$\hat{b}_{2,T_2} = -6(N_f - 1) \ . \tag{259}$$

Note that $\hat{b}_{2,T_2}$ vanishes for $N_f = 1$, so that the two-loop beta function has no IR zero for this value of N_f.

In general, the IR zero of the rescaled two-loop beta function β_{x,T_2} is $x_{IR,T_2} = -\hat{b_{1,T_2}}/\hat{b}_{2,T_2}$, i.e.,

$$x_{IR,2\ell,T_2} = \frac{3 - N_f}{6(N_f - 1)} \ . \tag{260}$$

The only value of N_f for which this has a finite, nonzero value is $N_f = 2$, and for $N_f = 2$, $x_{IR,2\ell,T_2} = 1/6$. In this limit, the rescaled NSVZ beta function $\beta_{x,NSVZ,T_2}$ has an IR zero at

$$x_{IR,NSVZ,T_2} = \frac{3 - N_f}{4N_f} \ . \tag{261}$$

For $N_f = 2$, this has the value

$$x_{IR,NSVZ,T_2} = \frac{1}{8} \quad \text{for } N_f = 2 \ . \tag{262}$$

In the $\overline{\rm DR}$ scheme, the three-loop coefficient in β_{x,T_2} is

$$\hat{b}_{3,T_2} = -7(N_f - 1)(3 - N_f) \ . \tag{263}$$

Hence, if $N_f = 1$, the three-loop beta function in the $\overline{\rm DR}$ scheme is the same as the (scheme-independent) two-loop beta function, in which the two-loop coefficient also vanishes. Thus, if $N_f = 1$ here, the beta function reduces simply to the one-loop term, which has no IR zero.

The three-loop beta function, $\beta_{x,3\ell,T_2}$, for the S_2 and A_2 theories in this limit, with $\hat{b}_3$ calculated in the $\overline{\rm DR}$ scheme, is

$$\beta_{x,3\ell,T_2} = -2x^2(\hat{b}_{1,T_2} + \hat{b}_{2,T_2}x + \hat{b}_{3,T_2}x^2) \ . \tag{264}$$

From Eq. (173), it follows that the reduced three-loop beta function $\beta_{x,rd,3\ell,T_2}$ is

$$\begin{aligned} \beta_{x,rd,3\ell,T_2} &= 1 + \frac{\hat{b}_{2,T_2}}{\hat{b}_{1,T_2}}x + \frac{\hat{b}_{3,T_2}}{\hat{b}_{1,T_2}}x^2 \\ &= 1 - \frac{6(N_f - 1)}{3 - N_f}\, x - 7(N_f - 1)x^2 \ . \end{aligned} \tag{265}$$

If $N_f \neq 1$ (and $N_f \neq 3$), the equation $\beta_{x,rd,3\ell,T_2} = 0$ has, formally, two solutions, given by

$$x_{IR,3\ell,T_2,\pm} = \frac{1}{7(3 - N_f)} \Big[-3 \pm \sqrt{\frac{7N_f^2 - 33N_f + 54}{N_f - 1}} \ \Big] \ . \tag{266}$$

For $N_f = 2$, the solution with the + sign in front of the square root is equal to $x_{IR,3\ell,T_2,+} = 1/7 = 0.14286$, which is reasonably close to the NSVZ result of 1/8 given in Eq. (262). (The solution with the minus sign in Eq. (266) has the unphysical negative value -1 and hence is not relevant.)

Table 9: Values of zeros and poles, in the variable x, of Padé approximants to $\beta_{x,rd,2\ell}$ and $\beta_{x,rd,3\ell,\overline{\rm DR}}$ for the $\mathcal{N}=1$ supersymmetric gauge theory with $N_f=2$ copies of chiral superfields in the symmetric or antisymmetric rank-2 tensor representation and its conjugate, in the limit $N_c \to \infty$. Results are given to the indicated floating-point accuracy. The abbreviation NA means "not applicable".

n	$[p,q]$	zero(s)	pole(s)
2	[1,0]	$1/6 = 0.167$	NA
2	[0,1]	NA	$-1/6 = -0.167$
3	[2,0]	$-1,\ 1/7 = 0.143$	NA
3	[1,1]	$6/43 = 0.1395$	$6/7 = 0.857$
3	[0,2]	NA	$-0.0698 \pm 0.1356i$

3.4.2 Padé Approximants

We next calculate the Padé approximants to the two-loop and three-loop reduced beta functions, $\beta_{x,rd,2\ell,T_2}$ and $\beta_{x,rd,3\ell,T_2}$, respectively. As before, these functions are identical to the [1,0] and [2,0] approximants, respectively, so our analysis given above of the zeros of $\beta_{x,rd,2\ell,T_2}$ and $\beta_{x,rd,3\ell,T_2}$ applies to these approximants. We list these results in Table 9 and proceed to calculate and analyze the $[p,q]$ approximants with $q \neq 0$. With $\beta_{x,rd,2\ell,T_2}$ we can only calculate one $[p,q]$ approximant with $q \neq 0$, namely the [0,1] approximant. We find

$$[0,1]_{\beta_x,rd,2\ell,T_2} = \frac{1}{1+\frac{6(N_f-1)}{3-N_f}x} \ . \tag{267}$$

Thus, as a special case of the relation (184), this Padé approximant has a pole at

$$\begin{aligned} [0,1]_{T_2,pole} &= -[1,0]_{T_2,zero} = -x_{IR,2\ell,T_2} \\ &= -\frac{(3-N_f)}{6(N_f-1)} \ . \end{aligned} \tag{268}$$

For $N_f = 2$,, this pole occurs at $x = -1/6$.

At the three-loop level, assuming that $N_f \neq 1$ (where the three-loop and two-loop coefficients vanish), we calculate, for the [1,1] approximant, the

result

$$[1,1]_{\beta_x,rd,3\ell,T_2} = \frac{1 - \frac{(7N_f^2-6N_f+27)}{6(3-N_f)}x}{1 - \frac{7(3-N_f)}{6}x} \ . \tag{269}$$

The fact that $\hat{b}_2$ and $\hat{b}_3$ vanish at $N_f = 1$ is reflected in the property that this [1,1] Padé approximant reduces to unity at this value of N_f. For $N_f \neq 1$, this approximant has a IR zero at

$$[1,1]_{T_2,zero} = \frac{6(3-N_f)}{7N_f^2 - 6N_f + 27} \ . \tag{270}$$

and a pole at

$$[1,1]_{T_2,pole} = \frac{6}{7(3-N_f)} \ . \tag{271}$$

The polynomial $7N_f^2 - 6N_f + 27$ is positive for all (real) N_f. We note the inequality

$$[1,1]_{T_2,zero} < [1,1]_{T_2,pole} \ . \tag{272}$$

This is proved by calculating the difference,

$$[1,1]_{T_2,pole} - [1,1]_{T_2,zero} = \frac{6^3(3-N_f)}{7(N_f-1)(7N_f^2-6N_f+27)} \ . \tag{273}$$

Evidently, since $N_f \neq 0,\ 1$ and $N_f < 3$, the right-hand side of (273) is positive-definite. For $N_f = 2$, we have $[1,1]_{T_2,zero} = 6/43 = 0.1395$ and $[1,1]_{T_2,pole} = 6/7 = 0.8571$. These values are listed in Table 9.

We compute the [0,2] Padé approximant to $\beta_{x,rd,3\ell,T_2}$ to be

$$[0,2]_{\beta_x,rd,3\ell,T_2} = \frac{1}{1 + \frac{6(N_f-1)}{(3-N_f)}x + \frac{(N_f-1)(7N_f^2-6N_f+27)}{(3-N_f)^2}x^2} \ . \tag{274}$$

This has, formally, two poles, at the values

$$\begin{aligned} [0,2]_{T_2,pole} &= \frac{(3-N_f)}{(7N_f^2-6N_f+27)} \Big[-3 \\ &\pm \sqrt{\frac{-7N_f^2+15N_f-36}{N_f-1}} \ \Big] \ . \end{aligned} \tag{275}$$

However, recalling that $N_f \neq 0,\ 1$, one sees that these poles are both unphysical, because the polynomial in the square root, $-7N_f^2 + 15N_f - 36$, is negative-definite. Explicitly, for $N_f = 2$, Eq. (275) yields the pole values $x = (1/43)(-3 \pm \sqrt{34}\, i\ ) = -0.0698 \pm 0.1356i$, as is listed in Table 9.

Let us summarize our results for these theories with a nonzero number, N_f, of copies of chiral superfields in the S_2 or A_2 representation and their respective conjugates, in the limit $N_c \to \infty$. In this limit, $N_f < 3$ for asymptotic freedom. For $N_f = 1$, the (scheme-independent) two-loop term in the beta function β_{x,T_2} vanishes, as does the three-loop term with the latter calculated in the $\overline{\rm DR}$ scheme, so that the beta function, calculated to these loop orders, does not contain any IR zero or any indication, via Padé approximants, of a pole.

For this theory with $N_f = 2$, our analysis of the two-loop and three-loop $\overline{\rm DR}$ beta functions, and the [1,1] Padé approximant to the latter all give evidence of an IR zero, with respective values 1/6, 1/7, and 6/43=0.1395, which decrease monotonically, approaching the the value $x_{IR,NSVZ,T_2} = 1/8$ from the NSVZ beta function. Thus, we find reasonably good agreement between these IR zeros calculated in different schemes. We come next to the questions of whether, for this theory, the $[p,q]$ Padé approximants with $q \neq 0$ to the two-loop and three-loop beta function give some indication of a (physical) pole and whether this pole occurs at a value close to the value $x = 1/2$ in the NSVZ beta function. Our result is that neither the [0,1] nor the [0,2] Padé approximants has any physical pole, while the [1,1] Padé does exhibit a pole, although it is roughly twice the value $x = 1/2$. As in the case of the theory containing chiral superfields in the fundamental and antifundamental representations, this suggests that it is necessary to calculate the beta function in the $\overline{\rm DR}$ scheme to higher-loop order and calculate higher-order Padé approximants to test for indications of a pole.

4 Renormalization-Group Evolution of the Finite-N Gross-Neveu Model

In this section we discuss our results on the renormalization-group evolution of the finite-N Gross-Neveu model, which were published in Ref. [4]. We begin with a review of some background.

The Gross-Neveu (GN) model [72] is a quantum field theory in $d = 2$ spacetime dimensions with an N-component massless fermion ψ_j, $j = 1, ..., N$, defined by the path integral

$$Z = \int \prod_x [\mathcal{D}\psi][\mathcal{D}\bar{\psi}]\, e^{i\int d^2x\, \mathcal{L}} \ , \tag{276}$$

with the Lagrangian density [73]

$$\mathcal{L}_{GN} = i\bar{\psi}\gamma^\mu\partial_\mu\psi + \frac{g}{2}(\bar{\psi}\psi)^2 \ . \tag{277}$$

This model is of interest because it exhibits, albeit in a lower-dimensional, non-gauge-theory context, some properties of quantum chromodynamics (QCD), namely asymptotic freedom, dynamical symmetry breaking of a certain chiral symmetry, and the formation of a massive bound state of fermions. These properties were shown by an exact solution of the model in [72] in an $N \to \infty$ limit that enabled Gross and Neveu to obtain nonperturbative information about the theory. A semiclassical calculation of the bound-state spectrum of the model was carried out in [74].

The Gross-Neveu model has also been studied at finite N, where it is not, in general, exactly solvable. In these studies, one again makes use of a property that the model shares with QCD, namely asymptotic freedom, which allows one to carry out reliable perturbative calculations at high Euclidean energy/momentum scales μ in the deep ultraviolet (UV), where the running four-fermion coupling, $g(\mu)$, approaches zero. In this context, there is an interesting and fundamental question: how does this running coupling $g(\mu)$ change as the scale μ decreases from the deep UV to the infrared (IR) limit at $\mu = 0$? This change of $g(\mu)$ as a function of μ is described by the renormalization group (RG) [5] and the associated beta function, $\beta = dg/dt$, where $dt = d\ln\mu$. The asymptotic freedom property is equivalent to the fact that β is negative in the vicinity of the origin, $g = 0$, so that this point is a UV fixed point (UVFP) of the renormalization group. As μ decreases from

the UV toward the IR, several different types of behavior of a theory are, *a priori*, possible. One is that the (perturbatively calculated) beta function has no IR zero, so that as μ decreases, $g(\mu)$ eventually increases beyond the range where perturbative methods can be used to study its RG evolution. An alternative possibility is that β has an IR zero at sufficiently small coupling so that it can be studied using perturbative methods. An exact IR zero of β would be an IR fixed point (IRFP) of the renormalization group. In the $N \to \infty$ limit used in [72] to solve the model, the resultant beta function (given below in Eq. (286)) does not exhibit any IR zero. Ref. [75] calculated $1/N$ corrections to the $N \to \infty$ limit in the Gross-Neveu model and excluded the presence of an IR zero to this order. However, to our knowledge, there has not been an analysis of the beta function of the GN model for finite N to higher-loop order to address the question of whether it exhibits evidence for an infrared fixed point.

In this section, we shall carry out this analysis of the beta function of the finite-N Gross-Neveu to address and answer the question of whether this function exhibits an IR zero in its beta function. We shall investigate the beta function to the highest loop order to which it has been calculated, namely four loops, making use of a recent computation of the four-loop term in Ref. [76].

Our discussion on this work is organized as follows. In Section 4.1 we review some background information about the Gross-Neveu model. In Section 4.2 we carry out our analysis of the beta function of the finite-N Gross-Neveu model up to the four-loop level. In Section 4.3 we extend this analysis using Padé approximants. Section 4.4 contains an analysis of the effect of scheme transformations on the beta function. In Section 4.5 we comment further on the large-N limit.

4.1 Some Relevant Background on the Gross-Neveu Model

Here we briefly review some relevant background concerning the Gross-Neveu model. We first comment on some notation. In Ref. [72], the coefficient in front of the $(\bar{\psi}\psi)^2$ operator was written as a squared coupling, which we denote as $(g_{GN}^2/2)$, while many subsequent works have written it as $g/2$, so one has

$$g \equiv g_{GN}^2 \ . \tag{278}$$

The analysis of the model in [72] made use of a functional integral identity to express the path integral as the $m \to \infty$ limit of a path integral containing an auxiliary real scalar field ϕ with a mass m and a Yukawa interaction

$$\mathcal{L}_Y = g_{GN} m [\bar{\psi}\psi]\phi \ . \tag{279}$$

Since ϕ is a real field, the hermiticity of $\mathcal{L}_Y$ implies that g_{GN} must be real, which, in conjunction with Eq. (278), implies that g must be non-negative:

$$g \geq 0 \ . \tag{280}$$

For $d = 2$ (as more generally, for any even spacetime dimension), one can define a product of Dirac gamma matrices, denoted γ_5, that satisfies the anticommutation relation $\{\gamma_5, \gamma_\mu\} = 0$ for all γ_μ. This γ_5 matrix also satisfies $\gamma_5^2 = 1$ and $\gamma_5^\dagger = \gamma_5$. (An explicit representation is $\gamma_0 = \sigma_1$, $\gamma_1 = \sigma_2$, with $\gamma_0\gamma_1 = i\gamma_5 = i\sigma_3$, where σ_j are the Pauli matrices.) One can then define chiral projection operators $P_{L,R} = (1/2)(1 \pm \gamma_5)$. As usual, one then defines left and right chiral components of the fermion field as $\psi_L = P_L\psi$ and $\psi_R = P_R\psi$.

The Gross-Neveu model is invariant under a discrete global $\mathbf{Z}_2$ group generated by the identity and the chiral transformation

$$\psi \to \gamma_5 \psi \ . \tag{281}$$

This discrete chiral transformation (281) takes $\bar{\psi}\psi \to -\bar{\psi}\psi$, and hence this $\mathbf{Z}_2$ symmetry forbids (i) a mass term in the Lagrangian (277) and (ii) the generation of a nonzero condensate $\langle\bar{\psi}\psi\rangle$. This is true to all (finite) orders of perturbation theory.

The Gross-Neveu model is also invariant under the continuous global (cg) symmetry group

$$G_{cg} = \mathrm{U}(N) \tag{282}$$

defined by the transformation

$$\psi \to U\psi \ , \tag{283}$$

where $U \in \mathrm{U}(N)$ (so $\bar{\psi} \to \bar{\psi}U^\dagger$). In terms of the chiral components of the fermion field, the continuous global symmetry transformation (283) is $\psi_L \to U\psi_L$, $\psi_R \to U\psi_R$. In contrast to the discrete γ_5 symmetry, the continuous symmetry G_{cg} leaves the operator $\bar{\psi}\psi$ invariant.

An exact solution of the theory was obtained in [72] in the limit $N \to \infty$ and $g_{GN} \to 0$ with the product

$$\lambda \equiv g_{GN}^2 N \equiv gN \tag{284}$$

a fixed and finite function of μ. We shall denote this as the LN limit (i.e., the large-N limit with the condition (284) imposed). In this limit, there is a nonperturbative generation of a nonzero bilinear fermion condensate, $\langle \bar{\psi}\psi \rangle$, dynamically breaking the discrete $\mathbf{Z}_2$ chiral symmetry. In this limit, there is also the formation of a massive bound state of fermions.

The beta function for g_{GN} is

$$\beta_{GN} = \frac{dg_{GN}}{dt} \ , \tag{285}$$

where $dt = d\ln\mu$. (The μ dependence of the coupling will often be suppressed in the notation.) This beta function is [72, 77]

$$\beta_{GN} = -\frac{g_{GN}\lambda}{2\pi} \ . \tag{286}$$

The fact that this beta function is negative is an expression of the asymptotic freedom of the theory. This beta function does not exhibit any zero away from the origin, i.e., any infrared zero. However, since the calculation in [72] was performed in the LN limit, this leaves open the possibility that at finite N, there could be an IR zero in the beta function that would disappear in the LN limit. We discuss this LN limit further in Section 4.5 below.

4.2 Beta Function for General N

Although the Gross-Neveu model is not, in general, solvable away from the LN limit, there has also been interest over the years in analyzing it for finite N. In terms of the coupling g, the beta function of the finite-N GN model is

$$\beta = \frac{dg}{dt} \ , \tag{287}$$

where, as before, $dt = d\ln\mu$. For our purposes, it will be convenient to introduce a variable a that includes the factor $1/(2\pi)$ resulting from Feynman integrals in $d = 2$ dimensions, namely

$$a = \frac{g}{2\pi} = \frac{g_{GN}^2}{2\pi} \ . \tag{288}$$

The $\ell = 1$ and $\ell = 2$ loop terms in β are independent of the scheme used for regularization and renormalization, while the terms at loop order $\ell \geq 3$ are scheme-dependent. The beta function was calculated up to two-loop level in [78], with the results

$$b_1 = -2(N-1) \tag{289}$$

and

$$b_2 = 2(N-1) \ . \tag{290}$$

The fact that b_1 in Eq. (289) is negative means that in $d = 2$, this theory is asymptotically free for any finite $N > 1$ as well as in the $N \to \infty$ limit considered in [72].

The three-loop coefficient, b_3, was calculated in [79, 80] in the $\overline{\rm MS}$ scheme, with the result

$$b_3 = \frac{(N-1)(2N-7)}{2} \ . \tag{291}$$

Recently, the four-loop coefficient, b_4 has been calculated, again in the $\overline{\rm MS}$ scheme, to be [76]

$$b_4 = \frac{1}{3}(N-1)\Big[-2N^2 - 19N + 24 - 6(11N-17)\zeta_3 \Big] \ , \tag{292}$$

where $\zeta_s = \sum_{n=1}^{\infty} n^{-s}$ is the Riemann zeta function.

We comment on the dependence of the beta function coefficients on N. The property that these coefficients all contain a factor of $(N-1)$ is a consequence of the fact that for $N = 1$ the GN model is equivalent to the massless abelian Thirring model [81], which has an identically zero beta function [82, 83]. Note that this statement about the beta function of the Thirring model is scheme-independent; if a beta function vanishes in one scheme, then it vanishes in all other schemes reached by acceptable (nonsingular) scheme transformations [37]. It follows that all of the coefficients b_ℓ contain a factor of $(N-1)$. Therefore, it is only necessary to analyze the beta function of the Gross-Neveu model for $N > 1$, where it is nonvanishing, and we will thus restrict to the physical integral values $N \geq 2$ henceforth. We next discuss how the b_ℓ depend on N in the relevant range $N > 1$. For this discussion, we consider N to be extended from the positive integers to the real numbers. The three-loop coefficient b_3 is a monotonically increasing function of N that is negative for $N < 7/2$, vanishes for $N = 7/2$, and is positive for $N > 7/2$. Thus, for physical, integral values, $b_3 < 0$ if $N = 2$ or $N = 3$ and $b_3 > 0$ if

$N \geq 4$. The coefficient b_4 is negative for large N and is positive for N in the interval

$$N_{b4z,m} < N < N_{b4z,p} \ , \tag{293}$$

where the subscript $b4z$ stands for "b_4 zero" and

$$N_{b4z,(p,m)} = \frac{-19 - 66\zeta_3 \pm \sqrt{553 + 3324\zeta_3 + 4356\zeta_3^2}}{4} \tag{294}$$

with (p, m) corresponding to the $\pm$ sign. These have the values $N_{b4z,m} = -50.616$ and $N_{b4z,p} = 1.448$ to the given floating-point accuracy. Thus, in the relevant range $N > 1$ under consideration here, b_4 is negative.

We proceed to investigate the question of whether the beta function for the Gross-Neveu model at finite N exhibits evidence for an infrared zero. We denote an IR zero of the n-loop beta function $\beta_{n\ell}$ as $a_{IR,n\ell}$, and the corresponding value of g as $g_{IR,n\ell} = 2\pi a_{IR,n\ell}$. This IR zero of beta is a zero for positive a closest to the origin (if there is such a zero), which one would thus reach as μ decreases from the deep UV at large μ to the IR at small μ and a increases from 0. At the two-loop level, $\beta_{2\ell}$ has an IR zero at

$$a_{IR,2\ell} = -\frac{b_1}{b_2} = 1 \ , \tag{295}$$

i.e., $g_{IR,2\ell} = 2\pi$. Note that this value is independent of N. To judge whether this constitutes convincing evidence of an IR zero in the beta function, it is necessary to determine if higher-loop calculations confirm it. We next carry out this task.

At the three-loop level, the condition that $\beta_{3\ell} = 0$ away from the origin is the quadratic equation $b_1 + b_2 a + b_3 a^2 = 0$. This has two solutions,

$$a = \frac{2[-1 \pm \sqrt{2(N-3)}\,]}{2N-7} \ . \tag{296}$$

If $N < 3$, then these solutions are complex and hence unphysical. If $N = 3$, these roots coincide, so that $a_{IR,3\ell} = 2$, i.e., $g_{IR,3\ell} = 4\pi$. For $N \geq 3$, there is only one physical root, namely

$$a_{IR,3\ell} = \frac{2[-1 + \sqrt{2(N-3)}\,]}{2N-7} \ . \tag{297}$$

However, this is not, in general, close to the two-loop zero of the beta function at $a_{IR,2\ell} = 1$. Furthermore, while $a_{IR,2\ell} = 1$ is independent of N, $a_{IR,3\ell}$ has a completely different behavior as a function of N; it decreases monotonically with N in the interval $N \geq 3$ over which it is physical and approaches zero asymptotically like

$$a_{IR,3\ell} \sim \sqrt{\frac{2}{N}} - \frac{1}{N} + O\Big(\frac{1}{N^{3/2}}\Big) \quad \text{as } N \to \infty \ . \tag{298}$$

At the four-loop level, the condition that $\beta_{4\ell} = 0$ away from the origin is the cubic equation

$$b_1 + b_2 a + b_3 a^2 + b_4 a^3 = 0 \ . \tag{299}$$

The nature of the roots of this equation is determined by the discriminant,

$$\Delta_3 = b_2^2 b_3^2 - 27 b_1^2 b_4^2 - 4(b_1 b_3^3 + b_4 b_2^3) + 18 b_1 b_2 b_3 b_4 \ . \tag{300}$$

This discriminant is negative for the relevant range $N \geq 2$ (indeed, it is negative for all real N). This implies that Eq. (299) has one real root and a pair of complex-conjugate roots. The real root is negative and hence is unphysical, since it violates the positivity requirement (280). Moreover, since it is negative, it is clearly incompatible with the values of $a_{IR,2\ell}$ and $a_{IR,3\ell}$, which are positive (discarding the unphysical complex value of $a_{IR,3\ell}$ at $N = 2$). We therefore do not label this root as $a_{IR,4\ell}$, but instead as $a_{rt,4\ell}$, where rt stands simply for the real root of Eq. (299). We find that the magnitude of $a_{rt,4\ell}$ decreases toward zero monotonically as N increases in the relevant interval $N \geq 2$, with the asymptotic behavior

$$a_{rt,4\ell} \sim -\frac{3^{1/3}}{N^{2/3}} + \frac{1}{2N} + O\Big(\frac{1}{N^{4/3}}\Big) \quad \text{as } N \to \infty \ . \tag{301}$$

We list the values of $a_{IR,2\ell}$, $a_{IR,3\ell}$, and $a_{rt,4\ell}$ in Table 10 for N from 2 to 10 and for three representative larger values, $N = 100$, 300, and 10^3.

In our discussion above, we had stated that in order to judge whether the result for $a_{IR,2\ell}$ constitutes convincing evidence of an IR zero in the beta function, it is necessary to determine if higher-loop calculations confirm it. A necessary condition for the reliability of a perturbative calculation is that if one calculates some quantity to a given loop order, then there should not be a large fractional change in this quantity if one computes it to one higher order in the loop expansion. This condition applies, in particular, to

Table 10: Values of $a_{IR,2\ell}$, $a_{IR,3\ell}$, and $a_{rt,4\ell}$ for the beta function of the Gross-Neveu model, as a function of N. Here, the three-loop and four-loop coefficients b_3 and b_4 are calculated in the $\overline{\rm MS}$ scheme. If $N = 2$, then the zeros of $\beta_{3\ell}$ at nonzero a form an unphysical complex (cmplx) pair. As indicated, all of the values of $a_{rt,4\ell}$ are negative and hence unphysical. See text for further details.

N	$a_{IR,2\ell}$	$a_{IR,3\ell}$	$a_{rt,4\ell}$
2	1	cmplx	-0.573
3	1	2.000	-0.370
4	1	0.828	-0.302
5	1	0.667	-0.264
6	1	0.580	-0.239
7	1	0.522	-0.220
8	1	0.481	-0.205
9	1	0.448	-0.194
10	1	0.422	-0.184
100	1	0.134	-0.0567
300	1	0.0788	-0.0295
10^3	1	0.0438	-0.0138

the calculation of a putative zero of the beta function. Quantitatively, in order for the perturbative calculation of the IR zero of a beta function to be reliable, it is necessary that the fractional difference

$$\frac{|a_{IR,(n-1)\ell} - a_{IR,n\ell}|}{\frac{1}{2}[a_{IR,(n-1)\ell} + a_{IR,n\ell}]} \tag{302}$$

should be reasonably small and should tend to decrease with increasing loop order, n. As is evident both from our analytic formulas and from the numerical results listed in Table 10, this necessary condition is not satisfied in the present case.

The reason for this is clear from a plot of the beta functions $\beta_{n\ell}$ at loop orders $n = 2$, $n = 3$, and $n = 4$. This shows that the IR zero in the two-loop beta function occurs at a value of a that is too large for the perturbative calculation to be reliable. In Fig.5 and 6 we plot the two-loop, three-loop, and four-loop beta functions for the Gross-Neveu model as functions of a for two illustrative values of N, namely $N = 3$ and $N = 10$. As is evident from these plots, the beta function does not satisfy the necessary criterion for the reliability of a calculation of an IR zero. For the IR zero of the two-loop beta function at $a_{IR,2\ell} = 1$ to be reliable, one requires that the curves for the three-loop and four-loop beta functions should agree approximately with the curve for the two-loop beta function for $a \simeq 1$, and that these higher-loop beta functions should thus have respective IR zeros that are close to the two-loop zero at $a_{IR,2\ell} = 1$. But this is not the case; for $N = 3$, $\beta_{3\ell}$ has a double zero at the larger value, $a_{IR,3\ell} = 2$ and then goes negative again, while $\beta_{4\ell}$ has no IR zero in the physical region, $a > 0$. For $N = 10$ the three-loop beta function $\beta_{3\ell}$ vanishes at a smaller value of a than $a = 1$ (and this value, $a_{IR,3\ell}$ decreases as N increases), while the four-loop beta function $\beta_{4\ell}$ again has no IR zero in the physical region, $a > 0$. The behavior illustrated for $N = 10$ is generic for other values of $N \geq 4$. Indeed, the curves for these beta functions at loop order $n = 2,\ 3,\ 4$ only agree with each other close to the origin, and deviate strongly from each other before one gets to values of a where a zero occurs. Specifically, for $N = 3$, $\beta_{2\ell}$ and $\beta_{3\ell}$ only agree with each other for a up to about 0.5, while $\beta_{4\ell}$ deviates from these lower-loop beta functions as a increases beyond approximately 0.2. As N increases, these deviations occur for smaller a. Thus, for $N = 10$, $\beta_{2\ell}$ and $\beta_{3\ell}$ only agree with each other for a up to roughly 0.15, while $\beta_{4\ell}$ deviates from these lower-loop beta functions as a increases beyond about 0.08.

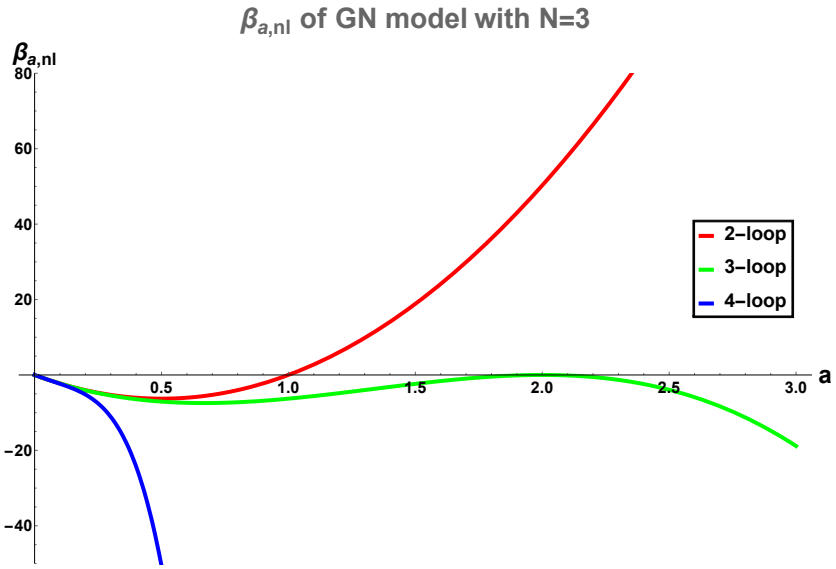

Figure 5: Plot of the n-loop β function $\beta_{a,n\ell}$ of the Gross-Neveu model as a function of a for $N = 3$ and (i) $n = 2$ (red), (ii) $n = 3$ (green), and (iii) $n = 4$ (blue) (colors in online version). At $a = 0.16$, going from bottom to top, the curves are $\beta_{4\ell}$, $\beta_{2\ell}$, and $\beta_{3\ell}$.

4.3 Analysis with Padé Approximants

In this section we carry out a further investigation of a possible IR fixed point in the renormalization-group flow for the Gross-Neveu model by calculating and analyzing Padé approximants (PAs) to the beta function at three-loop and four-loop level. Since we are interested in a possible zero of the beta function away from the origin, it will be convenient to deal with a reduced (rd) beta function,

$$\beta_{rd} \equiv \frac{\beta}{2\pi b_1 a^2} = 1 + \frac{1}{b_1}\sum_{\ell=2}^{\infty} b_\ell a^{\ell-1} \ . \tag{303}$$

The n-loop reduced beta function with $n \geq 2$, denoted $\beta_{rd,n\ell}$, is obtained from Eq. (303) by replacing $\ell = \infty$ by $\ell = n$ as the upper limit in the summand. This n-loop reduced beta function is thus a polynomial of degree $n-1$ in a. The $[p,q]$ Padé approximant to this polynomial is the rational function

$$[p,q]_{\beta_{rd,n\ell}} = \frac{1 + \sum_{j=1}^{p} n_j x^j}{1 + \sum_{k=1}^{q} d_k \, x^k} \tag{304}$$

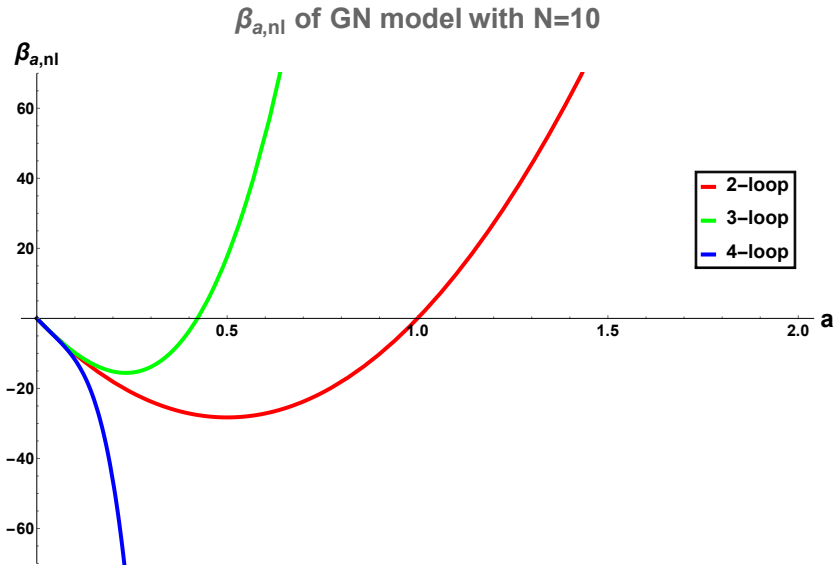

Figure 6: Plot of the n-loop β function $\beta_{a,n\ell}$ of the Gross-Neveu model as a function of a for $N = 10$ and (i) $n = 2$ (red), (ii) $n = 3$ (green), and (iii) $n = 4$ (blue) (colors in online version). At $a = 0.2$, going from bottom to top, the curves are $\beta_{4\ell}$, $\beta_{2\ell}$, and $\beta_{3\ell}$.

with

$$p + q = n - 1 \ , \tag{305}$$

where the n_j and d_k are a-independent coefficients of the respective polynomials in the numerator and denominator of $[p, q]_{\beta_{rd,n\ell}}$. (Our notation follows [71].) Hence, at a given n-loop order, there are n Padé approximants that one can calculate, namely

$$\{\ [n-k, k-1]_{\beta_{rd,n\ell}}\ \} \quad \text{with } 1 \le k \le n \ . \tag{306}$$

These provide rational-function approximations of the series expansion for $\beta_{rd,n\ell}$ that fits this series to the loop order n. As in our earlier work, e.g., [14, 30, 35], these provide an alternate approach to investigating zeros of a beta function.

We shall label one of the p zeros of a $[p, q]_{\beta_{rd,n\ell}}$ Padé approximant as $[p, q]_{zero}$ and one of the q poles of this approximant as $[p, q]_{pole}$; in each case, the value of n is given by Eq. (305) as $n = p+q+1$. At the n-loop level, the Padé approximant $[n-1, 0]_{\beta_{rd,n\ell}}$ is equal to the reduced n-loop beta function $\beta_{rd,n\ell}$ itself, which we have already analyzed in the previous section, and the PA $[0, n-1]_{\beta_{rd,n\ell}}$ has no zeros, and hence is not useful for our study. Hence, at

the n-loop level, we focus on the $n-2$ PAs $[p,q]_{\beta_{rd,n\ell}}$ with $[p,q]=[n-k,k-1]$ having $2 \leq k \leq n-1$.

At the $n=3$ loop level, we thus consider the $[1,1]_{\beta_{rd,3\ell}}$ Padé approximant. This is

$$[1,1]_{\beta_{rd,3\ell}} = \frac{1+\left(\frac{b_2}{b_1}-\frac{b_3}{b_2}\right)a}{1-\left(\frac{b_3}{b_2}\right)a} = \frac{1-\left(\frac{2N-3}{4}\right)a}{1-\left(\frac{2N-7}{4}\right)a} \ . \tag{307}$$

where the coefficients b_1, b_2, and b_3 were given in Eqs. (289)-(291) above. This [1,1] PA has a zero at

$$[1,1]_{zero} = \frac{4}{2N-3} \tag{308}$$

and a pole at

$$[1,1]_{pole} = \frac{4}{2N-7} \ . \tag{309}$$

The $a=[1,1]_{pole}$ is not relevant, since if $N=2$ or 3, it has the respective negative and hence unphysical values $-4/3$ and -4, while for $N \geq 4$, it lies farther from the origin than the zero. This is clear from the fact that the difference

$$[1,1]_{pole} - [1,1]_{zero} = \frac{16}{(2N-3)(2N-7)} \tag{310}$$

is positive for this range $N \geq 4$. Since the $[1,1]_{pole}$ lies farther from the origin than $[1,1]_{zero}$, the coupling $a=a(\mu)$ never reaches the pole as μ decreases from large values in the UV to $\mu=0$ and thus $a(\mu)$ increases from 0 to $[1,1]_{zero}$. We list the values of the zero of the $[1,1]_{\beta_{rd,3\ell}}$ Padé approximant in Table 11. For $N \geq 3$, the value of $a=[1,1]_{zero}$ is smaller than $a_{IR,3\ell}$ and decreases more rapidly to zero as $N \to \infty$ than $a_{IR,3\ell}$. If $N=3$, the comparison cannot be made, since $a_{IR,3\ell}$ is complex. Thus, this analysis of the [1,1] Padé approximant to the reduced three-loop beta function, $\beta_{rd,3\ell}$ yields further evidence against a (reliably calculable) IR zero in the beta function up to the three-loop level.

At the $n=4$ loop level, there are two Padé approximants to analyze, namely $[2,1]_{\beta_{rd,4\ell}}$ and $[1,2]_{\beta_{rd,4\ell}}$. We calculate

$$[2,1]_{\beta_{rd,4\ell}} = \frac{1+\left(\frac{b_2}{b_1}-\frac{b_4}{b_3}\right)a+\left(\frac{b_3}{b_1}-\frac{b_2 b_4}{b_1 b_3}\right)a^2}{1-\frac{b_4}{b_3}a} \ , \tag{311}$$

where the coefficients b_n were given in Eqs. (289)-(292). The zeros of the numerator occur at $a = [2,1]_{zero,(i,ii)}$, where

$$[2,1]_{zero,(i,ii)} = \frac{b_2 b_3 - b_1 b_4 \pm \left[b_1^2 b_4^2 + b_2^2 b_3^2 - 4 b_1 b_3^3 + 2 b_1 b_2 b_3 b_4\right]^{1/2}}{2(b_2 b_4 - b_3^2)} \ . \tag{312}$$

and the subscripts i and ii correspond to the $\pm$ sign in front of the square root. It is straightforward to substitute the explicit expressions for the coefficients b_2, b_3, and b_4 in Eq. (312), but the resultant expressions for these quadratic roots in terms of the explicit coefficients b_n, $1 \le n \le 4$ are somewhat lengthy, so we do not display them. The pole of the $[2,1]_{\beta_{rd,4\ell}}$ PA occurs at $a = [2,1]_{pole}$, where

$$\begin{aligned} [2,1]_{pole} &= \frac{b_3}{b_4} \\ &= -\frac{3(2N-7)}{2[2N^2 + 19N - 24 + 6(11N-17)\zeta_3]} \ . \end{aligned} \tag{313}$$

If one has a series expansion of a function that contains n_{zero} zeros and n_{pole} poles, and one calculates $[r,s]$ Padé approximants to this series with $r > n_{zeros}$ and $s > n_{poles}$, the approximants typically exhibit sets of nearly coincident zero-pole pairs in addition to fitting the actual zeros and poles of the function (e.g., see [71, 35]). These nearly coincident zero-pole pairs may thus be ignored. This happens in the present case. For example, for $N = 3$, the $[2,1]_{\beta_{rd,4\ell}}$ PA has a zero at $a = 0.99773$, a zero at $a = 0.009015$ and a pole at $a = 0.009015$, and similarly for other values of N. In Table 11 we list the first zero, denoted $[2,1]_{zero,i}$, as a function of N.

We calculate the $[1,2]_{\beta_{rd,4\ell}}$ Padé approximant to be

$$[1,2]_{\beta_{rd,4\ell}} = \frac{1 + \left[\frac{b_1^2 b_4 + b_2^3 - 2 b_1 b_2 b_3}{b_1(b_2^2 - b_1 b_3)}\right] a}{1 + \left(\frac{b_1 b_4 - b_2 b_3}{b_2^2 - b_1 b_3}\right) a + \left(\frac{b_3^2 - b_2 b_4}{b_2^2 - b_1 b_3}\right) a^2} \ . \tag{314}$$

The two poles of the $[1,2]_{\beta_{rd,4\ell}}$ approximant occur at $a = [1,2]_{pole,(i,ii)}$, where

$$[1,2]_{pole,(i,ii)} = \frac{b_1 b_4 - b_2 b_3 \pm \left[b_1^2 b_4^2 - 3 b_2^2 b_3^2 + 4 b_1 b_3^3 + 4 b_2^3 b_4 - 6 b_1 b_2 b_3 b_4\right]^{1/2}}{2(b_2 b_4 - b_3^2)} \ . \tag{315}$$

Table 11: Values of $[1,1]_{zero}$ from [1,1] Padé approximant to the reduced three-loop beta function, $\beta_{rd,3\ell}$, and $[2,1]_{zero,i}$ from the [2,1] Padé approximant to the four-loop beta function, $\beta_{rd,4\ell}$. See text for further details.

N	$[1,1]_{zero}$	$[2,1]_{zero,i}$
2	4.000	0.940
3	1.333	0.998
4	0.800	0.999
5	0.571	0.992
6	0.444	0.982
7	0.364	0.9725
8	0.308	0.963
9	0.267	0.953
10	0.235	0.943
100	0.0203	0.683
300	0.00670	0.615
10^3	0.00200	0.585

The zero of this approximant occurs at $a = [1,2]_{zero}$, where

$$[1,2]_{zero} = \frac{b_1(b_1 b_3 - b_2^2)}{b_1^2 b_4 + b_2^3 - 2b_1 b_2 b_3}$$
$$= -\frac{3(2N-3)}{2[2N^2 + 13N - 9 + 6(11N-17)\zeta_3]} \ . \tag{316}$$

Both of the poles $[1,2]_{pole,i}$ and $[1,2]_{pole,ii}$ are negative. Furthermore, we find that this approximant has nearly coincident zero-pole pairs, which thus can both be ignored. For example, for $N = 3$, the zero occurs at $a = -0.027540$ while one of the poles occurs at the nearly equal value, $a = -0.027556$, and the other pole is at $a = -0.97919$. Similar results hold for other values of N, i.e., the $[1,2]_{\beta_{rd,4\ell}}$ PA has a nearly coincident zero-pole pair (at negative a) together with a second unphysical pole at negative a.

As we have discussed, the four-loop beta function yields a negative real root, in strong disagreement with the two-loop and three-loop beta functions. At this four-loop level, the [1,2] PA does not exhibit any true zero, but only a zero that is nearly coincident with a pole and hence can be identified as an

artifact. The [2,1] PA yields a zero, but it is at a completely different value than the only real root of the actual four-loop beta function, $a_{rt,4\ell}$. Thus, our analysis of the [2,1] and [1,2] Padé approximants to the four-loop (reduced) beta function yield further evidence against a robust IR zero in this four-loop beta function.

4.4 Analysis Using Scheme Transformations

Since the coefficients b_ℓ with $\ell \geq 3$ in the beta function are scheme-dependent, it is necessary to check that the conclusions from our analysis of the beta function with b_3 and b_4 calculated in the $\overline{\rm MS}$ scheme are robust with respect to scheme transformations. The contents and notations for scheme transformation formalism follow Sec.1.4. To begin with, we study scheme transformations that are designed to remove higher-loop terms in the beta function.

Ref. [37] gave the first explicit scheme transformation to set $b'_\ell = 0$ for $\ell \geq 3$, at least in the local vicinity of the origin, but it also showed that this does not, in general, work to remove these higher-loop terms at a point located away from the origin, i.e., an IR zero in an asymptotically free theory or a UV zero in an IR-free theory. The reason is that, as shown in [37, 38, 39], if one attempts to apply such a scheme transformation to remove these higher-loop terms at a point away from the origin, then the transformation violates one or more of the conditions $\rm C_1$-$\rm C_4$ for acceptability. As in [38, 39], we denote the scheme transformation presented in [37] (with $s_{max} = m$) that removes the coefficients in the beta function up to loop order $\ell = m + 1$, at least near the origin, as $S_{R,m}$.

We proceed with our analysis with the $S_{R,m}$ scheme transformation. The $S_{R,2}$ transformation has [37]

$$k_2 = \frac{b_3}{b_1} \tag{317}$$

and the $S_{R,3}$ transformation has this k_2 and

$$k_3 = \frac{b_4}{2b_1} \ . \tag{318}$$

We begin by determining whether the scheme transformation $S_{R,2}$ can be applied in the relevant region of a where we need to apply it to set $b'_3 = 0$ and thus remove the three-loop term in the beta function. Since the (scheme-independent) two-loop value is $a_{IR,2\ell} = a'_{IR,2\ell} = 1$, the relevant region is in

the neighborhood of $a = 1$. This $S_{R,2}$ transformation is defined by Eq. (22) with $s_{max} = 2$ and k_2 given by Eq. (317). If the application of this $S_{R,2}$ transformation in the vicinity of $a =$ were possible, then it would follow from Eq. (32) that $b'_4 = b_4$. For $S_{R,2}$, Eq. (20) is

$$S_{R,2} \implies a = a'[1 + k_2(a')^2] = a'\Big[1 + \frac{b_3}{b_1}(a')^2\Big] \ . \tag{319}$$

Solving Eq. (319) for a', we obtain three roots, and we require that at least one of these should be a physical (real, positive) value for a in the relevant range of values comparable to $a_{IR,2\ell} = 1$. We find that this necessary condition, C_1, is not satisfied. Instead, two of the solutions of Eq. (319) for a' form a complex-conjugate pair, while the third is negative. For example, for $a = a_{IR,2\ell} = 1$ and $N = 4$, the three solutions for a' are $1.191 \pm 0.509i$ and -2.383, while for $N = 10$, the three solutions for a' are $0.4125 \pm 0.450i$ and -0.825. The Jacobian also exhibits pathological behavior; J is given by

$$\begin{aligned} S_{R,2} \implies J &= 1 + 3k_2(a')^2 = 1 + \frac{3b_3}{b_1}(a')^2 \\ &= 1 - \frac{3(2N-7)}{4}\,(a')^2 \ . \end{aligned} \tag{320}$$

For $a_{IR,2\ell} = a'_{IR,2\ell} = 1$, $J = (25 - 6N)/4$, which decreases through zero as N (continued to the real numbers) increases through the value $N = 25/6$, violating condition C_3. It is therefore not possible to use this scheme transformation to remove the three-loop term in the beta function in the region of a where we are trying to do this, namely the neighborhood of the (scheme-independent) value $a = a_{IR,2\ell} = 1$.

We can also investigate whether the scheme transformation $S_{R,3}$ is physically acceptable to be applied in the relevant range of values of a, namely $a = a_{IR,2\ell} = 1$. This transformation is defined by Eq. (22) with $s_{max} = 3$ and k_2 and k_3 given by Eqs. (317) and (318):

$$\begin{aligned} S_{R,3} \implies a &= a'[1 + k_2(a')^2 + k_3(a')^3] \\ &= a'\Big[1 + \frac{b_3}{b_1}(a')^2 + \frac{b_4}{2b_1}(a')^3\Big] \ . \end{aligned} \tag{321}$$

The Jacobian for this transformation is

$$\begin{aligned} S_{R,3} \implies J &= 1 + 3k_2(a')^2 + 4k_3(a')^3 \\ &= 1 + \frac{3b_3}{b_1}(a')^2 + \frac{2b_4}{b_1}(a')^3 \ . \end{aligned} \tag{322}$$

With this $S_{R,3}$ scheme transformation we find that for the relevant range of $a \simeq 1$, J can deviate excessively far from unity, violating condition C_1. For example, for $a = 1$ and $N = 10$, we find that $J = 339.8$, much larger than unity.

One can also apply the various scheme transformations that we have devised in [1, 2, 14, 30, 36, 37, 38, 39, 40, 41, 35] to the beta function calculated in the $\overline{\rm MS}$ scheme and compare the resulting value(s) of the zero(s) of the beta function with the value(s) obtained at the three-loop and four-loop level in the $\overline{\rm MS}$ scheme. Our general analyses in [1, 2] (see also [53]) have shown that, for moderate values of the parameters determining these scheme transformations, the resultant values of the zero(s) are similar to those obtained in the original $\overline{\rm MS}$ scheme. In particular, the negative, unphysical value of $a_{rt,4\ell}$ will still be present in the transformed scheme.

Summarizing this section, we have shown that our conclusion, that the beta function of the finite-N Gross-Neveu model, calculated up to four-loop order, does not exhibit an IR zero, is robust with respect to scheme transformations.

4.5 Comparison with Results in the LN Limit and Behavior for $d > 2$

In this section we discuss how the conventional perturbative beta function reduces in the LN limit, and we also comment on some properties of the theory for spacetime dimension $d > 2$. From Eq. (284), the quantity that remains finite and nonzero in the LN limit is $\lambda = gN$, and hence the corresponding beta function that is finite in this limit is

$$\beta_\lambda = \frac{d\lambda}{dt} = \lim_{LN} N \frac{dg}{dt} = \lim_{LN} N\beta \ . \tag{323}$$

With the limit $N \to \infty$ having been taken, β_λ has the series expansion, for $d \geq 2$, with $\epsilon_d = d - 2$,

$$\beta_\lambda = \lambda\Big[\epsilon_d + \sum_{\ell=1}^{\infty} \hat{b}_\ell \xi^\ell\Big] \ , \tag{324}$$

where

$$\xi = \lim_{LN} Na = \frac{\lambda}{2\pi} \tag{325}$$

and

$$\hat{b}_\ell = \lim_{LN} \frac{b_\ell}{N^\ell} \ . \tag{326}$$

Here we have used the fact that $b_\ell a^\ell = \hat{b}_\ell \xi^\ell$. We find

$$\hat{b}_1 = -2 \tag{327}$$

and

$$\hat{b}_\ell = 0 \quad \text{for } \ell \geq 2 \ . \tag{328}$$

The latter result follows from the fact that the structure of the bubble graphs in the calculation of b_ℓ in, e.g., the $\overline{\rm MS}$ scheme, means that, for $\ell \geq 2$, b_ℓ is a polynomial in N of degree $\ell - 1$. Although the b_ℓ with $\ell \geq 3$ are scheme-dependent, this property is maintained by scheme transformations that are finite in the LN limit [37]. Hence, for $\ell \geq 2$, $\lim_{LN} b_\ell/N^\ell = 0$, which is the result given in Eq. (328). Similarly, although $\hat{b}_\ell$ with $\ell \geq 3$ are, in general, scheme-dependent, if they are zero in one scheme, such as the $\overline{\rm MS}$ scheme, then they are also zero in any other scheme reached by a scheme transformation function that is finite in the LN limit [37]. It follows that in the LN limit, with $d = 2 + \epsilon \geq 2$,

$$\beta_\lambda = \lambda[\epsilon - 2\xi] = \lambda\Big[\epsilon - \frac{\lambda}{\pi}\Big] \ . \tag{329}$$

Hence,

$$d = 2 \implies \beta_\lambda = -\frac{\lambda^2}{\pi} \ , \tag{330}$$

with only the UV zero in this beta function at $\lambda = 0$, and no IR zero. We can relate this to the beta function that was calculated in [72] in the LN limit. From Eqs. (278) and (287), we have

$$\beta = \frac{dg}{dt} = 2g_{GN} \frac{dg_{GN}}{dt} = 2g_{GN}\beta_{GN} \ . \tag{331}$$

Explicitly, in the LN limit, from Eqs. (330) and (278),

$$\beta_\lambda = -\frac{\lambda^2}{\pi} = -\lim_{LN} \frac{g_{GN}^4 N^2}{\pi} \ . \tag{332}$$

Combining Eqs. (323), (331), and (332) yields $\beta_{GN} = -g_{GN}^3 N/(2\pi) = -g_{GN}\lambda/(2\pi)$, in agreement with Eq. (286) above, or equivalently, Eq. (3.7)

in Ref. [72]. This agreement was guaranteed, since the LN limit is a special limit of the result for finite N. Accordingly, our finding that there is no robust evidence for an IR zero in the finite-N beta function of the ($d = 2$) Gross-Neveu model is, *a fortiori*, in agreement with the fact that in the LN limit, the beta function β_λ in Eq. (330) (equivalently, β_{GN} in Eq. (286) above), does not exhibit an IR zero.

5 Conclusions

In this dissertation we studied transformations of schemes used for regularization and renormalization in quantum field theories, performed explicit construction of several scheme transformations and applied these to study renormalization group evolution of some asymptotically free quantum field theories. This research was done in collaboration with Prof. R. Shrock, and the results were published in the four papers [1]-[4], the last of which also involved Prof. T. Ryttov as a coauthor. In Sec.1 we reviewed some basic background for this research.

In Sec.2, corresponding to the two papers [1, 2], we constructed and studied several scheme transformations. As was discussed in Refs. [36]-[39], scheme transformations that are acceptable in the vicinity of zero coupling may not be acceptable for the study of zeros of the beta function at nonzero coupling (but still in the perturbative regime), in particular, at an infrared fixed point in an asymptotically free gauge theory. Motivated by this, we made progress in constructing new scheme transformations which can map coupling spaces of different renormalization schemes for the regime away from zero and still preserve perturbativity and unitarity. Applying those to an infrared zero $\alpha_{IR,zero}$ of the beta function of $SU(N_c)$ gauge theory with N_f massless fermion flavors in a representation of G, we could quantify the degree of scheme dependence of $\alpha_{IR,zero}$ calculated to a given loop order and show reduction of scheme dependence of $\alpha_{IR,zero}$ resulting from higher-loop corrections [1, 2].

In Sec.3, corresponding to the paper Ref. [3], we studied the renormalization-group evolution of an $\mathcal{N} = 1$ supersymmetric gauge theory with a non-Abelian gauge group $G = SU(N_c)$ and N_f massless chiral and anti chiral superfields in representations R and $\bar{R}$ of G by examining the beta function β_{NSVZ} calculated by Novikov, Shifman, Vainshtein, and Zakharov (NSVZ). This beta function has the form of a rational function of the coupling α and thus exhibits not only an infrared zero at $\alpha = \alpha_{IR,zero}$ in the non-Abelian Coulomb phase, but also a pole. To study the scheme dependence in a finite-loop calculation of the beta function for this theory, we compare properties of the NSVZ beta function with those of the beta function calculated to finite-loop order in a different scheme, namely the $\overline{\rm DR}$ scheme. We calculate Padé approximants to the beta functions for these theories in the $\overline{\rm DR}$ scheme up to four-loop order for the gluonic theory and up to three-loop order for the theories with matter superfields and compare results for IR zeros and poles with

results from the NSVZ beta function. Our calculations provide new insights, for these theories, of how well finite-order perturbative results calculated in one scheme reproduce properties of a known beta function calculated in a different scheme.

In Sec.4, corresponding to the paper [4], we discussed an investigation of the (two-dimensional) finite-N Gross-Neveu model. This model has a four-fermion interaction involving an N-component fermion and is asymptotically free, i.e., has a UV zero of the beta function at zero four-fermion coupling. The model was exactly solved in the limit $N \to \infty$ by Gross and Neveu [72]. In this limit, it did not exhibit an infrared fixed point of the renormalization group, but this left open the question of whether the beta function of the finite-N model might have an IR zero and associated IR fixed point. For our study, we calculate and analyze Padé approximants to the beta function and evaluate effects of scheme dependence. From our study, we find that in the range of coupling where the perturbative calculation of the four-loop beta function is reliable, it does not exhibit robust evidence for an infrared zero.

References

[1] G. Choi and R. Shrock, Phys. Rev. D **90**, 125029 (2014).

[2] G. Choi and R. Shrock, Phys.Rev. D **94** 065038 (2016).

[3] G. Choi and R. Shrock, Phys.Rev. D **93** 069905 (2016).

[4] G. Choi, T. A. Ryttov, and R. Shrock, Phys.Rev. D **95** 025012 (2017).

[5] Some early studies on the renormalization group in quantum field theory include E. C. G. Stueckelberg and A. Peterman, Helv. Phys. Acta **26**, 499 (1953); M. Gell-Mann and F. Low, Phys. Rev. **95**, 1300 (1954); N. N. Bogolubov and D. V. Shirkov, Doklad. Akad. Nauk SSSR **103**, 391 (1955); C. G. Callan, Phys. Rev. D **2**, 1541 (1970); K. Symanzik, Commun. Math. Phys. **18**, 227 (1970). See also K. Wilson, Phys. Rev. D **3**, 1818 (1971).

[6] G. 't Hooft and M. Veltman, Nucl. Phys B44 (1972) 199.

[7] G. 't Hooft, Nucl. Phys. B **61**, 455 (1973).

[8] W. A. Bardeen, A. J. Buras, D. W. Duke, and T. Muta, Phys. Rev. D **18**, 3998 (1978).

[9] J. Collins, *Renormalization* (Cambridge University Press, Cambridge, UK, 1992).

[10] W. A. Bardeen, B. W. Lee, and R. E. Shrock, Phys. Rev. D **14**, 985 (1976); E. Brézin and J. Zinn-Justin, Phys. Rev. B **14**, 3110 (1976); see also A. Polyakov, Phys. Lett. B **59**, 79 (1975).

[11] B. Holdom, Phys. Lett. B **694**, 74 (2010).

[12] R. Shrock, Phys. Rev. D **89**, 045019 (2014).

[13] E. Mølgaard and R. Shrock, Phys. Rev. D **89**, 105007 (2014).

[14] R. Shrock, Phys. Rev. D **90**, 065023 (2014).

[15] R. Shrock, Phys. Rev. D **94**, 125026 (2016).

[16] R. Shrock, Phys. Rev. D **96**, 056010 (2017).

[17] D. J. Gross and F. Wilczek, Phys. Rev. Lett. **30**, 1343 (1973); H. D. Politzer, Phys. Rev. Lett. **30**, 1346 (1973); G. 't Hooft, unpublished.

[18] W. E. Caswell, Phys. Rev. Lett. **33**, 244 (1974); D. R. T. Jones, Nucl. Phys. B **75**, 531 (1974).

[19] D. J. Gross, in R. Balian and J. Zinn-Justin, eds. *Methods in Field Theory*, Les Houches 1975 (North Holland, Amsterdam, 1976).

[20] O. V. Tarasov, A. A. Vladimirov, and A. Yu. Zharkov, Phys. Lett. B **93**, 429 (1980); S. A. Larin and J. A. M. Vermaseren, Phys. Lett. B **303**, 334 (1993).

[21] T. van Ritbergen, J. A. M. Vermaseren, and S. A. Larin, Phys. Lett. B **400**, 379 (1997).

[22] F. Herzog, B. Ruijl, T. Ueda, J. A. M. Vermaseren, and A. Vogt, JHEP 1702 (2017) 090 .

[23] P. A. Baikov, K. G. Chetyrkin, and J. H. Kühn, Phys. Rev. Lett. **118**, 082002 (2017).

[24] K. Yamawaki, M. Bando, and K. Matumoto, Phys. Rev. Lett. **56**, 1335 (1986); T. Appelquist, D. Karabali, and L. C. R. Wijewardhana, Phys. Rev. Lett. **57**, 957 (1986); V. A. Miransky, *Dynamical Symmetry Breaking in Quantum Field Theories* (World Scientific, Singapore, 1993).

[25] W. Goldberger, B. Grinstein, and W. Skiba, Phys. Rev. Lett. **100**, 111802 (2008); B. Coleppa, T. Gregoire and H. Logan, Phys. Rev. D **85**, 055001 (2012)

[26] For reviews of lattice work, see SCGT15 (Strongly Coupled Gauge Theories 2015), Nagoya University at http://www.kmi.nagoya-u.ac.jp/workshop/SCGT15; and Lattice-2015 at http://www.aics.riken.jp/sympo/lattice2015; Lattice-2016 at https://www.southampton.ac.uk/lattice2016; Lattice for BSM 2017 Workshop at http://www-hep.colorado.edu/(tilde)eneil/lbsm17; Lattice-2017 at http://wpd.ugr.es/(tilde)lattice2017, and Ref. [27].

[27] A recent workshop on both lattice studies and theoretical and phenomenological aspects of these theories (T. Ryttov and R. Shrock, organizers) is "Continuum and Lattice Approaches to the Infrared Behavior of Conformal and Quasi-Conformal Gauge Theories", Simons Center, Stony Brook University, Jan. 2018, available at http://scgp.stonybrook.edu/archives/21358.

[28] T. Banks and A. Zaks, Nucl. Phys. B **196**, 189 (1982).

[29] E. Gardi and M. Karliner, Nucl. Phys. B **529**, 383 (1998); E. Gardi and G. Grunberg, JHEP 03, 024 (1999).

[30] T. A. Ryttov, R. Shrock, Phys. Rev. D **83**, 056011 (2011).

[31] R. Shrock, Phys. Rev. D **87**, 105005 (2013).

[32] R. Shrock, Phys. Rev. D **87**, 116007 (2013).

[33] T. A. Ryttov and R. Shrock, Phys. Rev. D **85**, 076009 (2012).

[34] R. Shrock, Phys. Rev. D **91**, 125039 (2015).

[35] T. A. Ryttov and R. Shrock, Phys. Rev. D **94**, 105015 (2016).

[36] T. A. Ryttov and R. Shrock, Phys. Rev. D **86**, 065032 (2012)

[37] T. A. Ryttov and R. Shrock, Phys. Rev. D **86**, 085005 (2012)

[38] R. Shrock, Phys. Rev. D **88**, 036003 (2013).

[39] R. Shrock, Phys. Rev. D **90**, 045011 (2014).

[40] T. A. Ryttov, Phys. Rev. D **89**, 016013 (2014); Phys. Rev. D **89**, 056001 (2014).

[41] T. A. Ryttov, Phys. Rev. D **90**, 056007 (2014).

[42] T. A. Ryttov, Phys. Rev. Lett. **117**, 071601 (2016).

[43] T. A. Ryttov and R. Shrock, Phys. Rev. D **94**, 105014 (2016).

[44] T. A. Ryttov and R. Shrock, Phys. Rev. D **94** 125005 (2016).

[45] T. A. Ryttov and R. Shrock, Phys. Rev. D **95**, 085012 (2017).

[46] T. A. Ryttov and R. Shrock, Phys. Rev. D **95**, 105004 (2017); Phys. Rev. D **96**, 105015 (2017); Phys. Rev. D **97**, 025004 (2018); Phys. Rev. D **97**, 016020 (2018).

[47] T. A. Ryttov and R. Shrock, Phys. Rev. D **96**, 105018 (2017).

[48] G. Choi, with C.-T. Chiang, and M. Loverde, to appear.

[49] G. 't Hooft, in *The Whys of Subnuclear Physics, Proc. 1977 Erice Summer School*, ed. A. Zichichi (Plenum, New York, 1979), p. 943.

[50] For recent reviews, see, X.-G. Wu, S. J. Brodsky, and M. Mojaza, Prog. Part. Nucl. Phys. **72**, 44 (2013); A. Deur, S. J. Brodsky, and G. F. de Teramond, Prog. Part. Nuc. Phys. **90**, 1 (2016).

[51] Here and elsewhere, when an expression is given for N_f that formally evaluates to a non-integral real value, it is understood implicitly that one infers an appropriate integral value from it, either the greatest integer smaller than the real value, or the least integer greater than the real value, or the closest integer, depending on the context.

[52] W. Celmaster and R. J. Gonsalves, Phys. Rev. D **20**, 1420 (1979); E. Braaten and J. P. Leveille, Phys. Rev. D **24**, 1369 (1981); J. A. Gracey, Phys. Lett. B **700**, 79 (2011); J. A. Gracey, J. Phys. A **46**, 225403 (2013).

[53] J. A. Gracey and R. M. Simms, Phys. Rev. D **91**, 085037 (2015).

[54] P. M. Stevenson, Phys. Rev. D **23**, 2916 (1981); S. J. Brodsky, G. P. Lepage, and P. B. MacKenzie, Phys. Rev. D **28**, 228 (1983).

[55] V. A. Novikov, M. A. Shifman, A. I. Vainshtein, and V. I. Zakharov, Nucl. Phys. B **229**, 381, 407 (1983); Phys. Lett. B **166**, 329 (1986); M. A. Shifman and A. I. Vainshtein, Nucl. Phys. B **277**, 426 (1986).

[56] M. A. Shifman, Prog. Part. Nucl. Phys. **39**, 1 (1997).

[57] I. I. Kogan and M. Shifman, Phys. Rev. Lett. **75**, 2085 (1995).

[58] N. Seiberg, Phys. Rev. D **49**, 6857 (1994); K. A. Intriligator and N. Seiberg, Nucl. Phys. B **431**, 551 (1994); N. Seiberg, Nucl. Phys. B **435**, 129 (1995).

[59] A review is M. Shifman, Prog. Part. Nucl. Phys. **39**, 1 (1997) [hep-th/9704114].

[60] S. Ferrara and B. Zumino, Nucl. Phys. B **79**, 413 (1974); D. R. T. Jones, Nucl. Phys. B **87**, 127 (1975).

[61] The Casimir invariants C_R and T_R are defined as $\sum_a \sum_j \mathcal{D}_R(T_a)_{ij}\mathcal{D}_R(T_a)_{jk} = C_R\delta_{ik}$ and $\sum_{i,j} \mathcal{D}_R(T_a)_{ij}\mathcal{D}_R(T_b)_{ji} = T_R\delta_{ab}$, where R is the representation and T_a are the generators of G, so that for SU(N_c), $C_A = N_c$ for the adjoint (A) and $T_{fund} = 1/2$ for the fundamental representation, etc. C_f denotes C_R for the fermion representation.

[62] M. Machacek and M. Vaughn, Nucl. Phys. B **222**, 83 (1983); A. J. Parkes and P. C. West, Phys. Lett. B **138**, 99 (1984); Nucl. Phys. B **256**, 340 (1985); D. R. T. Jones and L. Mezincescu, Phys. Lett. B **136**, 242 (1984); Phys. Lett. B **138**, 293 (1984); I. Jack, D. R. T. Jones, and C. G. North, Nucl. Phys. B **473**, 308 (1996).

[63] I, Jack, D. R. T. Jones, and A. Pickering, Phys. Lett. B **435**, 61 (1998).

[64] W. Siegel, Phys. Lett. B **84**, 193 (1979); W. Siegel, Phys. Lett. B **94**, 37 (1980); D. M. Capper, D. R. T. Jones, and P. van Nieuwenhuizen, Nucl Phys. B **167**, 479 (1980); W. Stöckinger, JHEP 0503, 076 (2005).

[65] I. Jack, D. R. T. Jones, and C. G. North, Nucl. Phys. B **486**, 479 (1997); I. Jack, D. R. T. Jones, and A. Pickering, Phys. Lett. B **435**, 61 (1998).

[66] F. A. Chishtie, V. Elias, V. A. Miransky, and T. G. Steele, Prog. Theor. Phys. **104**, 603 (2000).

[67] V. Elias, J. Phys. G **27**, 217 (2001).

[68] T. Appelquist, A. Nyffeler, and S. B. Selipsky, Phys. Lett. B **425**, 300

[69] T. A. Ryttov and F. Sannino, Phys. Rev. D **76**, 105004 (2007).

[70] F. Sannino and J. Schechter, Phys. Rev. D **82**, 096008 (2010).

[71] I-H. Lee and R. E. Shrock, Phys. Rev. B **36**, 3712 (1987); I-H. Lee and R. E. Shrock, J. Phys. A **21**, 3139 (1988); V. Matveev and R. Shrock, J. Phys. A **28**, 1557 (1995).

[72] D. J. Gross and A. Neveu, Phys. Rev. D **10**, 3235 (1974).

[73] Here the copy indices j on the fermion field ψ_j are implicit in the notation, i.e., $\bar\psi \not\partial\psi \equiv \sum_{j=1}^N \bar\psi_j \gamma^\mu \partial_\mu \psi_j$ and $(\bar\psi\psi)^2 \equiv (\sum_{j=1}^N \bar\psi_j \psi_j)^2$.

[74] R. F. Dashen, B. Hasslacher, and A. Neveu, Phys. Rev. D **12**, 2443 (1975).

[75] J. Schonfeld, Nucl. Phys. B **95**, 148 (1975).

[76] J. A. Gracey, T. Luthe, and Y. Schröder, Phys. Rev. D94, 125028 (2016).

[77] In our Eq. (286) we are quoting the result from Eq. (3.7) of Ref. [72]. An alternate calculation of β_{GN} was given in Eq. (4.16) of Ref. [72], with the result $\beta_{GN} = -(2\pi)^{-1}\lambda g_{GN}/[1 + (\lambda/(2\pi))]$. As was noted in [72], their expressions for β_{GN} in their Eqs. (3.7) and (4.16) agree to leading order in λ.

[78] W. Wetzel, Phys. Lett. B **153**, 297 (1985).

[79] J. A. Gracey, Nucl. Phys. B **341**, 403 (1990); J. A. Gracey, Nucl. Phys. B **367**, 657 (1991).

[80] C. Luperini and P. Rossi, Ann. Phys. (NY) **212**, 371 (1991).

[81] W. Thirring, Ann. Phys. (NY) **3**, 91 (1958).

[82] B. Klaiber, *1967 Boulder Lectures in Theoretical Physics*, ed. A. O. Barut and W. E. Brittin (Gordon and Breach, NY, 1968), p. 141.

[83] A. J. Mueller and T. L. Trueman, Phys. Rev. D **4**, 1635 (1971); M. Gomes and J. Lowenstein, Nucl. Phys. B **45**, 252 (1972).